Electronic Theses and Dissertations

Theses, Dissertations, and Major Papers

8-1-1969

# Theoretical investigation of critical sections in inclined prestressed roof girders.

M. A. Saeed
*University of Windsor*

Follow this and additional works at: https://scholar.uwindsor.ca/etd

THEORETICAL INVESTIGATION OF CRITICAL SECTIONS

IN

INCLINED PRESTRESSED ROOF GIRDERS

Submitted in partial fulfillment of the
requirements for the Degree of
Master of Applied Science
from the University of
Windsor

By

M. A. Saeed

Windsor, August, 1969

UMI Number: EC52769

INFORMATION TO USERS

The quality of this reproduction is dependent upon the quality of the copy submitted. Broken or indistinct print, colored or poor quality illustrations and photographs, print bleed-through, substandard margins, and improper alignment can adversely affect reproduction.

In the unlikely event that the author did not send a complete manuscript and there are missing pages, these will be noted. Also, if unauthorized copyright material had to be removed, a note will indicate the deletion.

# UMI®

UMI Microform EC52769
Copyright 2008 by ProQuest LLC.
All rights reserved. This microform edition is protected against unauthorized copying under Title 17, United States Code.
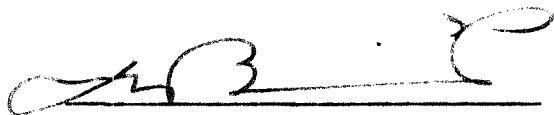
ProQuest LLC
789 E. Eisenhower Parkway
PO Box 1346
Ann Arbor, MI 48106-1346

ABT9013

APPROVED BY:

_____

_G. Abdel - Sayged_____

_B. Kennedy_____

275370

# TABLE OF CONTENTS

ii

# TABLE OF CONTENTS
## (Continued)

# TABLE OF CONTENTS
## (Continued)

## TABLE OF CONTENTS
### (Continued)

v

# ACKNOWLEDGEMENTS

The author wishes to extend his sincere thanks and gratitude for aid and encouragement given by Dr. J. B. Kennedy during the course of this project.

Thanks are also extended to the National Research Council of Canada which contributed greatly to the financing of this work.

The efforts of Mr. M. Malone, third year student in Mechanical Engineering, and Mr. W. C. Wong, graduate student in Civil Engineering, in drawing the figures are acknowledged with thanks.

Last, but not least, appreciation and gratitude are extended to my wife for typing the manuscript and who together with our two childern have coped with so many inconveniences as a result of my decision of returning to university.

# ABSTRACT

In this paper an investigation is made of the critical design sections in bonded pretensioned inclined roof girders with straight tendons. Various inclinations of the top flanges are treated. The lateral stability of such girders is considered briefly. The critical sections include flexural critical sections, principal tensile stress, and other critical sections such as the section through the crown of the girder, if any, see Fig. 1.

In establishing the flexural critical sections, two approaches are followed. The first approach is based on simplified assumptions together with equilibrium and geometrical conditions, excluding creep, and shrinkage deformations. The second approach is by means of a general computer programme which considers the pertinent parameters essential in the design of prestressed concrete structures. The flexural critical sections which are derived through simplified assumptions are compared with the flexural critical sections derived from the general computer programme.

The critical sections for principal tensile stress are ascertained from the computer programme, taking into account the effect of inclination on the shear force reduction.

Several computer programmes were written to evaluate critical sections for different girder cross-sections and to plot the location of the critical section versus the girder length.

# NOTATION

## English Letters

$A$ = cross-sectional area in general

$A_c$ = cross-sectional area of concrete = $A_g - A_s$

$A_g$ = gross cross-sectional area = $A_c + A_s$

$A_s$ = cross-sectional area of prestressing steel

$A_{s1}$ = cross-sectional area of bottom layer of prestressing steel

$A_{s2}$ = cross-sectional area of top layer of prestressing steel

$A_e$ = effective cross-sectional area = $A_c + n A_s$

$A_i$ = area of the section comprised between the horizontal edge of girder and level i – i

$A_\xi$ = cross-sectional area at dimensionless distance $\xi$ from midspan

$a$ = lever arm between compressive and tensile forces; average thickness of inclined flange in I-section with constant flange thickness at inclined edge throughout girder length

$a_x$ = lever arm at distance x from support or midspan as defined locally in text

$a_{cr}$ = lever arm at critical section location $x_{cr}$

$B$ = $(d_m - d_s)/d_m$

$b$ = width of cross-section; width of compression flange; width of cross-section at any given level

$b_i$ = width of cross-section at level i – i

$b_s$ = width of cross-section at inclined edge of girder

$C$ = compressive force; $C_1$, $C_2$ ... and $C_{10}$ are constants as defined locally in text

viii

$c$ = width of the overhanging portion of the inclined flange; distance form point of application of load to centre of twist (shear centre) ; $c_1$ , $c_2$ ... and $c_5$ are constants as defined locally in text

$d$ = effective depth of girder in general, i.e., the distance from extreme compressive fibre to centroid of bottom prestressing force

$d_{cr}$ = effective depth at critical section distance $x_{cr}$

$d_m$ = effective depth of girder at midspan

$d_s$ = effective depth of girder at support

$d_x$ = effective depth at distance $x$ from the support or midspan as defined locally in text

$E$ = modulus of elasticity

$E_c$ = modulus of elasticity for concrete

$E_{co}$ = short-term loading modulus of elasticity for concrete

$E_{cf}$ = fictitious modulus of elasticity for concrete

$E_{ef}$ = effective fictitious modulus of elasticity for concrete (modulus of deformation)

$E_s$ = modulus of elasticity for steel

$e$ = eccentricity in general

$e_c$ = eccentricity of unit load relative to c.g. of concrete part

$e_s$ = eccentricity of unit load relative to c.g. of steel part

$F_t$ = vertical tensile force at crown of girder (tearing force)

$f$ = stress in general

$f_c$ = stress in concrete; flexural stress acting on section at any given level; stress in concrete fibre adjacent to steel centroid at any given time $t$ after creep has taken place

ix

$f_{co}$ = initial stress in concrete fibre adjacent to the centroid of steel at beginning of creep in concrete

$\Delta f_{co}$ = loss in concrete stress = $f_{co} - f_c$

$f_{cb}$ = stress at extreme bottom concrete fibre

$f_{cbot}$ = stress at extreme bottom concrete fibre

$f_{ct}$ = stress at extreme top concrete fibre

$f_{ctop}$ = stress at extreme top concrete fibre

$f_{cmax}$ = maximum stress in concrete along the girder

$f'_c$ = cylinder crushing strength for concrete at 28 days of age under standard curing (design strength)

$f_{cs}$ = stress in concrete at inclined edge of girder

$f_e$ = stress in equivalent section at level of steel centroid

$\overline{f}_c$ = stress in concrete due to unit load in unbonded composite section

$f_s$ = stress in steel

$f_{s1}$ = stress in bottom layer of prestressing steel tendon

$f_{s2}$ = stress in top layer of prestressing steel or stress in a non-tensioned conventional steel layer replacing top layer of prestressing steel

$f_{so1}$ = initial prestressing stress in bottom layer of prestressing steel

$f_{so2}$ = initial prestressing stress in top layer of prestressing steel

$f_{su}$ = stress in prestressing steel at ultimate load
= $f'_s(1 - 0.5 f'_c / f'_s)$

$f'_s$ = ultimate strength of prestressing steel

$\overline{f}_s$ = stress in steel due to unit load in unbonded composite section

$G$ = modulus of rigidity, modulus of elasticity in shear
= $E/2(1 + \nu)$

x

$h_b$ = distance of centroid of bottom prestressing force to extreme bottom concrete fibre

$h_t$ = distance of centroid of top prestressing force to extreme top concrete fibre

$h_{cr}$ = height of girder at critical section location $x_{cr}$

$h_m$ = height of girder at midspan

$h_s$ = height of girder at support

$h_x$ = height of girder at distance $x$ from support or midspan as locally defined in text

$h_\zeta$ = height of girder at dimensionless distance $\zeta$ from midspan

$h_{ft}$ = distance of shear centre to centroid of top flange

$h_{fb}$ = distance of shear centre to centroid of bottom flange

$I$ = moment of inertia of cross-section in general

$I_e$ = moment of inertia of effective cross-section

$I_y$ = moment of inertia of section about vertical axis $y - y$

$I_{yfb}$ = moment of inertia of bottom flange about vertical axis $y - y$

$I_{yft}$ = moment of inertia of top flange about vertical axis $y - y$

$I_{yf}$ = $(2 I_{yft} I_{yfb})/(I_{yft} + I_{yfb})$

$I_\zeta$ = moment of inertia of cross-section at dimensionless distance $\zeta$ from midspan

$I_{const,c}$ = construction moment of inertia relative to $E_c$ = $I_c + n I_s$ , see also below

$I_{const,s}$ = $I_s + I_c/n$ , construction moment of inertia of unbonded composite section relative to $E_s$. $I_c$ and $I_s$ are moment of inertia of concrete and steel parts respectively

$J$ = St. Venant's torsional resistance constant of section, comparable to polar moment of inertia of a circular solid shaft

xi

$K$ = constant; $K_1$, $K_2$, $K_3$ and $K_4$ are constants as defined locally in text

$k_o$ = constant as defined locally in text

$k$ = $(1/3 - 2t\eta/h)$, see Appendix, Section A.2

$L$ = length of girder, distance between centre lines of supports

$M$ = bending moment in general

$M_a$ = applied bending moment

$M_{co}$ = applied bending moment within concrete part in unbonded composite section ($M_{co}$ to be carried by both concrete and steel parts according to their relative stiffnesses)

$M_c$ = applied moment carried by concrete part of an unbonded composite section

$M_{max}$ = maximum applied moment at midspan

$M_r$ = resisting moment capacity, carrying moment capacity

$M_p$ = bending moment due to prestressing force

$M_{ip}$ = induced bending moment due to prestressing force

$M_t$ = internal resisting torsional moment, resisting torque

$N$ = applied normal force on section

$N_p$ = applied prestressing force on section

$N_{ip}$ = induced normal force due to prestressing force

$n$ = modular ratio, $n = E_s / E_c$

$P_1$ = total initial prestressing force in bottom layer of prestressing steel ($P_1 = A_{s1} f_{so1}$)

$P_2$ = total initial prestressing force in top layer of prestressing steel ($P_2 = A_{s2} f_{so2}$)

$p$  $=$  percentage of bottom layer of prestressing steel

$= A_{sl}/(b \, d_{cr})$

$p_{cr}$  $=$  uniformly distributed critical load in lateral instability

$Q$  $=$  first moment of area, static moment

$Q_i$  $=$  first moment of area, $A_i$, about the centroid of section

$S$  $=$  distance between point of intersection of top edge with bottom edge of an inclined girder and the section under consideration

$S_t$  $=$  principal tensile stress

$S_c$  $=$  principal compressive stress

$T$  $=$  total tensile force in bottom layer of prestressing steel

$t$  $=$  time in hours;  thickness of rectangle (see Appendix, Section A.2

$t_{max}$  $=$  maximum thickness of rectangle

$V$  $=$  shear force on a section;  volume under deflected membrane

$V_a$  $=$  applied shear force on section

$V_{ia}$  $=$  induced shear force due to applied shear force

$V_{ip}$  $=$  induced shear force due to prestressing force

$V_r$  $=$  reduced shear force accounting for the inclination of girder

$v$  $=$  shear stress at any given level

$x$  $=$  distance of any arbitrary section from support or midspan as locally defined in text

$x_{cr}$  $=$  distance of critical section from support or midspan as defined locally in text

$x_{comp}$  $=$  location of maximum compressive stress at top concrete fibre from support

$x_{ten}$ = location of the maximum tensile stress (minimum compressive) at bottom concrete fibre from support

$x_{st1}$ = location of the maximum stress in the bottom layer of prestressing steel from support

$x_{st2}$ = location of the minimum stress in top layer of prestressing steel from support; location of maximum stress in top layer of conventional steel from support

$y$ = distance of centroid of section from soffit of girder

$y_{cr}$ = position of maximum principal tensile stress relative to soffit of girder at critical section

$y_s$ = distance of inclined edge to the c.g. of the section; distance between the c.g. of concrete and c.g. of steel

$y_e$ = distance between the c.g. of effective section and the c.g. of bottom layer of steel

$y_{\xi 1}$ = distance between gross c.g. of the section and centroid of bottom layer of prestressing steel

$y_{\xi 2}$ = distance between gross c.g. of the section and centroid of top layer of steel

$Z$ = modulus of section in general

$Z_{\xi}$ = modulus of section at distance $\xi$ from midspan

$z$ = distance between centroids of flanges in an I-section

## Greek Letters

$\alpha$ = angle between inclined and horizontal edges of a girder

$\alpha_o$ = stiffness coefficient of reinforcements in a section, i.e., contribution of reinforcements in supporting applied loads

$\beta$ = $(h_m - h_s)/h_m$ ; angle between horizontal axis and c.g. of an inclined girder

$\beta_p$ = concrete prism strength after 28 days of standard curing in general

$\beta_{p90}$ = concrete prism strength after 90 days of standard curing

$\gamma$ = $d_m / d_s$ ; angle between direction of principal tensile stress and horizontal axis

$\gamma_{cr}$ = angle between direction of maximum principal tensile stress and horizontal axis at critical section

$\delta$ = coefficient accounting for position of point of application of load in lateral instability

$\varepsilon$ = strain in general

$\varepsilon_c$ = strain in concrete, strain in concrete at any given time

$\varepsilon_{cel}$ = elastic strain in concrete

$\varepsilon_{cpl}$ = plastic strain due to creep in concrete under sustained loading

$\varepsilon_{ct}$ = total strain in concrete at any given time, t , after sustained loading becomes operative

$\bar{\varepsilon}_{co}$ = strain in concrete in unbonded composite section

$\bar{\varepsilon}_{com}$ = strain in concrete due to moment $M_c$ at eccentricity $e_c$ from centroid of concrete part in an unbonded composite section

$\varepsilon_e$ = strain in an equivalent section

xv

$\varepsilon_{s,t}$ = strain in concrete due to shrinkage at any given time $t$

$\varepsilon_{st}$ = strain in steel

$\varepsilon_{s\infty}$ = final shrinkage strain in concrete ($t = \infty$)

$\bar{\varepsilon}_{sto}$ = strain in steel at a common level of steel and concrete in an unbonded composite section

$\zeta$ = coefficient accounting for inherent stiffness of the flanges in an I-section girder

$\zeta_{cr}$ = $y_{cr} / h_{cr}$

$\eta$ = coefficient accounting for volume reduction in deflected membrane at the corners of a rectangular section

$\theta$ = angle between direction of total compression, C , and bottom edge of an inclined girder: angle of twist in radian per unit length

$\lambda$ = constant depending on concrete quality and ambient conditions

$\nu$ = Poisson's ratio

$\xi$ = $2x/L$ , dimensionless distance from midspan or support as defined locally in text

$\xi_{cr}$ = $2x_{cr} / L$ , dimensionless distance of the critical section from support or midspan as defined locally in text

$\frac{1}{2}\xi$ = $x/L$ from support

$\frac{1}{2}\xi_{cr}$ = $x_{cr} / L$ from support

$\xi_{comp}$ = dimensionless location of maximum compressive stress at top concrete fibre from midspan

$\xi_{ten}$ = dimensionless location of the maximum tensile stress (minimum compressive) at bottom concrete fibre from midspan

$\xi_{stl}$ = dimensionless location of the maximum stress in the bottom layer of prestressing steel from midspan

$\zeta_{st2}$ = dimensionless location of the minimum stress in top layer of prestressing steel from midspan; dimensionless location of maximum stress in top layer of conventional steel from midspan

$\sigma$ = standard deviation; $\sigma_1$ , $\sigma_2$ , $\sigma_3$ , $\sigma_4$ and $\sigma_5$ standard deviation for constants $c_1$ , $c_2$ , $c_3$ , $c_4$ and $c_5$ respectively

$\phi$ = creep factor in general

$\phi_t$ = creep factor at any given time $t$ after the sustained load becomes operative

$\phi_\infty$ = final creep factor ($t = \infty$)

$\psi$ = coefficient accounting for effects of reinforcement in section on concrete fictitious modulus of elasticity

$\Delta f_{co}$ = loss in concrete stress = $f_{co} - f_c$

# ARRANGEMENT OF FIGURES

# ARRANGEMENT OF FIGURES
## (Continued)

xix

# INTRODUCTION

Roof trusses are mainly used to dispense with interior columns in buildings such as industrial assembly halls, indoor industrial plants, gymnasiums, and theaters etc., where the presence of such columns are not desired. Prestressed concrete girders with inclined flanges can often be substituted for these roof trusses, since such girders can support large spans. In particular, pretensioned roof girders with straight tendons and inclined flanges offer the following advantages:

1- They provide adequate slope to ease water drainage.

2- Water proofing material in roof construction is reduced.

3- Snow loads are reduced if the angle of inclination is greater than the angle of repose of the snow.

4- Their capacity to resist bending moment is large in the region of high moment. This reduces the amount of prestressing steel.

5- The inclination of the flange affects a reduction in the shear forces.

6- Their self-weight is less than that of parallel flanged girders of the same bending capacity, thus, less transportation costs.

7- The use of straight tendons will save considerable amount of work in production, (e.g., by using Hoyer's method).

-1-

8- The bonding of the tendons saves end anchors.

9- Deflections are reduced due to large moment of inertia, and particularly in the region of midspan.

10- By their use, requirements for the provision of false ceiling etc., are not difficult when these are envisaged in advance.

However, in addition to the inherent disadvantages of prestressed concrete in general, the inclined roof girders have the following additional disadvantages:

1- If the girders are to be prefabricated, the maximum span of such girders is limited to approximately 100 ft., because of difficulties in transportation and erection.

2- For heavily loaded short span girders having a large depth at the supports and large flange inclination, the resisting capacity against shear force is not large and is somewhat comparable to those of ordinary reinforced concrete when the amount of prestressing steel area is based on the flexural requirements, i.e., the favourable effect of the prestressing force on reducing the principal tensile stress is not significant.

3- The design of such girder with utility openings is quite involved and presents difficulties to the design engineer.

The theoretical analysis of uniformly loaded inclined pretensioned roof girders with straight tendons include:

1. Critical Sections for Flexure

Critical sections for flexure are categorized into two loading cases:

Working Loads

The following critical sections for flexure under service loads are established:

1- A formula derived from the geometrical relationship which predict the approximate location of the critical section.

2- Critical section for bottom fibre of the concrete.

3- Critical section for top fibre of the concrete.

4- Critical section for the bottom layer of the pre-stressing steel.

5- Critical section for the top layer of the prestressing steel.

The first of the above five critical sections is derived from geometrical relationship, while the last four critical sections are established in two ways: the first from the differentiation of the stress formulae of a girder having rect-angular cross-section without considering shrinkage and creep deformations, the second from a general computer programme considering all the pertinent parameters that enter in the

-3-

analysis and design of prestressed concrete structures.

### Ultimate Loads

Here, the critical section is found from geometrical con-
siderations only. Such formula is more relevant to predict
the critical section since the assumptions in the derivation
are based on Whitney's simplified assumption of the stress
block diagram.

2. ## Critical Sections for Principal Tensile Stresses

For reasons which will be explained later, the critical
sections for the principal tensile stresses are considered only
for uncracked sections; these are also categorized into two
loading cases:

### Working Loads

This loading case can become an important criterion when
cracks are not desirable in an environment detrimental to
the prestressing steel tendons. This is further sub-divided
into two cases:

1- Critical section considering maximum effects of creep
and shrinkage.

2- Critical section considering minimum effects of creep
and shrinkage.

### Ultimate Loads

Ultimate load consideration is a criterion here because of

-4-

safety reasons. Critical sections are subdivided into
two cases:

1- Critical section taking into account maximum effects
   of creep and shrinkage. It should be noted that this
   case is the most important case of all, since it yields
   the largest principal tensile stress and normally it
   is sufficient for design purposes.

2- Critical section considering minimum effects of creep
   and shrinkage.

As long as a concrete section remains uncracked, the shear
and normal stresses combine to produce principal compressive
and tensile stresses, the latter being of utmost importance
in prestressed concrete structures. However, in roof
trusses, the tensile flexural stresses occur in sections
away from the support where the shear stresses are usually
not too large. In these sections, the principal tensile
stresses reflect predominantly the effects of the tensile
flexural stresses. To show the effects of shear stresses
in producing principal tensile stresses, at these sections,
it is assumed that the tensile flexural stresses are
relieved from the concrete and resisted solely by an
adequate steel reinforcement. If such reinforcement is
provided in the inclined roof girders, then it is appro-
priate to substitute zero for the tensile flexural stresses
in the elastic equation which combines the shear stress

-5-

and the flexural stress.

With this concept in mind, the procedure for finding the locations of the critical sections for principal tensile stresses is the same as in the foregoing cases.

3. Upward Tearing Force at the Crown of the Girder

This upward tearing force is caused by the discontinuity of the inclinations of the girder at the crown point, thus inducing some tensile force to be resisted by the web or an adequate steel reinforcement.

4. Lateral Instability of the Girder

The problem of lateral instability arises only when the roof girders are not stiffened laterally. However, under sustaining loads, the critical loads are reduced because of creep phenomena of concrete. Such critical loads may well be the criterion in the design of the inclined roof girders in some cases.

5. Shipping and Erection

Prefabricated roof girders should be shipped and erected with great care and in such a manner that nowhere in the girder will the concrete crack and crush due to excessive temporary stresses and with steel reaching its yield point which will incur losses in its prestressing forces. Thus,

-6-

the shipping and erection procedures should be carried out in
a fashion which will ascertain that the temporary stresses do
not exceed their limits.

1. <u>Critical Sections for Flexure</u>

1.1 <u>Working Loads</u>

The location of the critical sections for flexure under
service loads is derived from the following considerations:

1.1.1 <u>Geometrical Considerations</u>

The assumptions made in the derivation are:

1- The girder is carrying a uniformly distributed load,
i.e., the moment diagram has a parabolic shape.

2- The lever arm of the resisting moment capacity at any
section is proportional to the effective depth at that
section. This assumption utilizes the Whitney's
stress block diagram which is more justified under
the ultimate loads.

3- The bottom layer of the prestressing steel has a con-
stant cross-sectional area throughout the girder.

4- The stress in the bottom layer of the prestressing
steel is the same throughout the girder when the bending
moment carrying capacity becomes fully developed.

The critical section is established from the fact that
the applied moment and the resisting moment diagrams are
equal in magnitude and have a common tangent at that section.

From the geometry of the girder (see Fig. 2) it can

be readily shown that the inclination

$$\tan \alpha = \frac{d_m - d_s}{L/2} = (d_m - d_s)\,2/L \qquad (1a)$$

and

$$d_m = d_s + \frac{L}{2}\tan \alpha \qquad (1b)$$

where

$\alpha$ = the angle of inclination of the girder

$L$ = the length of the girder

$d_s$ = the effective depth of the girder at the support

$d_m$ = the effective depth of the girder at the midspan

Thus, the effective depth at a distance x from the support is:

$$d_x = d_s + (d_m - d_s)\,2x/L \qquad (2a)$$

or

$$d_x = d_s + x \tan \alpha \qquad (2b)$$

Furthermore, from the assumption made before, the lever arm of the resisting bending moment at a distance  x  from the support is:

$$a_x = K\,d_x \qquad (3a)$$

where  K  is a constant. Then from Eqs. (2b) and (3a),

$$a_x = K\,(d_s + x \tan \alpha ) \qquad (3b)$$

-9-

The resisting moment capacity, $M_r$, at a distance x from the support is

$$M_r = f_s A_s a_x \tag{4a}$$

where

$f_s$ = the stress in the prestressing steel

$A_s$ = the area of the prestressing steel

From Eqs. (3b) and (4a)

$$M_r = f_s A_s K (d_s + x \tan \alpha) \tag{4b}$$

It is evident from the assumptions made before that $f_s A_s K$ is a constant quantity. Denoting that quantity by C

$$M_r = C (d_s + x \tan \alpha) \tag{4c}$$

The applied moment, $M_a$, at a distance x from the support

$$M_a = M_{max} (4x/L - 4x^2/L^2) \tag{5a}$$

where $M_{max}$ is the maximum applied moment at midspan.

At the critical section, a distance $x_{cr}$ from the support, the applied moment is equal to the resisting moment capacity, or

$$M_a = M_r \tag{6a}$$

Thus from Eqs. (5a) and (4c)

$$M_{max} (4x_{cr}/L - 4x^2_{cr}/L^2) = C (d_s + x_{cr} \tan \alpha) \tag{6b}$$

-10-

or

$$M_{max} = \frac{C\,(d_s + x_{cr}\,\tan\alpha)}{(4x_{cr}/L - 4x_{cr}^2/L^2)} \tag{6c}$$

The tangents of the applied and the resisting moments curves at a distance, $x$ , from the support are obtained by differentiating Eqs. (5a) and (4c) with respect to $x$ . Thus

$$\frac{dM_a}{dx} = (4/L - 8x/L^2)\,M_{max} \tag{7a}$$

$$\frac{dM_r}{dx} = C\,\tan\alpha \tag{7b}$$

The applied and the resisting moment diagrams have the same tangent at $x = x_{cr}$

Hence from Eqs. (7a), (7b), and (6c),

$$C\,\tan\alpha = (4/L - 8x_{cr}/L^2)\,C\,\frac{(d_s + x_{cr}\,\tan\alpha)}{(4x_{cr}/L - 4x_{cr}^2/L^2)} \tag{8a}$$

or

$$\frac{\tan\alpha}{L}\,x_{cr}^2 + \frac{2d_s}{L}\,x_{cr} - d_s = 0 \tag{8b}$$

The applicable root of the Eq. (8b) is:

$$x_{cr} = \sqrt{\frac{d_s}{\tan\alpha}\left(\frac{d_s}{\tan\alpha} + L\right)} - \frac{d_s}{\tan\alpha} \tag{9a}$$

for $\tan\alpha \neq 0$

-11-

The foregoing equation gives directly the distance of
the critical section from the support.

However, it is often desirable to express the location of
the critical section in dimentionless form. Substituting
Eq. (1a) into Eq. (9a) and denoting $2x_{cr}/L = \xi_{cr}$

$$x_{cr} = \sqrt{\frac{L^2}{4}(\frac{d_s}{d_m - d_s})(\frac{d_s}{d_m - d_s} + 2)} - \frac{L}{2}\frac{d_s}{d_m - d_s}$$

$$\frac{x_{cr}}{L/2} = \xi_{cr} = \sqrt{(\frac{d_s}{d_m - d_s})(\frac{d_s}{d_m - d_s} + 2)} - \frac{d_s}{d_m - d_s} \tag{10a}$$

putting

$$\gamma = \frac{d_m}{d_s} \tag{11a}$$

Equation (10a) is reduced to

$$\xi_{cr} = \frac{1}{\gamma - 1}(\sqrt{2\gamma - 1} - 1) \tag{12a}$$

Furthermore, denoting

$$B = \frac{d_m - d_s}{d_m} \tag{13a}$$

Equation (10a) takes the following form

$$\xi_{cr} = \frac{1}{B}(\sqrt{1 - B^2} - 1 + B) \tag{14a}$$

From Eq. (12a) or (14a), the location of the critical section
is given as:

$$x_{cr} = 0.5\,\xi_{cr}\,L \tag{15a}$$

-12-

## 1.1.2 Derivation by the Calculus

Critical sections are found by differentiating the stresses
with respect to the distance of the sections from the sup-
port, thus, establishing the locations of the maxima and
minima of the stresses in the girder. The stress locations
which are of interest to a designer are the location of
the maximum compressive stress at the top fibre, location
of maximum tensile stress at the bottom fibre and locations
of maximum stresses in the top and bottom layers of prestress-
ing steel. The practicality of this approach is very limited
owing to the complexity of the procedure. This is due to
the number of parameters to be included such as variable
moment of inertia of the cross-sections, creep and shrinkage
deformations. However, excluding creep and shrinkage defor-
mations and confining the cross-sections to rectangular
sections only, four formulae are derived to predict the
critical sections in the inclined roof girders under working
loads. These are:

    1- flexural critical section for bottom concrete fibre

    2- flexural critical section for top concrete fibre

    3- critical section for bottom prestressing steel layer

    4- critical section for top prestressing steel layer

In deriving the foregoing formulae the following assumptions
are made:

    1- The girders are sustaining uniformly distributed loads,

        i.e., the bending moment diagram has a parabolic shape.

-13-

2- The concrete behaves as an elastic material and remains uncracked.

3- The gross cross-section of the rectangular is used to determine the section properties, i.e., the centroid of the section lies at the middle of the section under consideration.

Taking the origin at midspan, see Fig. 3, and defining

$$\xi = 2x/L \tag{16a}$$

$$\beta = (h_m - h_s)/h_m \tag{16b}$$

$$\tan \alpha = (h_m - h_s)\, 2/L \tag{16c}$$

Further, adopting the following notations:

$b$ = the width of the rectangular cross-section

$h_s$ = the height of the girder at the support

$h_m$ = the height of the girder at the midspan

$h_\xi$ = the height of the girder at the distance $\xi$ from the midspan

$A_\xi$ = the area of the cross-section at the distance $\xi$ from the midspan

$Z_\xi$ = the top and bottom section modulus of the section at $\xi$ from the midspan

$I_\xi$ = the moment of inertia of the cross-section at $\xi$ distance from the midspan

$A_{sl}$ = cross-sectional area of the bottom layer of the prestressing steel

-14-

$A_{s2}$ = cross-sectional area of the top layer of the prestressing steel

$f_{so1}$ = initial prestressing stress in the bottom layer of the prestressing steel (prestressing bed stress)

$f_{so2}$ = initial prestressing stress in the top layer of the prestressing steel (prestressing bed stress)

$P_1$ = the total initial prestressing force in the bottom layer of the prestressing steel ($P_1 = A_{s1} f_{so1}$)

$P_2$ = the total initial prestressing force in the top layer of the prestressing steel ($P_2 = A_{s2} f_{so2}$)

$h_b$ = the distance of the centroid of the bottom prestressing force to the concrete bottom fibre

$h_t$ = the distance of the centroid of the top prestressing force to the concrete top fibre

$M_{max}$ = the maximum bending moment at midspan due to the applied loads

$M_\zeta$ = the bending moment at distance $\zeta$ from midspan

$E_s$ = the modulus of elasticity of the prestressing steel

$E_c$ = the modulus of elasticity of the concrete

$n$ = the modular ratio of the prestressing steel to the concrete ($n = E_s/E_c$)

$\zeta_{comp}$ = the distance of the maximum compressive stress at the top concrete fibre from midspan (dimensionless)

$\xi_{ten}$ = the distance of the maximum tensile stress at the bottom concrete fibre from midspan (dimensionless)

$\xi_{stl}$ = the distance of the maximum stress in the bottom layer of the prestressing steel from midspan (dimensionless)

$\xi_{st2}$ = the distance of the minimum stress in the top layer of the prestressing steel from midspan (dimensionless)

Then from the geometry of the girder it can be readily shown that:

$$h_\xi = h_m (1 - \beta\xi) \tag{17a}$$

$$A_\xi = b\, h_\xi \tag{17b}$$

$$Z_\xi = b\, h_\xi^2 / 6 \tag{17c}$$

$$I_\xi = b\, h_\xi^3 / 12 \tag{17d}$$

$$M_\xi = M_{max} (1 - \xi^2) \tag{17e}$$

## 1- Critical Section for Top Compressive Concrete Fibre

The stress at the extreme top concrete fibre, $f_{ctop}$ , at any section $\xi$ :

$$f_{ctop} = - \left[ \frac{M_\xi}{Z_\xi} + \frac{P_1 + P_2}{A_\xi} - \frac{1}{Z_\xi}\left[ P_1\left(\frac{h_\xi}{2} - h_b\right) - P_2\left(\frac{h_\xi}{2} - h_t\right)\right]\right] \tag{18a}$$

-16-

Substituting equations (17a), (17b), (17c), (17d) and (17e) into Eq. (18a) and rearranging result in:

$$f_{ctop} = - \frac{2}{bh_m^2(1-\beta\xi)^2} \left[ 3M_{max}(1-\xi^2)-h_m(P_1-2P_2)(1-\beta\xi) + 3P_1h_b - 3P_2h_t \right] \qquad (18b)$$

The location of maximum value of the compressive stress at top concrete fibre along the girder is obtained by differentiating $f_{ctop}$ with respect to $\xi$ and equating the derivative to zero, i.e.

$$\frac{df_{ctop}}{d\xi} = 0$$

thus:

$$\left[ 6M_{max} - \beta^2 h_m(P_1 - 2P_2) \right] \xi + \beta h_m(P_1 - 2P_2) - 6\beta(M_{max} + P_1h_b - P_2h_t) = 0 \qquad (19a)$$

Denoting the location of maximum $f_{ctop}$ along the girder by $\xi_{comp}$ and rearranging the Eq. (19a)

$$\xi_{comp} = \frac{\beta\left[6M_{max} + 6P_1h_b - 6P_2h_t - h_m(P_1-2P_2)\right]}{6M_{max} - \beta^2 h_m(P_1-2P_2)} \qquad (20a)$$

When the top layer of the prestressing steel is omitted, the above equation reduces to:

$$\xi_{comp} = \frac{\beta\left[6M_{max} + 6P_1h_b - h_m P_1\right]}{6M_{max} - \beta^2 h_m P_1} \qquad (20b)$$

-17-

The distance of the maximum compressive stress at concrete top fibre from the support being:

$$x_{comp} = 0.5 (1 - \xi_{comp}) L \qquad (20c)$$

### 2- Critical Section for Bottom Tensile Concrete Fibre

The stress at the extreme bottom concrete fibre, $f_{cbot}$, at any given section is:

$$f_{cbot} = \frac{M_\xi}{Z_\xi} - \frac{P_1+P_2}{A_\xi} - \left[ P_1(\frac{h_\xi}{2} - h_b) - P_2(\frac{h_\xi}{2} - h_t) \right] \frac{1}{Z_\xi} \qquad (21a)$$

Again substituting Eqs. (17) into Eq. (21a) and rearranging yield:

$$f_{cbot} = \frac{2}{bh_m^2(1-\beta\xi)^2} \left[ 3M_{max}(1-\xi^2) - h_m(2P_1 - P_2)(1-\beta\xi) \right.$$
$$\left. + 3P_1h_b - 3P_2h_t \right] \qquad (21b)$$

The location of maximum value of the tensile stress (or location of minimum compressive stress) at the bottom concrete fibre along the girder is obtained by differentiating $f_{cbot}$ with respect to $\xi$ and equating the derivative to zero, i.e.

$$\frac{df_{cbot}}{d\xi} = 0$$

or

$$\left[ 6M_{max} - \beta^2 h_m(2P_1-P_2) \right] + \beta h_m(2P_1 - P_2)$$
$$- 6\beta(M_{max} + P_1h_b - P_2h_t) = 0 \qquad (22a)$$

-18-

Denoting the location of maximum tensile (or minimum compressive) $f_{cbot}$ along the extreme bottom concrete fibre of the girder by $\zeta_{ten}$ and rearranging Eq. (22a)

$$\zeta_{ten} = \frac{\beta\left[6M_{max} + 6P_1h_b - 6P_2h_t - h_m(2P_1 - P_2)\right]}{6M_{max} - \beta^2 h_m(2P_1 - P_2)} \tag{23a}$$

In the absence of the top layer of prestressing steel, Eq.(23a) reduces to:

$$\zeta_{ten} = \beta\frac{\left[6M_{max} + 6P_1h_b - 2h_mP_1\right]}{6M_{max} - 2\beta^2 h_mP_1} \tag{23b}$$

The critical section distance of the maximum tensile stress at the bottom concrete fibre from the support becomes:

$$x_{ten} = 0.5\,(1 - \zeta_{ten})\,L \tag{23c}$$

3- <u>Critical Section for the Bottom Prestressing Steel Tendons</u>

The stress in the bottom layer of the prestressing steel tendons, $f_{sl}$ , at any section is given as:

$$f_{sl} = f_{sol} - \frac{nf_{sol}A_{sl}}{A_\zeta}\left(1 + \frac{A_\zeta}{I_\zeta}y_{\zeta 1}^2\right)$$

$$- \frac{nf_{so2}A_{s2}}{A_\zeta}\left(1 - \frac{A_\zeta}{I_\zeta}y_{\zeta 1}y_{\zeta 2}\right) + \frac{nM_\zeta}{I_\zeta}y_{\zeta 1} \tag{24a}$$

where

$$f_{sol} = \frac{P_1}{A_{sl}}$$

-19-

$$f_{so2} = \frac{P_2}{A_{s2}}$$

$$y_{\xi 1} = \frac{h_\xi}{2} - h_b$$

$$y_{\xi 2} = \frac{h_\xi}{2} - h_t$$

Substituting the foregoing quantities and Eqs. (17) into Eq. (24a) give:

$$f_{s1} = \frac{P_1}{A_{s1}} - \frac{n(P_1+P_2)}{bh_m(1-\beta\xi)} - \frac{12nP_1}{bh_m^3(1-\beta\xi)^3}\left[\frac{h_m}{2}(1-\beta\xi) - h_b\right]^2$$

$$+ \frac{12nP_2}{bh_m^3(1-\beta\xi)^3}\left[\frac{h_m}{2}(1-\beta\xi) - h_b\right]\left[\frac{h_m}{2}(1-\beta\xi) - h_t\right]$$

$$+ \frac{12nM_{max}(1-\xi^2)}{bh_m^3(1-\beta\xi)^3}\left[\frac{h_m}{2}(1-\beta\xi) - h_b\right] \tag{24b}$$

The location of maximum stress in the bottom layer of the prestressing steel tendons is obtained by differentiating $f_{s1}$ with respect to $\xi$ and equating the derivative to zero, i.e.

$$\frac{df_{s1}}{d\xi} = -\beta h_m^2(2P_1-P_2)(1-\beta\xi)^2$$

$$+ 6\beta h_m\left[h_b(2P_1-P_2) - h_tP_2\right](1-\beta\xi)$$

$$- 18\beta h_b(P_1h_b - P_2h_t)$$

$$+ 6h_mM_{max}(\beta-\xi)(1-\beta\xi)$$

$$+ 6h_bM_{max}(\beta\xi^2+2\xi-3\beta) = 0 \tag{25a}$$

-20-

Now in order to simplify the foregoing equation let:

$$c_1 = \beta h_m^2 (2P_1 - P_2)$$

$$c_2 = 6\beta h_m \left[ h_b (2P_1 - P_2) - h_t P_2 \right]$$

$$c_3 = 18\beta h_b (P_1 h_b - P_2 h_t)$$

$$c_4 = 6h_m M_{max}$$

$$c_5 = 6h_b M_{max}$$

Thus, Eq. (25a) reduces to:

$$\beta (\beta c_1 - c_4 - c_5) \xi^2 - \left[ \beta (2c_1 - c_2) - (1 + \beta^2)c_4 + 2c_5 \right] \xi$$

$$+ \left[ c_1 - c_2 + c_3 - \beta (c_4 - 3c_5) \right] = 0 \qquad (25b)$$

again by letting:

$$K_1 = \frac{\beta (2c_1 - c_2) - (1 + \beta^2)c_4 + 2c_5}{\beta (\beta c_1 - c_4 - c_5)}$$

$$K_2 = \frac{c_1 - c_2 + c_3 - \beta (c_4 - 3c_5)}{\beta (\beta c_1 - c_4 - c_5)}$$

then Eq. (25b) reduces to:

$$\xi^2 - K_1 \xi + K_2 = 0 \qquad (25c)$$

Denoting the location of the maximum stress in the bottom layer of prestressing steel along the girder by $\xi_{stl}$ and taking only

-21-

the non-trivial root of the above equation yield:

$$\zeta_{stl} = \frac{K_1}{2} - \sqrt{\frac{K_1^2}{4} - K_2} \qquad (26a)$$

The distance of the location of the maximum stress in the bottom layer of the prestressing steel from the support becomes:

$$x_{stl} = 0.5 \, (1 - \zeta_{stl}) \, L \qquad (26b)$$

4- <u>Critical Section for the Top Layer of the Prestressing Steel</u>

The stress in the top layer of the prestressing steel tendons, $f_{s2}$ , at any section is given as:

$$f_{s2} = f_{so2} - \frac{nf_{so2}A_{s2}}{A_\zeta} \, (1 + \frac{A_\zeta}{I_\zeta} \, y_{\zeta 2}^2) \; - \frac{nf_{so1}A_{s1}}{A_\zeta} \, (1 - \frac{A_\zeta}{I_\zeta} \, y_{\zeta 2} y_{\zeta 1})$$
$$\div \frac{nM_\zeta}{I_\zeta} \, y_{\zeta 2} \qquad (27a)$$

Substituting for $f_{so1}$ , $f_{so2}$ in terms of $P_1$ , $P_2$ and Eqs. (17) into Eq. (27a):

$$f_{s2} = \frac{P_2}{A_{s2}} - \frac{n(P_1 + P_2)}{bh_m(1 - \beta\zeta)} - \frac{12nP_2}{bh_m^3(1 - \beta\zeta)^3} \left[ \frac{h_m}{2} \, (1 - \beta\zeta) - h_t \right]^2$$

$$+ \frac{12nP_1}{bh_m^3(1 - \beta\zeta)^3} \left[ \frac{h_m}{2} \, (1 - \beta\zeta) - h_b \right] \left[ \frac{h_m}{2} \, (1 - \beta\zeta) - h_t \right]$$

$$- \frac{12nM_{max}(1 - \zeta^2)}{bh_m^3 \, (1 - \beta\zeta)^3} \left[ \frac{h_m}{2} \, (1 - \beta\zeta) - h_t \right] \qquad (27b)$$

-22-

The location of minimum stress in the top layer of the pre-stressing steel tendons (or the location of maximum stress in conventional reinforcement which replaces the top layer of the prestressing steel tendons) is obtained by differentiating $f_{s2}$ with respect to $\zeta$ and equating the derivative to zero, i.e.

$$\frac{df_{s2}}{d\zeta} = -\beta h_m^2(2P_2 - P_1)(1 - \beta\zeta)^2$$

$$+ 6\beta h_m\left[h_t(2P_2 - P_1) - h_b P_1\right](1 - \beta\zeta)$$

$$- 18\beta h_t(P_2 h_t - P_1 h_b)$$

$$- 6h_m M_{max}(\beta - \zeta)(1 - \beta\zeta)$$

$$- 6h_t M_{max}(\beta\zeta^2 + 2\zeta - 3\beta) = 0 \qquad (28a)$$

Again in order to simplify the above equation let:

$$c_6 = \beta h_m^2(2P_2 - P_1)$$

$$c_7 = 6\beta h_m\left[h_t(2P_2 - P_1) - h_b P_1\right]$$

$$c_8 = 18\beta h_t(P_2 h_t - P_1 h_b)$$

$$c_9 = c_5 = 6h_m M_{max}$$

$$c_{10} = 6h_t M_{max}$$

Thus, Eq. (28a) reduces to:

$$\beta(\beta c_6 + c_9 + c_{10})\xi^2 - \left[\beta(2c_6 - c_7) + (1 + \beta^2)c_9 - 2c_{10}\right]$$

$$+ \left[c_6 - c_7 + c_8 + \beta(c_9 - 3c_{10})\right] = 0 \qquad (28b)$$

Letting:

$$K_3 = \frac{\beta(2c_6 - c_7) + (1 + \beta^2)c_9 - 2c_{10}}{\beta(\beta c_6 + c_9 + c_{10})}$$

$$K_4 = \frac{c_6 - c_7 + c_8 + \beta(c_9 - 3c_{10})}{\beta(\beta c_6 + c_9 + c_{10})}$$

leads to:

$$\xi^2 - K_3\xi + K_4 = 0 \qquad (28c)$$

Denoting the location of the minimum stress in the top layer of prestressing steel along the girder by $\xi_{st2}$ and taking only the non-trivial root of the above equation result in:

$$\xi_{st2} = \frac{K_3}{2} - \sqrt{\frac{K_3^2}{4} - K_4} \qquad (29a)$$

The distance of the location of the minimum stress in the top layer of the prestressing steel from the support is then given by:

$$x_{st2} = 0.5(1 - \xi_{st2})L \qquad (29b)$$

-24-

The significance of Eqs. (29a) and (29b) is not in predicting the location of minimum stress in the top prestressing steel layer but rather in predicting the location of maximum stress in non-tensioned steel top layer. In practice, the top prestressing steel layer is often replaced by conventional steel reinforcement.

The foregoing critical section distance, Eqs. (20), (23),(26) and (29) have been computed for girders ranging from 25 ft. to 105 ft. span with various inclinations. For these computations, the prestressing steel areas and the applied bending moments are evaluated according to the section 1.1.2.1 . By following the method described in that section, some degree of consistency in choosing the prestressing steel areas and the applied bending moments is achieved.

### 1.1.2.1 Amount of Prestressing Steel and Carrying Bending Moment Capacity under Working Load

The amount of prestressing steel is determined according to the CPCI (Canadian Prestressed Concrete Institute) prestressed handbook, paragraph 3.5.2, clauses 3.5.2.1, 3.5.2.2 and 3.5.2.3 (normally reinforced members). The bending moment resisting capacity under the working loads is derived from the amount of prestressing multiplied by an assumed lever arm for the rectangular cross-section. Thus, for normally reinforced rectangular section, the amount of prestressing steel, as given by CPCI prestressed handbook, is:

$$p \leqslant \frac{0.3 \ f'_c}{f_{su}} \qquad (30a)$$

where

$p$ = the percentage of bottom layer of prestressing steel

$\quad = A_{sl}/(b \ d_{cr})$

$f_{su}$ = the stress in prestressing steel at ultimate load

$\quad = f'_s \ (1 - 0.5 \ f'_s/f'_c)$

$f'_c$ = the cylinder crushing strength for concrete at 28 days of age under normal curing (design strength)

$f'_s$ = the ultimate strength of prestressing steel

$b$ = the width of the rectangular section (compression flange)

$A_{sl}$ = the cross-sectional area of the bottom prestressing steel layer

-26-

$d_{cr}$ = the distance from the extreme compressive fibre to the centroid of the bottom prestressing force at critical section obtained from Eq. (2), i.e.

$d_{cr} = d_s + x_{cr} \tan \alpha$ , where $x_{cr}$ is evaluated from Eq. (9a)

$a_{cr}$ = the internal moment lever arm at critical section

$\simeq 0.60 \, d_{cr}$ for rectangular cross-section

Thus, the bending moment resisting capacity at working load is given by:

$$M \simeq 0.80 \, A_{s1} \, f_{so1} \, a_{cr} \qquad\qquad (30b)$$

A small amount of prestressing steel $(A_{s2})$, is provided at the top. This is often dictated by the necessity of keeping the extreme top concrete fibres along the girder in compression to prevent the sections from cracking at transfer, shipping and/or erection. The top steel layer could be omitted if desired and its effects can be deleted by letting some of the parameters in the derived formulae equal to zero.

To show the effects of the amount of the prestressing force on variation of the critical section distances, two percentages of the prestressing steel are considered (p $f_{su}/f'_c$ = 0.3 and 0.25). The four critical distances obtained from Eqs. (20), (23), (26) and (29) as well as the one from Eq. (9a) (geometric consideration) are plotted versus the length of the girder on

-27-

the same graph for different inclinations. The ratio of the critical section distances to the length of the girder are also plotted on the same graph.

All computations and plottings were carried out by means of computer programmes, written in Fortran II for an IBM 1620 model 2.

### 1.1.3 Locations of Flexural Critical Sections by means of a General Computer Programme

A general computer programme was written in Fortran IV for an IBM model 40 to evaluate maximum normal stresses (flexural stresses) at top and bottom concrete fibres and top and bottom steel layers along the length of the girder. The solution programme takes into account elastic, creep and shrinkage deformations as well as cater for any arbitrarily shaped cross-section and any inclination. Fig. 4 shows the flow chart of the computer programme. It should be noted that the same approach employed in the section 1.1.2.1 regarding the amount of prestressing steels and bending moment resisting capacity under working load is employed in this section too. Results were plotted by an IBM 1620 model 2. The plotted results included the locations of the critical sections for:

1- top concrete fibre, i.e., maximum compressive stress at the extreme top concrete fibre under total working loads accounting for maximum creep and shrinkage

2- bottom concrete fibre, i.e., maximum tensile stress at the extreme bottom concrete fibre under total working loads accounting for maximum creep and shrinkage

3- bottom prestressing steel, i.e., maximum stress in

the bottom prestressing steel tendons under total

working loads accounting for maximum creep and

shrinkage

4- top prestressing steel, i.e., maximum stress in

the top prestressing steel tendons under total

working loads accounting for maximum creep and

shrinkage

5- top concrete fibre, i.e., maximum compressive stress

at the extreme top concrete fibre under total

working loads accounting for minimum creep and

shrinkage

6- bottom concrete fibre, i.e., maximum tensile stress

at the extreme bottom concrete fibre under total

working loads accounting for minimum creep and

shrinkage

7- bottom prestressing steel layer, i.e., maximum

stress in the bottom prestressing steel tendons

under total working loads accounting for minimum

creep and shrinkage

8- top prestressing steel layer, i.e., maximum stress

in the top prestressing steel tendons under total

working loads accounting for minimum creep and

shrinkage

-30-

All the foregoing critical section locations have been computed for girder length ranging from 25 ft. to 105 ft. and inclinations ranging from 0.0 to 0.125. Girders having rectangular, I and T cross-sections have been treated.

## 1.2 Ultimate Loads

Knowledge of the location of the flexural critical section
under ultimate loads is dictated by safety requirements.
An adequate resisting moment capacity under ultimate loads
is of utmost importance because the safety of the girder
depends on such moment. Furthermore, an analysis for
ultimate loads affords an advance warning of the failure.
This warning can be achieved when the girder is normally
reinforced[1] . For normally reinforced girders, an additional
steel strain of 0.5% to the prestretched steel strain
(elastic strain in the bottom layer of the prestressing
steel due to prestressing force and maximum creep and shrink-
age loading cases) is recommended by most codes including
the Canadian code. This state of affairs will lead to
about 5 cracks of 1 mm. width each, in 1 meter length
around the critical section. In this case, the stress in
the bottom layer of the prestressing steel is almost
constant and concrete stress in the compression zone is
non-linear which supports Whitney's assumption of the
stress block diagram. Refering to the assumptions made
in deriving the formulae under section 1.1.1 , it can be
clearly seen that such assumptions are more likely to be
realistic for normally reinforced girders under ultimate
loads. Thus, Eqs. (9a), (12a) and (14a) are adequate for
predicting the flexural critical section under ultimate loads.

-32-

## 2. Location of Critical Sections for Principal Tensile Stress

### 2.1 Uncracked Concrete Sections

Here, the concrete is considered to be elastic, isotropic, and of homogeneous material following Hooke's law (as long as it remains uncracked) and deflections are small. Thus, the equations of elasticity hold good as long as these conditions are satisfied.

Adopting positive sign to denote tensile stresses and negative sign to denote compressive stresses, the principal stresses at any level in a section are then given by:

$$S_t = \frac{f_c}{2} + \sqrt{\frac{f_c^2}{4} + v^2} \qquad\qquad (31a)$$

$$S_c = \frac{f_c}{2} - \sqrt{\frac{f_c^2}{4} + v^2} \qquad\qquad (31b)$$

where

$S_t$ = principal tensile stress acting on the section at the given level

$S_c$ = principal compressive stress acting on the section at the given level

$f_c$ = flexural stress acting on the section at the given level

$v$ = shear stress acting on the section at the given level

-33-

In prestressed concrete members, the compressive principal stress, $S_c$ , is generally less important than the principal tensile stress, $S_t$, because of the inherent characteristics of the concrete of being far better in resisting compressive stresses than tensile stresses. Thus, the discussions here will be limited to principal tensile stresses only.

The direction of the principal tensile stress with the horizontal axis, or the direction of the principal compressive stress with the vertical axis, is determined by:

$$\tan 2\gamma = \frac{2v}{f_c} \tag{31c}$$

Where $\gamma$ is the angle between the direction of the principal tensile stress and the horizontal axis. The direction of the principal tensile stress is modified by the amount of the prestressing force, for example, the direction of the principal tensile stress in a prestressed girder is sloped more steeply than in a non-prestressed girder. However, it should be also noted that the direction of principal tensile stress under working load has a steeper slope with the horizontal axis than the direction of the principal tensile stress under ultimate load. Furthermore, in an inclined girder uniformly loaded, with straight tendons, the direction of the maximum principal tensile stress has a steep slope with the horizontal axis of the girder near the support,

-34-

with such a slope flattening out gradually away from the support. This is due to the fact that the shear stresses become smaller and the flexural stresses larger away from the support.

In the prestressed concrete inclined roof girders with straight tendons, the effects of the moments and normal forces, due to the applied loads and prestressing forces, are to reduce the shear force induced in the section and modify the shear stress distribution accross the section[3].

### 2.1.1 Shear Stress Distribution taking into account the Inclination of the Girder, Moments and Normal Forces

The shear stress at any level on the section, at  x  distance from the support (see fig. 5) is given by:[2]

$$vb_i = \left[ \frac{V + N\tan\beta}{I} - \frac{M}{I^2} \frac{dI}{dx} \right] Q_i - \left[ \frac{N}{A^2} \frac{dA}{dx} - \frac{M}{I} \tan\beta \right] A_i$$

$$(32a)^*$$

where

  $v$ = the shear stress on the section at the level i - i

  $b_i$ = the width of the section at level i - i

  $V$ = the applied shear force on the section

  $N$ = the applied normal force on the section, (pre-stressing force)

  $M$ = the applied moments on the section

---

* This formula was derived for the first time by H. Bay, see Ingenieur-Archiv, April 1936.

$A_i$ = the area of the section comprised between the
horizontal edge and the level i - i

$Q_i$ = the first moment of the area $A_i$ about the centroid
of the section (static moment)

A = the area of the section under consideration

I = the moment of inertia of the section under con-
sideration

$\beta$ = the angle between the horizontal line and c.g. of
the girder, see Fig. 5 for the sign convention

Bonatz[4] has derived the following expression for girders
which do not possess a constant thickness at the inclined
flange (i.e. the thickness of the inclined flange is propor-
tional to the depth of the section under consideration):

$$ vb_i = \frac{Q_i}{I} \left[ V - y_s\, b_s\, f_{cs}\, \tan \alpha \right] - \frac{A_i}{A}\, b_s\, f_{cs}\, \tan \alpha \qquad (32b) $$

where

$\alpha$ = the angle between the horizontal line and the
inclined flange of the girder, see Fig. 5 for
the sign convention

$y_s$ = the distance of the inclined edge (sloped edge)
to the centroid of the section

$b_s$ = the width of the cross-section at the inclined
edge

$f_{cs}$ = the flexural stress at the inclined edge

-36-

For the rectangular section ($b_i = b_s = b$) and Eq. (32b) reduces to:

$$v = \frac{VQ_i}{Ib} - f_{cs}\, y_s\, \tan \alpha\, \frac{Q_i}{I} - f_{cs}\, \tan \alpha\, \frac{A_i}{A} \qquad (32c)$$

It is easily seen that for parallel-flanged girders (i.e., $\tan \alpha = 0$) the above equation takes the usual form:

$$v = \frac{VQ_i}{I\,b} \qquad (32d)$$

Weiss[5] has derived the following solution for girders having a constant thickness at the inclined edge with remaining part of the section being of any arbitrary shape, see Fig. 5,:

$$vb_i = \frac{Q_i}{I}\left[ V - y_s b_s f_{cs} \tan \alpha + a\,c\left[ f_{cs} + \frac{M}{I}(y_s + a)\right]\tan \alpha\right]$$

$$- \frac{A_i}{A}\left( b_s f_{cs} \tan \alpha - \frac{M}{I}\,a\,c\,\tan \alpha \right) \qquad (32e)$$

where

    a = the average thickness of the inclined flange, and

    c = the width of the overhanging portions of the inclined
        flange

It is worthwhile to note that the shear stress on the vertical section to the horizontal axis has the highest magnitude at the extreme top fibre along the inclined edge. However, this does not give rise to any principal tensile

stress when the top flange is in compression. This is
due to the nature of the free boundary condition, where
the flexural stress parallel to the edge is in fact
principal stress.  In the inclined roof girders, the
shear stress distribution on the vertical section to the
horizontal axis is largely concentrated on the upper
side of the centroid of the section.

## 2.1.2 Shear Force Reduction due to the Inclination

As mentioned before, the effects of the inclination is
to reduce the induced shear force acting on the section.
Refering to Fig. 6, one can assume that for small angles
of inclination, the induced flexural stresses meet at
a common point 0.  This state of affairs implies that their
resultant induces no moment about that point.  Taking
moments about  0  and from equilibrium conditions that
the sum of the applied moments and the induced moments
acting on the section is zero, one finds that moments due
to the applied loads are given by:

$$M_a - V_a \; S + V_{ia} \; S = 0 \tag{33a}$$

where

$M_a$ = the moment acting on the section due to the
applied loads

$V_a$ = the shear force acting on the section due to the applied loads

$V_{ia}$ = the induced shear force on the section due to the applied loads

S = the distance of the section under consideration from the point 0

Moments due to the prestressing force are:

$$N_p\, y - M_p - V_{ip}\, S = 0 \qquad\qquad (33b)$$

where

$N_p$ = the applied prestressing force on the section under consideration

$M_p$ = the moment due to the prestressing force

$V_{ip}$ = the induced shear force due to prestressing force

y = the distance of the centroid (c.g.) of the section from the soffit of the girder

Thus, summing up Eqs. (33a) and (33b) and rearranging:

$$(V_{ia} - V_{ip}) + (M_a - M_p)\,\frac{1}{S} - V_a + N_p\,\frac{y}{S} = 0 \qquad (33c)$$

Denoting $(V_{ia} - V_{ip})$ as the reduced shear force, $V_r$ , (see also the force diagram Fig. 6), assuming that the centroid of the section lies at the mid-depth of the section $(y = \frac{h_x}{2})$

-39-

and using the fact that:

$$\tan \alpha = \frac{h_x}{S} \quad ; \quad S = \frac{h_x}{\tan \alpha}$$

where $h_x$ is the total depth of the section under consideration.

Eq. (33c) reduces to:

$$V_r = V_a - (M_a - M_p) \frac{\tan \alpha}{h_x} - \frac{N_p}{2} \tan \alpha \qquad (33d)$$

When the prestressing force is absent or not operative as in the case of the prestressing steel being at yield point, Eq. (33d) reduces to:

$$V_r = V_a - M_a \frac{\tan \alpha}{h_x} \qquad (33e)$$

The shear stress at any level on the section can be derived from:

$$v = \frac{V_r Q_i}{I b_i} \qquad (34a)$$

It is obvious that Eq. (34a) does not give exact shear stress distribution along the vertical section through inclined girders. However, shear stresses determined from Eq. (34a) and substituted in Eq. (31a) will yield principal tensile stresses very close to those determined by means of exact methods.

-40-

Since the principal tensile stress depends on so many parameters, no attempt is made to find a simplified formula for the location of the critical section. Instead the general computer programme, whose flow chart is shown in Fig. 4, is written to evaluate the locations for the maximum principal tensile stresses in the inclined girders for the following loading cases:

## 2.1.3 Working Loads

The establishment of location and magnitude of the maximum principal tensile stress under service load is generally not a criterion for the design except for some special cases, such as in water retaining structures where cracks are not permitted, and also when the structure is in an aggressive environment having detrimental effects on the prestressing steel.

To show the effects of the losses in the prestressing force in the tendons on the locations of the maximum principal tensile stress, both maximum and minimum limits of creep and shrinkage are considered. Furthermore, the two cases where concrete resists or does not resist flexural tensile stress are also treated.

### 2.1.3.1 When Concrete Carries Normal Flexural Tensile Stress

Here, the concrete is considered fully elastic and it resists the tensile stresses within the allowable limits for the

-41-

following cases:

    1- location of maximum principal tensile stress under
       working loads accounting for maximum creep and shrinkage

    2- location of maximum principal tensile stress under
       working loads accounting for minimum creep and shrinkage

### 2.1.3.2 When Concrete does not Carry any Normal Flexural Tensile Stress

As mentioned before, concrete has a low and somewhat unreliable tensile strength. Since in inclined roof girders the normal tensile stresses generally occur where shear stresses have negligible magnitude, it can be assumed that these normal tensile stresses are resisted solely by an adequate horizontally laid steel reinforcement. If such reinforcements are adequately provided, then it is appropriate to substitute zero for the normal tensile stresses in Eq. (31a), i.e., $S_t = v$ in the region where normal tensile stresses occur.

Here again, the two possible limits of the creep and shrinkage are considered:

    1- location of maximum principal tensile stress under
       working loads with maximum creep and shrinkage effects

    2- location of maximum principal tensile stress under
       working loads with the minimum creep and shrinkage
       effects

-42-

## 2.1.4  Ultimate Loads

For safety reasons, an adequate resisting capacity of the girders against principal tensile stresses under ultimate loads is essential.  Thus, many codes including the Canadian code, specify that the ultimate load calculated with maximum possible loss of prestressing force is to be the only requirement for the principal tensile stress criterion in design. Thus, the requirement is to check whether the magnitude of the maximum principal tensile stress in the girder exceeds the allowable value.  If it does, the concrete is assumed to be cracked and will not follow the elasticity equation any more.  However, if the maximum principal tensile stress does not exceed the allowable concrete tensile strength, then the concrete is assumed to remain uncracked and this would require only nominal amount of reinforcement against shear.

Proceeding in the same as in section  2.1.3, this is also categorized into two cases:


## 2.1.4.1  When Concrete Resists Normal Flexural Tensile Stress

Here, the location of the maximum principal tensile stress along the girder, in a similar manner described in section 2.1.3.1, is predicted for the following cases:

1- location of maximum principal tensile stress under
   ultimate loads with maximum creep and shrinkage effects

-43-

2- location of maximum principal tensile stress under

ultimate loads with minimum creep and shrinkage effects

### 2.1.4.2 When Concrete does not Resist any Normal Flexural Tensile Stress

Again, the location of the maximum principal tensile stress

along the girder, in a similar manner described in section

2.1.3.2 , is predicted for the following cases:

1- location of maximum principal tensile stress under

ultimate loads with maximum creep and shrinkage effects

2- location of maximum principal tensile stress under

ultimate loads with minimum creep and shrinkage effects

-44-

## 2.2  Cracked Concrete Sections

In general, cracks develop in prestressed concrete under
ultimate loads.  In cracked concrete sections, drastic
changes in stress distribution take place and the sections
are reduced to merely ordinary reinforced sections with a
uniform shear stress across the cracked parts.  Furthermore,
the magnitude of the shear stress becomes a design criterion
instead of the principal tensile stress.  The shear force
acting on the section can be determined from either Eq. (33d)
or Eq. (33e) whichever is relevant.  Canadian code[1] requires
provision for shear reinforcement only for the shear force
in excess of the cracking shear.  Thus, the shear force
on the section is resisted by two components, first the
shear resistance of the concrete, which is calculated from
some arbitrary formulae based on experiments, and the
remaining shear resisted by steel reinforcement which is
calculated in the same manner as in ordinary reinforced
concrete.

A formula to predict in what portion of the girder the
principal tensile stress becomes larger than the allowable
tensile stress is indeed difficult to formulate because
so many parameters are involved.  For example, the effects
of creep and shrinkage will tend to increase the principal
tensile stress and enlarge the range where the principal
tensile stress exceeds the allowable tensile stress.  It

-45-

is evident from the foregoing discussions that there is
no question of a critical section for principal tensile
stress but a region where such stresses are larger than
the allowable concrete tensile stress. Thus, the question
of the boundaries of such region arises together with the
magnitude of the shear to be resisted by each of the concrete
and steel reinforcements individually at each section
within such region. No attempt has been made here to
investigate such regions. This can be best done by means
of a computer programme considering all the parameters
and possibilities involved.

## 3. Upward Tensile Tearing Force at Crown

The discontinuity of the inclinations of the inclined roof girder will introduce an upward force which tends to tear the girder through the web in a horizontal plane. For girders having the same inclination on both the left and right sides and the crown lies at the midspan of the girder, this upward force is derived as follows:

Refering to Fig. 7, the total compression, C , at any section is given as:

$$C = \sqrt{T^2 + V_r^2} \tag{35a}$$

where

    T = total tension in the prestressing steel

    $V_r$ = reduced shear force as determined by Eq. (33d)

The direction of the total compression, C , is:

$$\tan \theta = \frac{V_r}{T} \tag{36a}$$

where

    $\theta$ = the angle between the direction of total compression,

        C , and bottom edge of the girder ( $\sphericalangle \theta < \sphericalangle \alpha$ )

It can be readily shown that no shear force could exist in a section through the axis of the symmetry of a structure loaded in a symmetrical manner; however, for the girder under

-47-

consideration, one finds that any section cut, is acted upon by two equal shear forces but opposite in sign. The magnitude of these shear forces are given by Eq. (33d). However, because of the symmetry, such a state of affairs cannot exist at the crown. Instead both shear forces at the left and right hand sides are giving rise to a tensile force at the crown. This tensile force is in fact induced by the sudden change in the direction of the total compression acting on the section through the crown. The tensile force, $F_t$, is acting vertically, its magnitude is given by:

$$F_t = 2 V_r, \text{ at midspan}$$

$$= -2(M_a - M_p) \frac{\tan \alpha}{h_m} - N_p \tan \alpha \qquad (37a)$$

where $M_a$, $M_p$, $N_p$ and $h_m$ are values at midspan of the girder. See section 2.1.2 for their definitions.

Again, refering to Fig. 7, the tensile force, $F_t$, can be approximated, on the conservative side, as follows:

$$F_t \approx 2 C \sin \alpha \qquad (38a)$$

where

$$C \approx T \approx N_p = A_{sl} f_{sl}$$

Thus, Eq. (38a) reduces to:

$$F_t \approx 2 A_{sl} f_{sl} \sin \alpha \qquad (38b)$$

-48-

## 4. Lateral Instability of Inclined Roof Girders

In laterally unstiffened roof girders, lateral instability may be a criterion in the design of such girders. It is not intended here to derive such formulae for inclined roof girders; however, considering the most common case, the parallel-flanged I-section girder supported in fork type bearing, the critical uniformly distributed load acting at a distance c above the centre of twist is given as[3]:

$$p_{cr} = \frac{28.3}{L^3} \left( \sqrt{1 + 2.47\zeta + 0.52\delta^2} - 0.72\delta \right)\sqrt{EI_y GJ} \qquad (39a)$$

where

E = the modulus of elasticity

G = the modulus of rigidity, or the modulus of elasticity in shear, $G = E/2(1+\nu)$

$\nu$ = Poisson's ratio

$I_y$ = the moment of inertia of the section about the vertical axis y − y

J = St. Venant's torsional resistance (comparable to the polar moment of inertia in circular sections). See the Appendix section A.2

L = the effective length of the girder between supports

$\zeta$ = coefficient for taking account of the inherent stiffness of the flanges:

$$\zeta = \frac{EI_{yf}}{GJ} \frac{2z^2}{L^2}$$

-49-

$\delta$ = coefficient for taking account of the position of the point of application of the load:

$$\delta = \frac{2c}{L} \sqrt{\frac{EI_y}{GJ}}$$

c = distance from point of application of load to centre of twist, see Appendix section A.1

z = distance between centroids of the flanges

$I_{yft}$ = the moment of inertia of the top flange about the vertical axis y - y

$I_{yfb}$ = the moment of inertia of the bottom flange about the vertical axis y - y

$$I_{yf} = \frac{2 \, I_{yft} \, I_{yfb}}{I_{yft} + I_{yfb}}$$

It should be emphasized here, that Eq. (39a) is derived on basis of the elastic theory, for materials having a constant modulus of elasticity and with no consideration for creep deformation. Furthermore, the initial deformation due to the presence of the prestressing force is totally ignored. A straightforward solution of the differential equation of the problem considering all the pertinent parameters involved has not been yet derived. Thus, with regards to prestressed concrete inclined roof girders, we observe two important facts:

1- Geometrical Properties of the Section

Inspecting the Eq. (39a) with regard to the effect of the

-50-

height of the section on the critical load, $P_{cr}$ , we find only some terms are linearly proportional to the height of the section, while the other terms remain constant*. Thus, for the inclined roof girders, a good approximation could be achieved by taking the mid-section between the support and the crown for determining the section properties, such as, $I_y$ , $I_{yf}$ , $J$ etc. See Fig. 8.

## 2- Material Constants

One should keep in mind that the critical load for lateral instability is derived from deflection consideration, end conditions etc. and has very little to do with the ultimate stresses of the materials involved. Furthermore, since Eq. (39a) does not consider all the pertinent parameters involved in the problem of the instability for the prestressed concrete girders, one resorts to some modification. Thus, taking into account the effect of creep in concrete, a time dependent fictitious modulus of elasticity under sustaining loads is adopted. This will predict the combined elastic and creep deformation of the concrete at any given time and validate to some extend the use of Eq. (39a) in pre-stressed concrete girders.

---

* This fact is even clearer for the rectangular sections in fork type bearing[3].

- 51-

Lebelle[6] has given the following empirical values for time dependent modulus of elasticity of concrete under sustaining loads:

for sustaining load duration $t \leqslant 4$ hrs

$$E_c \text{ (in kg/cm}^2) = 18000 \left(1 - \frac{f_{cmax}}{\beta_p}\right) \sqrt{\beta_p} \qquad (40a)$$

for sustaining load duration $4 \text{ hrs} < t < 100$ hrs

$$E_c \text{ (in kg/cm}^2) = 18000 \left(1 - \frac{f_{cmax}}{\beta_p} \sqrt{\beta_p} \left(1 - \frac{t-4}{200}\right)\right) \qquad (40b)$$

for sustaining load duration $t \geqslant 100$ hrs

$$E_c \text{ (in kg/cm}^2) = 6000 \sqrt{\beta_{p90}} \qquad (40c)$$

In all cases the modulus of rigidity should be taken as:

$$G = 0.4 E_c \qquad (40d)$$

where

$f_{cmax}$ = the maximum stress in the concrete along the girder

$\beta_p$ = concrete prism strength after 28 days of normal curing in general

$\beta_{p90}$ = concrete prism strength after 90 days of normal curing

$t$ = time in hours

-52-

The concrete fictitious modulus of elasticity which fully takes into account the effect of creep in the concrete could be derived from deformation considerations. Thus, the short term loading modulus of elasticity, $E_{co}$, and the fictitious modulus of elasticity, $E_{cf}$, are given as follows:

$$E_{co} = \frac{f_c}{\varepsilon_{cel}} \qquad (41a)$$

$$E_{cf} = \frac{f_c}{\varepsilon_{ct}} \qquad (41b)$$

$$\varepsilon_{ct} = \varepsilon_{cel} + \varepsilon_{cpl}$$

$$= \varepsilon_{cel} ( 1 + \phi_t )$$

$$= \frac{f_c}{E_{co}} ( 1 + \phi_t ) \qquad (41c)$$

$$E_{cf} = \frac{E_{co}}{1 + \phi_t} \qquad (41d)$$

where

$f_c$ = the stress in the concrete

$\varepsilon_{cel}$ = the elastic strain of the concrete, i.e., short-term loading

$\varepsilon_{cpl}$ = the plastic strain due to the creep in concrete under sustained loading

-53-

$\mathcal{E}_{ct}$ = the total strain in the concrete at any given

time, t , after the sustained loading becomes

operative.

$\phi_t$ = the creep factor at any given time, t , the

ratio of the plastic strain under sustained

loading to the elastic strain ( $\phi_t = \mathcal{E}_{cpl}/\mathcal{E}_{cel}$ )

The short-term loading modulus of elasticity, $E_{co}$ , is

itself a function of time. Its value increases with time.

At the age of 5 years, the short-term loading modulus of

elasticity of concrete gains generally 25% more than its

value at 28 days of age. Roš[7] has suggested the following

empirical value:

$$E_{co} \text{ (in kg/cm}^2) = \frac{55000}{1 + 150/\beta_p} \qquad (42a)$$

For design purposes however, the short-term loading

modulus of elasticity, $E_{co}$ , is considered to have a

constant value. After a year of standard curing at

temperatures 64 - 68°F, crushing strengths for concrete

prisms, $\beta_p$ (and also crushing strengths for concrete

cylinders, $f'_c$ ) , made with the ordinary Portland cement

and the high early strength cement attain about 30% and

15% higher values than their respective values at 28

days of age under the same conditions[10].

The fictitious modulus of elasticity of the concrete,

-54-

Eq. (41d), which was first introduced by Dischinger[8], is for plane uncracked concrete and ignores the presence of the steel reinforcements in the section.

The inclusion of the steel reinforcement effects on the concrete fictitious modulus of elasticity when creep of the concrete under sustained loading is fully operative, can be shown as follows:

Considering the concrete stress in a fibre adjacent to the steel centroid (c.g.s.)[*,9] .

$$f_c = f_{co} \ e^{-\alpha_o \phi_t} \qquad (43a)$$

or

$$f_{co} = f_c \ e^{+\alpha_o \phi_t} \qquad (43b)$$

where

$f_{co}$ = the initial stress in the concrete fibre adjacent to steel centroid at the beginning of creep in the concrete

$f_c$ = the stress in the concrete fibre adjacent to the steel centroid at any given time, t , after creep has taken place

---

\* For the derivation of creep and shrinkage formula for bonded sections, see Appendix,section A.3 .

$\alpha_o$ = the stiffness coefficient of the reinforcements in the section; the contribution of the reinforcements in supporting the loads. It is function of the cross-sectional area of the steel, $A_s$ , and its location.

$$\alpha_o = \frac{I_c + A_c\, y_s^2}{\dfrac{I_c A_c}{n A_s} + I_c + A_c\, y_s^2} = \frac{n A_s}{A_e}\left(1 + \frac{A_e}{I_e}\, y_e^2\right) \qquad (43c)$$

A and I stand for area and moment of inertia respectively. The subscripts c , s , and e denote concrete, steel and effective properties of the section

$y_s$ = the distance between concrete centroid (c.g.c.) and the steel centroid (c.g.s.)

$y_e$ = the distance between the centroid of the effective section (c.g.e.) and the steel centroid (c.g.s.)

The concrete fictitious modulus of elasticity accounting for creep in concrete is defined as:

$$E_{cf} = \frac{f_c}{\varepsilon_c} \qquad (44a)$$

For the same strain in the concrete, the difference in the stress arising from the use of the short-term modulus of elasticity and fictitious modulus of elasticity is given as:

-56-

$$( E_{co} - E_{cf} ) \, \mathcal{E}_c = \int_0^{\phi_t} f_c \, d\phi_t \qquad (45a)$$

Substituting Eqs. (43a) and (44a) into (45a) and carrying out the integration result in:

$$E_{co} \, \mathcal{E}_c = f_c + f_{co} \frac{1 - e^{-\alpha_o \phi_t}}{\alpha_o} \qquad (45b)$$

Again substituting Eq. (43b) into Eq. (45b) and rearranging the result yields:

$$\frac{f_c}{\mathcal{E}_c} = E_{cf} = \frac{E_{co}}{1 + \left( \dfrac{e^{\alpha_o \phi_t} - 1}{\alpha_o \phi_t} \right) \phi_t} \qquad (46a)$$

The above eqation is reduced to:

$$E_{cf} = \frac{E_{co}}{1 + \psi \phi_t} \qquad (46b)$$

where

$$\psi = \frac{e^{\alpha_o \phi_t} - 1}{\alpha_o \phi_t} \qquad (46c)$$

Thus, $\psi$ takes care of the effects of the reinforcement in the section on the concrete fictitious modulus of elasticity. For $\alpha_o \longrightarrow 0$ , $\psi = 1$ , then Eq. (44b) takes the form of Eq. (41d).

Once, the stress in any concrete fibre, in a composite section, is known, the corresponding concrete strain in that fibre can be evaluated in the same way as in the elastic theory by substituting the concrete fictitious modulus of elasticity instead of Young's modulus.

The creep in concrete of a composite section induces stress relaxation in the concrete part and stress concentration in the steel part. Thus, in the course of time neither the stresses in the concrete part nor the stresses in the steel part remain constant.

In problems concerning lateral instability, one is interested only in the overall deflection of the composite structure. This implies that the composite structure should be treated as if it is an equivalent structure made of one homogeneous material exhibiting creep phenomenon and having the same deflection configuration of the composite structure. As a result of this assumption, the stresses in this 'equivalent structure' remain constant in course of time, but not the strains. Thus, the modulus of elasticity of the hypothesized material making up the equivalent structure changes in the course of time too. It is also assumed that the equivalent structure has the same geometrical properties as the effective properties of the composite structure and the material making up such structure has an effective fictitious modulus of

-58-

elasticity $E_{ef}$ .

Now considering strains at the level of the steel centroid, both in the composite structure and the equivalent structure described before, one finds that:

strain in any section of the composite structure,

$$\varepsilon_{st} = \varepsilon_c = \frac{f_c}{E_{cf}} \tag{47a}$$

and strain in the corresponding section of the equivalent structure,

$$\varepsilon_e = \frac{f_e}{E_{ef}} \tag{47b}$$

where $f_e$ is the stress in the equivalent section at the level of the steel centroid. This stress does not change in time and it has the same value as the initial stress in concrete, $f_{co}$ , at time $t = 0$ , i.e., at the beginning of creep in the concrete.

Thus, it follows that:

$$f_e = f_{co} \tag{48a}$$

For the same deformation in both composite and equivalent structures at the level of the steel centroid:

$$\varepsilon_c = \varepsilon_e \tag{49a}$$

-59-

or

$$\frac{f_c}{E_{cf}} = \frac{f_e}{E_{ef}} \qquad (49b)$$

The above relationship holds good for all similar fibres in corresponding sections as long as the materials involved follow Hooke's law and the sections have the same geometrical properties. Such deformations result in similar overall deflection configuration in both of the composite and the equivalent structures.

Substituting Eq. (48a) into Eq. (49b) and rearranging yield:

$$E_{ef} = \frac{f_{co}}{f_c} E_{cf} \qquad (50a)$$

Again, substituting Eqs. (46a) and (43b) into Eq. (50a) result in:

$$E_{ef} = \frac{\alpha_o E_{co}}{(\alpha_o - 1) e^{-\alpha_o \phi_t} + 1} \qquad (50b)$$

For no reinforcements in the composite section (i.e. $\alpha_o \longrightarrow 0$) Eq. (50b) takes the form of Eq. (41d), thus

$$E_{ef} = \frac{E_{co}}{1 + \phi_t} \qquad (50c)$$

Furthermore, disregarding the creep in the concrete part

-60-

of the composite section, i.e., $\phi_t = 0$ , Eq. (50b) reduces to:

$$E_{ef} = E_{co} \qquad (50d)$$

It is evident from Eqs. (43c) and (50b), that in prestressed concrete inclined roof girders with straight tendons, the effective fictitious modulus of elasticity varies from section to section along the length of the girder. This fact necessitates evaluation of a single mean value of the effective fictitious modulus of elasticity for the entire inclined girder. Such evaluation by means of integration, however, is difficult and tedious. An approximate mean value for the effective fictitious modulus of elasticity in inclined girders could be achieved by substituting the stiffness coefficient of the mid-section between the support and the crown (midspan) in Eq. (50b).

However, since in the prestressed concrete inclined roof girders, the stiffness coefficient, $\alpha_o$ , ranges from about 0.05 to 0.10 , the effect of the reinforcements on the effective fictitious modulus of elasticity could be neglected if the creep factor involved is not too large.

The effective fictitious modulus of elasticity calculated from Eq. (50b) yields lower values than the empirical values given in Eqs. (40). This may be due to the fact

-61-

that Eq. (39a) is only an approximate solution of the lateral stability problems of I-section girders, because in deriving this equation, the prestressed force as well as the initial deflection due to the prestressed force is totally ignored.

## 5. Shipping, Handling and Erection

This problem arises only if the roof girders are prefabricated. The shipping, handling, and erection of the girders should be carried out in a predetermined fashion, thereby the concrete remains uncracked and uncrushed and the steel does not reach its yield point which would incur permanent strains in the prestressing steel leading to losses in the prestressing force. In shipping, the girders are usually supported in such a way that their ends protrude slightly in a cantilever fashion. The lateral stiffness should be given due consideration more particularly with regard to erection. Quite frequently such girders have buckled laterally when lifted from the ground. Usually such mishaps are not so much due to lateral elastic instability of the girder, or to inadequate safety of the compressive flange against buckling produced by high compressive stresses, as due to additional flexural stresses in the highly precompressed tensile flange when the girder is slightly tilted.

Auxiliary steel girder frames, especially designed for handling and erection purposes, should be used to prevent possible damage done to the girders due to tilting, lateral buckling in erection, etc. In handling of heavy girders, it may be necessary to use one lifting appliance (crane or sling) at each end. The following practical rules should be observed in shipping, handling and erection:

1- The prefabricated inclined roof girder must be supported
   or lifted at the ends to ensure that the full load of
   the girder will be acting.

2- The lifting point should be located accurately in the
   vertical centroidal plane, above the top flange if possible.

3- Any tilting of the girder out of its vertical plane must
   be avoided.

For any other handling situation which deviates from the
recommended ones above, the resulting handling stresses should
be determined to see whether they are within the allowable
temporary stresses.  Should they exceed such limits
adequate handling reinforcements should be provided to keep
these stresses within the allowable range.

# 6. Discussion of Results

The results discussed here are related only to locations of critical sections for flexure and principal tensile stress in inclined roof girders. Girders having I-, T-, and rectangular sections are investigated. Computerized results for inclined roof girders ranging from 25 ft. to 105 ft. span with inclinations (tan $\alpha$) ranging from 0.0 to 0.125 are displayed by means of graphs. To compare results, some parameters are kept constant so that the effect of other parameters could be studied. In order to reduce the volume of the work only girders having I-section profile are fully discussed. However, empirical formulae based on calculated results for all three types of sections mentioned before are derived.

## 6.1 Critical Sections for Flexure

### 6.1.1 Critical Section Location according to the Formula from Geometrical Consideration

Figure 10[*] shows the location of critical section as predicted by Eqs. (9a), (12a) and (15a). It is evident that $x_{cr}$ versus L is almost a straight line relationship while $(\frac{1}{2}\zeta_{cr})$ versus L , $x_{cr}$ versus tan $\alpha$ and $(\frac{1}{2}\zeta_{cr})$ versus tan $\alpha$ closely resemble exponential relationships.

---

[*] For legend and list of symbols used in Figs. 10 to 40 inclusive see pages 108 and 109 .

-65-

### 6.1.2 Critical Section Locations according to the Formulae Derived by means of Calculus

Figures 11 and 12 present $x_{cr}$ versus $L$ or $(\frac{1}{2}\xi_{cr})$ versus $L$ relationships for $f_{ct}$, $f_{cb}$, $f_{s1}$ and $f_{s2}$.

It is observed that the relationships $x_{cr}$ versus $L$ maintain a straight line form while those for $(\frac{1}{2}\xi_{cr})$ versus $L$ maintain an exponential form. It should be noted that $x_{cr}$ and $(\frac{1}{2}\xi_{cr})$ move closer to the support for larger $\tan\alpha$, and this shift does not appear to be linearly proportional to $\tan\alpha$.

Figures 13 and 14 show the critical section locations for girders having inclinations 0.05 and 0.125 for both tensioned and non-tensioned top steel layer. Using a small prestressing force in the top of the section has little bearing on the locations of critical sections. The critical section locations for stresses mentioned before do not coincide with each other. All locations of critical sections predicted by Eqs. (20) , (23) , (26) and (29) as well as the critical section predicted by the formula from the geometrical consideration are shown on the same graph for comparison.

Figures 13 and 15 exhibit the effects of the amount of applied moments (partially prestressed girders are subjected to larger applied moments than the fully prestressed girders). Increasing the applied moments leads to a

-66-

decrease in the distance of critical locations from the
support, particularly for $f_{cb}$ and $f_{sl}$ . However,
computations (not included here) show that upon increasing
the prestressing force, distances of critical sections
from the support will increase and in particular for $f_{cb}$
and $f_{sl}$ .

Figure 16 presents the location of critical sections for
80 ft. span girders for both fully and partially prestressed
cases. The observation regarding the effect of the applied
moments on the shift of the critical section locations
toward the support is also noted here.

Figures 17, 18, 19 and 20 exhibit the flexural stress
distribution along 80 ft. span girders for various combina-
tions of the relevant parameters. The location of maximum
(or minimum) stress are indicated by the notation —•—
and the location of the critical section as predicted by
the formula from geometrical consideration is denoted by
the broken line — — — .

It is to be noted that some variations of the critical
section locations produce no significant change in the
amount of the actual stress. Furthermore, it is observed
that Eq. (9a) predicts closely the critical section loca-
tions for $f_{cb}$ and $f_{sl}$ while the critical section
locations for $f_{ct}$ and $f_{s2}$ deviate from the location

-67-

predicted by Eq. (9a).

With regards to the critical section location for $f_{s2}$ , it is readily seen that Eq. (29) predicts the location of minimum tensile stress in a prestressed top steel layer as well as the location of maximum compressive stress when a non-tensioned conventional steel replace the top layer of the prestressing steel.

For non-tensioned conventional steel replacing both top and bottom layers of prestressing steels (hypothetically an uncracked concrete member), the critical section locations for $f_{ct}$ , $f_{cb}$ , $f_{s1}$ and $f_{s2}$ tend to converge to the same position. This position does not coincide with the position predicted by the formula from geometrical consideration. This divergency is due to the fact that in Eq. (9a) Whitney's stress block diagram (on which the derivation of the geometrical formula is partially based) is assumed rather than the usual Bernoulli's linear stress distribution which follows from the assumption that plain sections remain plain before and after deformations.

### 6.1.3 General Computer Solution Programme

Locations of critical sections for flexure have been determined by means of a computer solution programme in which all the pertinent parameters involved in prestressed concrete structures have been considered. In evaluating

the results four ranges of spans were considered.  In each range, all the cross-sectional dimensions other than heights at support are kept constant.  Minimum practical heights at support based on safety requirements were used for each span.  The four span ranges are:

25 ft. to 45 ft. inclusive

50 ft. to 65 ft. inclusive

70 ft. to 85 ft. inclusive

90 ft. to 105 ft. inclusive

The calculations are carried out for normally reinforced girders (see section 1.1.2.1) and the cross-sections considered are  I- , T-  and rectangular sections.  For brevity, only some representative samples of I-section girders are shown.

Figures 21 and 22 present the location of critical sections for various inclinations and accounting for maximum creep and shrinkage effects.  The same trends displayed in the previous graphs (Figs. 10 to 20) are also noted here, except that the critical section location for maximum stress in the top layer of prestressing steel exhibit sudden change in the critical location for larger  $\tan \alpha$ . This indicates that for smaller inclinations the maximum stress in the top layer of prestressing steel occurs at the support and as the inclination increases, the location of maximum stress suddenly shifts to midspan.

-69-

Figures 23 and 24 compare the results of identical girders, with identical prestressing and load, taking into account maximum and minimum creep and shrinkage effects. It is noted that the location of critical sections relative to the support varies with the amount of the deformations due to creep and shrinkage .... the larger the deformations the closer the critical sections are to the support. In some cases the differences are significant and in particular for the location of maximum $f_{cb}$ as expected.

Figure 25 shows the critical sections for an 80 ft. span girder with various inclinations and degree of deformations due to creep and shrinkage. It is to be noted that differences in the locations of critical sections for various stresses and both degrees of deformations due to creep and shrinkage increase with inclination.

Due to the sudden changes in the dimensions of the cross-section at the demarcation points between the span ranges used, distinct discontinuities in Figs. 21 to 25 are observed. Furthermore, the location of the critical section was determined by comparing the maximum flexural stresses at fifty sections taken between the end block zone and the centre of the girder. It is quite possible that the section so chosen will not coincide with the true critical section; however, the error involved in this procedure will be insignificant due to the number of the sections

-70-

considered.

As indicated before, Figs. 21, 22, 23, 24 and 25 are only some representative samples displaying the location of critical sections for an I-section girder. In order to draw a comparison between girders having different cross-sections, an exponential form for $x_{cr}$ versus L is assumed. It has been found by trial and error that the following expressions, Eqs. (51) , closely predict the relationship between the location of the critical sections and the other pertinent parameters.

1- Location of Maximum Stress in Extreme Top Fibre $(f_{ct})$

$$x_{cr} = 0.5 \ L \ e^{- \ cl \ \tan \alpha \ \sqrt[4]{L \ h_s}} \qquad (51a)$$

where

$x_{cr}$ = the distance of critical section from the support in ft.

L = length of girder in ft.

cl = constant*, depends on loading, degree of prestressing and deformations due to effects of creep and shrinkage (the value given here is for normally reinforced girders)

$\tan \alpha$ = inclination of the girder

$h_s$ = height of the girder at the support in inches

* Average from 85 values.

-71-

Mean values for the constant $c_1$, together with its standard
deviation, $\sigma_1$, for the different cross-sections are listed
below:

| Section | with maximum creep and shrinkage effects | with minimum creep and shrinkage effects |
|---|---|---|
| I-section | $c_1 = 1.166$ $\sigma_1 = 0.005$ | $c_1 = 1.151$ $\sigma_1 = 0.006$ |
| T-section | $c_1 = 1.397$ $\sigma_1 = 0.011$ | $c_1 = 1.375$ $\sigma_1 = 0.013$ |
| rectangular section | $c_1 = 1.350$ $\sigma_1 = 0.006$ | $c_1 = 1.289$ $\sigma_1 = 0.010$ |

Note that by virtue of the exponential form of Eq. (51a),
it is readily seen that the locations of the critical sections
of the T-section girders are closest to the support,
followed by the rectangular and the I-section girders
respectively.

2- Location of Maximum Stress in Extreme Bottom Concrete Fibre $(f_{cb})$

$$x_{cr} = 0.5 \, L \, e^{-c_2 \tan \alpha \sqrt[2]{h_s}} \tag{51b}$$

where

c2 = constant[*], depends on loading, degree of pre-
stressing and deformations due to effects of
creep and shrinkage (the value given here is
for normally reinforced girders)

---

* Average from 85 values.

-72-

Mean values for the constant $c_2$, together with its standard deviation, $\sigma_2$, for the different cross-sections are listed below:

| Section | with maximum creep and shrinkage effects | with minimum creep and shrinkage effects |
|---|---|---|
| I-section | $c_2 = 1.010$ $\sigma_2 = 0.006$ | $c_2 = 0.903$ $\sigma_2 = 0.007$ |
| T-section | $c_2 = 1.214$ $\sigma_2 = 0.010$ | $c_2 = 1.066$ $\sigma_2 = 0.014$ |
| rectangular section | $c_2 = 1.096$ $\sigma_2 = 0.005$ | $c_2 = 0.916$ $\sigma_2 = 0.007$ |

By virtue of the exponential form of Eq. (51b), it is readily seen that the locations of the critical sections of the T-section girders are closest to the support, followed by the rectangular and the I-section girders respectively.

3- Location of Maximum Stress in Bottom Layer of Prestressing Steel ($f_{s1}$)

$$x_{cr} = 0.5 \, L \, e^{- c_3 \tan \alpha \sqrt[2]{h_s}} \qquad (51c)$$

where

$c_3$ = constant[*], depends on loading, degree of prestressing and deformations due to effects of creep and shrinkage (the value given here is for normally reinforced girders)

---

[*] Average from 85 values.

-73-

Mean values for the constant $c_3$, together with its standard deviation, $\sigma_3$, for the different cross-sections are listed below:

| Section | with maximum creep and shrinkage effects | with minimum creep and shrinkage effects |
|---|---|---|
| I-section | $c_3 = 0.630$ $\sigma_3 = 0.008$ | $c_3 = 0.618$ $\sigma_3 = 0.008$ |
| T-section | $c_3 = 0.618$ $\sigma_3 = 0.009$ | $c_3 = 0.595$ $\sigma_3 = 0.010$ |
| rectangular section | $c_3 = 0.557$ $\sigma_3 = 0.009$ | $c_3 = 0.519$ $\sigma_3 = 0.010$ |

Here again by virtue of the exponential form of Eq. (51c), it is readily seen that the locations of critical sections of the I-section girders are closest to the support, followed by the T-section and rectangular section girders respectively.

## 6.2 Critical Section Locations for Principal Tensile Stress

The object of the computer solution programme was to establish location (relative to the support), position (relative to the soffit of the girder) and inclination (relative to the horizontal axis) of the maximum principal tensile stress.

It is worthwhile to note that the direction of the principal tensile stress within the compression zone in concrete lies between $45^\circ$ to $90^\circ$, whereas in the concrete tensile zone (uncracked) it lies between $0^\circ$ to $45^\circ$.

Furthermore, it is well established that as a result of using linear stress distribution in the concrete (which is not strictly true), a larger allowable tensile strength in flexure is specified to justify the validity and use of the linear stress distribution method of analysis. For this reason, the following two cases of critical section locations for principal tensile stress are investigated.

Case I : Flexural Tensile Stresses Carried by the Concrete
(see Sections 2.1.3.1 and 2.1.3.2)

In this case maximum principal tensile stress is established for the entire section whether the whole section is in compression or partly in compression and partly in tension. Equation (31a) shows that the compressive flexural stress has a reducing effect on the principal tensile stress while the flexural tensile stress tends to augment considerably

-75-

the principal tensile stress; thus, in a section with a
tensile zone the maximum principal tensile stress will in
most cases appear in the tensile zone with a very small angle
of inclination with the horizontal axis (if not zero) and
near or at the extreme tensile fibre.  This state of affairs
will give rise to a maximum principal tensile stress almost
equal to the flexural tensile stress itself, overwhelming
the effect and the amount of the shearing stresses acting
on the section.  Thus, any reinforcement provided to resist
such maximum principal tensile stress will have virtually
no vertical component.  However, on cracking stress
re-distribution takes place and a uniform vertical shear
stress appears immediately in the cracked zone with little
or no reinforcements.  If such shear stress is large, it
may lead to a sudden shear failure of the girder.
Furthermore, location, position and inclination of maximum
principal tensile stress resulting from the shortcomings
of the linear stress distribution method of analysis may
lead to predict false location, position and direction of
maximum principal tensile stress.

Case II :  Flexural Tensile Stresses Assumed to be Carried
           by Adequate Steel Reinforcement (see Sections
           2.1.4.1  and  2.1.4.2)

In this case either maximum principal tensile stress in
compression zone or maximum shear stress in the tensile

zone of a section is considered as a criterion for design against shear failure. This state of affairs is valid only by assuming that concrete remains uncracked and the flexural tensile stress in the concrete is resisted by an adequate steel reinforcement which relieves the concrete part from the flexural tensile stresses. This implies that the flexural tensile stresses should be within its allowable limit. Experiments have shown that the provision of steel reinforcement will impede the appearance of cracks when they are adequately positioned and improve the resistance of concrete to tensile forces.

By assuming that the flexural tensile stress in the section is carried by an adequate steel reinforcement, the shear resisting capacity of a prestressed member is considerably improved since the allowable tensile strength of concrete in flexure is fairly large compared to the axial or principal tensile stresses. It should be also noted that the direction of principal tensile force in the compression zone of concrete is between $45^{\circ}$ to $90^{\circ}$ from the horizontal and the direction of the assumed principal tensile stress due to shear stress in the tensile zone of concrete is $45^{\circ}$ (state of pure shear stress). Thus, providing reinforcements for such conditions give rise to large vertical components of reinforcements which will serve to resist the shear in the cracked section and prevent sudden failures.

-77-

Location, position relative to the soffit of girder, and inclination relative to horizontal axis of the critical section for maximum principal tensile stress are evaluated by means of the computer solution programme for working and ultimate loads with maximum and minimum creep and shrinkage effects for cases I and II as described before.

For brevity, only representative samples of I-section girders have been re-drawn from the numerous plottings carried out by the computer. Unless otherwise indicated, all the graphs, Figs. 26 to 40 , are for girders having an I-profile cross-section, see Fig. 8 . Comparison with other types of cross-sections are made by means of empirical formulae as was performed in the case of flexure.

It is relevant to mention that the working load capacity of the girders are evaluated according to section 1.1.2.1 and the ultimate load is taken as 1.8 of working loads (see CPCI prestressed handbook, paragraph 3.4[1]). It should be noted that 80% overload used is considered as live load with no creep effects taken into account.

For clarity in what follows, the section of the girder which borders next to the end block zone is refered to as the transition section.

Figure 26 shows location of critical section for maximum principal tensile stress under working and ultimate loads,

-78-

with maximum and minimum creep and shrinkage effects for both cases I and II . The girders considered, have parallel flanges (tan $\alpha$ = 0). In case I , the critical locations are either at transition or midspan section for all loading cases. The latter location coincide with the location of maximum flexural tensile stress. However, in case II the critical locations are either at transition section or at a section L/6 to L/4 away from the support depending on the degree of deformations caused by creep and shrinkage.

Figures 27 and 28 exhibit the effect of inclinations on critical section locations for both cases I and II and their relative locations with regard to loadings and the degree of deformations due to creep and shrinkage. It is also to be noted that the critical section under working load coincide, in almost all cases, with the transition section and under ultimate loads it shifts further away from the support. Occasionally the maximum deformation due to creep and shrinkage will cause the critical section locations under working load (in case I only) to shift further away from the support than the case for ultimate load.

Figures 29, 30, 31 and 32 show the shift of critical section locations due to inclination for each individual loading and degree of deformation for cases I and II .

-79-

It is evident from these graphs that there are two distinct possible critical section locations, the first at the transition section .... this is most likely to occur under working load, and the second will be further away from the support when the girders under ultimate loads. The distance of the second critical section relative to the support depend largely on the inclination, degree of prestressing, amount of the applied load, degree of deformation due to creep and shrinkage, and whether it is case I or case II .

The linear relationship between $x_{cr}$ and L is maintained for all cases of the second critical section locations except for some sudden shift. The same observation was also noted for all other results not included in this paper.

Figures 33 and 34 show the variation of critical section locations with $\tan\alpha$ for 80 ft. span girders. For both cases I and II the two possible critical section locations are distinctly confirmed again. The second critical section location is approximately related to $\tan\alpha$ by an exponential form (see Eq. (52a) ). In case I , the second location of critical section is further away from the support than that of case II .

Figure 33 shows that in case I , the second critical section location for principal tensile stress coincides with the critical section for flexural tensile stress at extreme

-80-

bottom fibre. This can also be deduced from Figs. 35 and 37, case I (i.e. $\zeta_{cr} = 0$).

Figure 34 presents a comparison of case II critical section locations under working and ultimate loads with maximum and minimum deformations due to creep and shrinkage for various types of cross-sections. There is an insignificant difference in the second critical section locations various types of cross-sections.

The foregoing observations regarding the critical section locations together with the corresponding observations made for I- , T- and rectangular sections, in calculations not included in this paper, are classified now as follows:

## 6.2.1 Case I

### 6.2.1.1 Critical Section Location Under Working Loads

The critical sections occur both in the transition section and at a section very close but slightly further away from the critical section under ultimate load for case I . No intermediate location for the critical section between these two locations was observed.

### 6.2.1.2 Critical Section Location Under Ultimate Loads

By trial and error, the following exponential expression has been found to fit closely the results obtained from

-81-

the general computer solution programme.

$$x_{cr} = 0.5 \, L \, e^{-c4 \, \tan \alpha \sqrt[2]{h_s}}$$ (52a)

where

c4 = constant[*], depends on loading, degree of pre-
stressing and deformations due to effects of
creep and shrinkage (the value given here is
for normally reinforced girders)

Mean values for the constant c4 , together with its standard
deviation, $\sigma 4$ , for the different cross-sections are listed
below:

| Section | with maximum creep and shrinkage effects | with minimum creep and shrinkage effects |
|---|---|---|
| I-section | c4 = 1.198<br>$\sigma 4$ = 0.005 | c4 = 1.121<br>$\sigma 4$ = 0.004 |
| T-section | c4 = 1.461<br>$\sigma 4$ = 0.005 | c4 = 1.358<br>$\sigma 4$ = 0.007 |
| rectangular section | c4 = 1.405<br>$\sigma 4$ = 0.008 | c4 = 1.282<br>$\sigma 4$ = 0.005 |

It should be noted that by virtue of the exponential form
of Eq. (52a), it is readily seen that the locations of the
critical sections of the T-section girders are closest to
the support, followed by the rectangular and the I-section
girders respectively.

---

* Average from 85 values.

## 6.2.2 Case II

### 6.2.2.1 Critical Section Location Under Working Loads

The critical section occurs at the transition section for all types of sections considered and for both limits of deformation due to creep and shrinkage.

### 6.2.2.2 Critical Section Location Under Ultimate Loads

Here, the critical section location occurs at a distance further away from the transition section but not so far as the critical section for case I mentioned in 6.2.1.2 . By trial and error, the following exponential expression has been found to fit closely the results obtained from the general computer solution programme:

$$x_{cr} = ko \ L \ e^{- c5 \ \tan \alpha \ \sqrt[2]{h_s}} \tag{52b}$$

where

> ko and c5 are constants which depend on the type of the cross-sections, prestressing force and degree of deformations due to creep and shrinkage effects.

For normally reinforced girders and different types of cross-sections; the constant ko , and mean values for the constant $c5^{*}$ together with its standard deviation $\sigma 5$ are listed below:

---

* Average for 60 values.

| Section | with maximum creep and shrinkage effects | with minimum creep and shrinkage effects |
|---------|------------------------------------------|------------------------------------------|
| I-section | $k_o = 0.190$<br>$c_5 = 1.540$<br>$\sigma_5 = 0.020$ | $k_o = 0.240$<br>$c_5 = 1.597$<br>$\sigma_5 = 0.059$ |
| T-section | $k_o = 0.215$<br>$c_5 = 1.861$<br>$\sigma_5 = 0.020$ | $k_o = 0.245$<br>$c_5 = 1.522$<br>$\sigma_5 = 0.018$ |
| rectangular section | $k_o = 0.225$<br>$c_5 = 1.858$<br>$\sigma_5 = 0.018$ | $k_o = 0.260$<br>$c_5 = 1.531$<br>$\sigma_5 = 0.013$ |

It is evident from Eq. (52b) that the location of the critical sections of the I-section girders are closest to the support, followed by T-section and rectangular section girders respectively.

Figures 35 and 36 illustrate the position of maximum principal tensile stress relative to the soffit of the girder for cases I and II respectively. It is noted that for case I this position, under working loads, occurs above the c.g. of the section; whereas under ultimate loads it occurs below the c.g. of the section at or very close to the soffit of the girder. However, for case II the position of maximum tensile stress at the critical location occurs under working loads above the c.g. and under ultimate loads just below the c.g. of the section and close to the location of the maximum shear stress.

-84-

Figures 37 and 38 show the inclination of the maximum principal tensile stress with the horizontal axis at the critical section. For case I under working loads, the direction of the maximum principal tensile stress is either horizontal coinciding with the flexural stresses at top or bottom extreme fibre, or very steep above the c.g.; while, for ultimate loads it is always horizontal at the soffit of the girder. However, for case II under working loads the inclinations are always steep relative to horizontal axis, whereas under ultimate loads it is around $45^\circ$ .

Figures 39 and 40 show the variation of critical section locations, positions, relative to the soffit of the girder, and inclination of maximum principal tensile stress with $\tan \alpha$ for 80 ft. span girders. These figures give comparisons between cases I and II . The observations made before are also applicable in this case. The most important observation is that case II is 'shift free' i.e., without abrupt change in position and direction giving smooth variation unlike case I . Furthermore, it should be noted that in case II and for prestressed girders having I-section profile, the position of maximum principal tensile stress under working loads is quite likely to occur at section A — A , whereas under ultimate loads it may occur either at the c.g. or section B — B . See Fig. 8 .

## 7. Conclusions

Although the following conclusions are made for normally reinforced girders, it is believed that the results presented can be readily modified to deal with under- and over-reinforced girders either fully or partially prestressed.

### 7.1 Critical Section Locations for Flexure

The conclusions to be drawn here are that the location of critical sections relative to the support is governed by the stresses in the following order: $f_{ct}$ , $f_{cb}$ and $f_{sl}$ respectively, i.e., critical section for the stress $f_{ct}$ is the one nearest to the support followed by those for $f_{cb}$ and $f_{sl}$ respectively. The critical distances relative to the support decrease with the applied moments and increase with the prestressing force in the bottom steel layer. With regard to the critical section location governed by the top layer of prestressing steel, the maximum stress occurs either at the support (transition section) or at midspan depending on the inclination. Generally, for larger inclination it is more likely that the maximum stress in the top layer of the prestressing steel will occur at midspan. This is on one hand, on the other hand for non-tensioned conventional steel replacing the top layer of prestressing steel, the maximum compressive stress can be predicted by Eq. (29).

-86-

For larger $\tan \alpha$ the divergency among the critical section locations are much more than those for smaller $\tan \alpha$ .

It is evident from Eqs. (20), (23), (26) and (29) that the locations of critical sections are not constant and will depend largely upon the magnitude of the applied moment and the prestressing force. However, Eq. (9a) predicts a fixed location for the critical section, and indeed it gives a good assessment for the location of maximum stresses for smaller $\tan \alpha$ and in particular the critical locations for stresses $f_{cb}$ and $f_{sl}$ . This is due to the inherent characteristics of slow variation of stresses in the vicinity of the location predicted by Eq. (9a). These results are also confirmed by these obtained from the computer solution programme.

It is evident from the results obtained from the general computer solution programme that the abrupt change in the dimension of the cross-sections at the demarcation points of span ranges does not produce large discontinuities. This signifies that the height of the section at the support has a larger effect on the critical section location than do other dimensions of the section. Thus, the application of Eqs. (20), (23), (26) and (29) for sections other than rectangular sections are still justified.

As was expected, the effects of creep and shrinkage

-87-

deformations on the location of the critical sections are to shift these locations towards the support depending on the magnitude of loss in the prestressing force in the tendons due to such effects. Moreover, these effects are more noticeable in the critical section locations for the stresses $f_{cb}$ and $f_{sl}$.

It should be noted that the formula derived from geometrical consideration $\left[\text{Eq. (9a)}\right]$ together with the formulae derived by means of calculus $\left[\text{Eqs. (20), (23), (26) and (29)}\right]$ as well as the empirical formulae $\left[\text{Eqs. (51a), (51b) and (51c)}\right]$ for normally reinforced prestressed roof girders provide a good tool to locate the critical sections for flexure in uncracked concrete sections. However, for cracked concrete sections, only Eq. (9a) will provide the location of the critical section.

## 7.2 Critical Section Location for Principal Tensile Stress

The critical section location for principal tensile stress is
dictated by the magnitude of loading, amount of prestressing
force and degree of deformation due to creep and shrinkage
effects. It was established that for each case I and II ,
two critical section locations exist depending on the magnitude
of the applied loads. The first critical section location
occurs at transition section and the second one further away
from it. This is, however, based on the assumption that under
working loads, a small tensile zone is induced in the upper
part of the transition section (i.e., extreme top concrete
fibre of the transition section is in tension) giving rise to
a maximum principal tensile stress within the girder.
Nevertheless, this tensile zone will disappear under ultimate
loads and instead tensile stresses at extreme bottom fibres
in a region further away from the support will appear. This
gives rise to a maximum principal tensile stress in a section
within the region mentioned above. Thus, for normally reinforced
prestressed girders, it can generally be assumed that under
working loads the first critical section occurs at transition
section, whereas under ultimate loads the second critical
section occurs further away from the support. Slight variation
of the second critical section location has been observed ... the
larger the applied external loadings or the smaller the pre-
stressing force, the shorter is the distance of this critical

-89-

section from the support. Furthermore, the larger the deforma-
tions due to creep and shrinkage effects the closer is the
second critical section to the support.

However, the largest maximum principal tensile stress occurs
under ultimate loads with maximum deformations due to creep
and shrinkage. This makes this latter case the criterion
in design.

### 7.2.1 Case I

#### 7.2.1.1 Under Working Loads

Here, the location of the critical section generally occurs
at the transition section. For maximum creep and shrinkage
effects, occasional shift of this location to one close
but slightly further than the critical location under
ultimate loads has also been noticed. Therefore, this
location could be readily predicted approximately by Eq. (52a)
and taking the constant $c_4$ for minimum creep and
shrinkage.

If the critical location is at the transition section,
the maximum principal tensile stress would lie above the
c.g. with a steep inclination to the horizontal; whereas,
if the critical section location is further away from the
transition section, the position of maximum principal
tensile stress is at the soffit and its direction coincides

with the horizontal axis.

### 7.2.1.2 Under Ultimate Loads

The location of critical section occurs further away from the transition section. The approximate critical section location for various inclination can be predicted by Eq. (52a). The position and direction of maximum principal tensile stress generally coincide with the position and direction of maximum flexural tensile at extreme bottom concrete fibre.

## 7.2.2 Case II

### 7.2.2.1 Under Working Loads

Here, the critical section location occurs at the transition section above the c.g. with steep inclination to the horizontal axis.

### 7.2.2.2 Under Ultimate Loads

The critical section location occurs further away from the transition section. The approximate location of the critical section is given by Eq. (52b). A slight adjustment of the constants involved (ko and c5) may be made to meet the requirements as described in section 7.2 . The location of the maximum principal tensile stress is below the c.g.

of the section and its direction is about 45° to the horizontal.

Case I has no significance in design against the shear because it generally fails to predict any vertical component of reinforcements. Nevertheless, it may be useful in checking the position of cracks in some special structures where cracks have to be minimized. However, case II , under ultimate loads and maximum deformations due to creep and shrinkage, will yield a location where the maximum principal tensile stress is largest. Equation (52b) with adequate constants will provide a good tool in finding the critical section location. Slight variation of the location of the critical section will yield no significant change in the magnitude of the maximum principal tensile stress because of the inherent characteristics of bending moment and shear force diagrams in inclined roof girders. Thus, case II provides a good criterion for design against shear since it predicts large component of vertical reinforcements which will be neccessary in a cracked section with shear stress exceeding its allowable limit.

# REFERENCES

1. CPCI Presressed Handbook "Canadian Prestressed Institute, Prestressed Handbook, by L. Cazaly and M. W. Huggins", 1st edition, 1st printing, April 1964.

2. Mörsch, E., "Static der Gwölbe und Rahmen, Teil A", Seite 694-700, Karl Wittwer Verlag, Stuttgart 1947.

3. Leonhardt, F.,"Prestressed Concrete, Design and Construction", 2nd edition, Wilhelm Ernst & Sohn, Berlin 1964.

4. Bonatz, P.,"Schubspannungen und lotrechte Pressungen im Balken mit veränderlicher Höhe". Bauingenieur 24 (1949) Heft 4, Seite 125-128.

5. Weiss, W., Berechnung der Schubspannungen bei Balken mit veränderlicher Querschnitthöhe". Bauplanung - Bautechnik 14 (1960) Heft 11, Seite 498-500.

6. Lebelle, P., "Stabilité élastique des poutres en béton précontraint a l'égard du déversement lateral". Annales de l'Institut Technique du Bâtiment et des Travaux Publics 12 (1959) No. 141, p. 779-831.

7. Roš, M. u. Sarrasin, A., "Die Materialtechnischen Grundlagen und Probleme des Eisenbetons im Hinblick auf die zukünftige Gestaltung der Stahlbeton-Bauweise." EMPA Bericht Nr. 162, Zürich 1950.

8. Dischinger, F., "Elastische und Plastische Verformungen der Eisenbetontragwerke und insbesondere der Bogenbrücken". Bauingenieur 20, Jahrgang (1939), Hefte 5/6, 21/6, 31/32 and 47/48.

9. Fritz, B., "Verbundträger", Springer-Verlag, Berlin 1961.

10. Hummel, A., "Das Beton-ABC", 11. Auflage, Wilhelm Ernst & Sohn, Berlin 1953 (12. Auflage 1959).

11. Borg, S. F., and Gennaro, J. J., "Advanced Structural Analysis", D. Van Nostrand Company, Inc. Princeton, New Jersey 1959.

# FIGURES

-95-
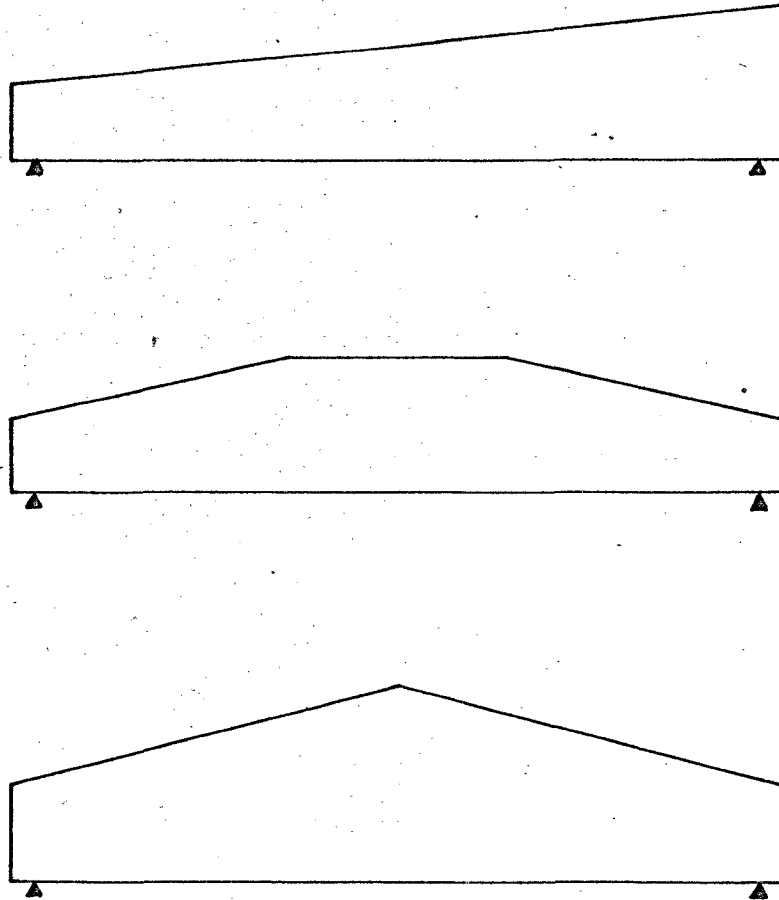
(a) TYPICAL INCLINED PRESTRESSED GIRDERS
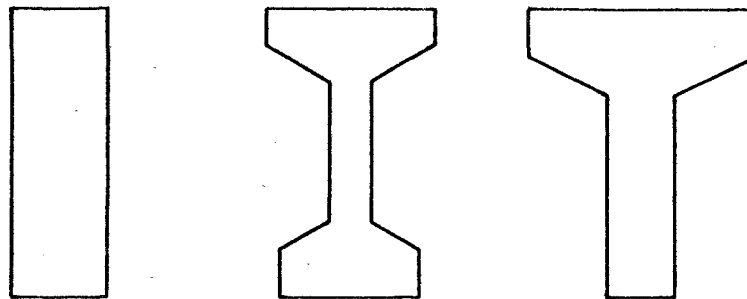


(b) TYPICAL CROSS - SECTIONS

FIGURE 1.

-96-

FIGURE 2.

(a)

(b)

PARABOLA

$M_{MAX}$   $M_\xi$

(c)

FIGURE 3.

-98-

**Read girder data**
1- initial prestressing stress, properties of prestressing steel and concrete
2- maximum and minimum creep factors and shrinkage strains

$\boxed{A}$ ⟶ **Read inclination**

1- Choose a girder length from 25 ft. to 105 ft. in increments of 5 ft.
2- Initialize the stresses for the girder under consideration
3- Choose dimensions of the girder c/s from the 4 ranges specified
4- Compute the critical section according to Eq.(9a) given in section 1.1.1
5- Compute area of prestressing steel according to CPCI 3.5.2 , i.e., Eq. (30a)
6- Compute bending moment resistance capacity under working loads according to Eq. (30b)
7- Compute:
　　girder weight, $W_g$ , from the girder dimensions
　　total weights, $W_t$ , could be sustained by girder
　　superimposed load $W_s = 0.65 \, (W_t - W_g)$
　　live load　　　　$W_l = 0.35 \, (W_t - W_g)$

$\boxed{B}$

$\boxed{C}$ ⟶ **Choose a distance x from the support**
(50 increments between the end block zone and midspan)

**Compute:**
1- moments and shear forces
2- height of girder at x
3- gross and effective areas of concrete and composite section
4- centre of gravity of the section
5- moment of inertia
6- stiffness coefficients for prestressing steel

Fig. 4 – Flow chart of the general programme

-99-

Compute:
  normal stress on the sections in steel and concrete due to
  1- prestressing force
  2- girder weight
  3- superimposed load (permanent dead load except girder
     weight)
  4- live load
  5- max. (creep & shrinkage) accounting for prestressing
     force and girder weight
  6- max. creep accounting for superimposed load
  7- min. (creep & shrinkage) accounting for prestressing
     force and girder weight

Combinations of normal stresses due to the above 7 cases
   8- (1+2)         at transfer
   9- (1+2+3+7)     dead loads + min. (creep & shrinkage)
  10- (1+2+3+4+7)  total loads + min. (creep & shrinkage)
  11- (1+2+3+5+6)  dead loads + max. (creep & shrinkage)
  12- (1+2+3+4+5+6) total loads + max. (creep & shrinkage)

Compute:
  1- reduced shear force under working loads accounting
     for the effects of max. (creep & shrinkage)
  2- reduced shear force under working loads accounting
     for the effects of min. (creep & shrinkage)
  3- reduced shear force under ultimate loads accounting
     for the effects of max. (creep & shrinkage)
  4- reduced shear force under ultimate loads accounting
     for the effects of min. (creep & shrinkage)

Compute from shear stress and normal stresses, the principal
  tensile stresses at various levels accross the section
  under consideration and keep the largest principal tensile
  stress indicating length of the girder, distance of the
  section from the support, distance of the max. principal
  tensile stress from the soffit of the girder etc. This is
  done for the following cases:

(Fig. 4 - continuation 1)

-100-

```
1- largest principal tensile stress under working load
   accounting for the effects of max. (creep & shrinkage)
2- largest principal tensile stress under working load
   accounting for the effects of min. (creep & shrinkage)
3- largest principal tensile stress under ultimate load
   accounting for the effects of max. (creep & shrinkage)
4- largest principal tensile stress under ultimate load
   accounting for the effects of min. (creep & shrinkage)
```

```
Compare the following stresses with previous values and keep
   the largest stress, indicate the distance of the section
   from the support, length of the girder, location of the
   stress from soffit of the girder in case of principal tensile
   stress etc.

   1- normal stress at top concrete fibre accounting
      for the effects of max. (creep & shrinkage)
   2- normal stress at bottom concrete fibre accounting
      for the effects of max. (creep & shrinkage)
   3- stress in bottom layer of prestressing steel account-
      ing for the effects of max. (creep & shrinkage)
   4- stress in top layer of prestressing steel accounting
      for the effects of max. (creep & shrinkage)

   5- normal stress at top concrete fibre accounting
      for the effects of min. (creep & shrinkage)
   6- normal stress at bottom concrete fibre accounting
      for the effects of min. (creep & shrinkage)
   7- stress in bottom layer of prestressing steel account-
      ing for the effects of min. (creep & shrinkage)
   8- stress in top layer of prestressing steel accounting
      for the effects of min. (creep & shrinkage)

   9- principal tensile stress under working load account-
      ing for the effects of max. (creep & shrinkage)
  10- principal tensile stress under working load account-
      ing for the effects of min. (creep & shrinkage)
  11- principal tensile stress under ultimate load account-
      ing for the effects of max. (creep & shrinkage)
  12- principal tensile stress under ultimate load account-
      ing for the effects of min. (creep & shrinkage)
```

(Fig. 4 - continuation 2)

-101-
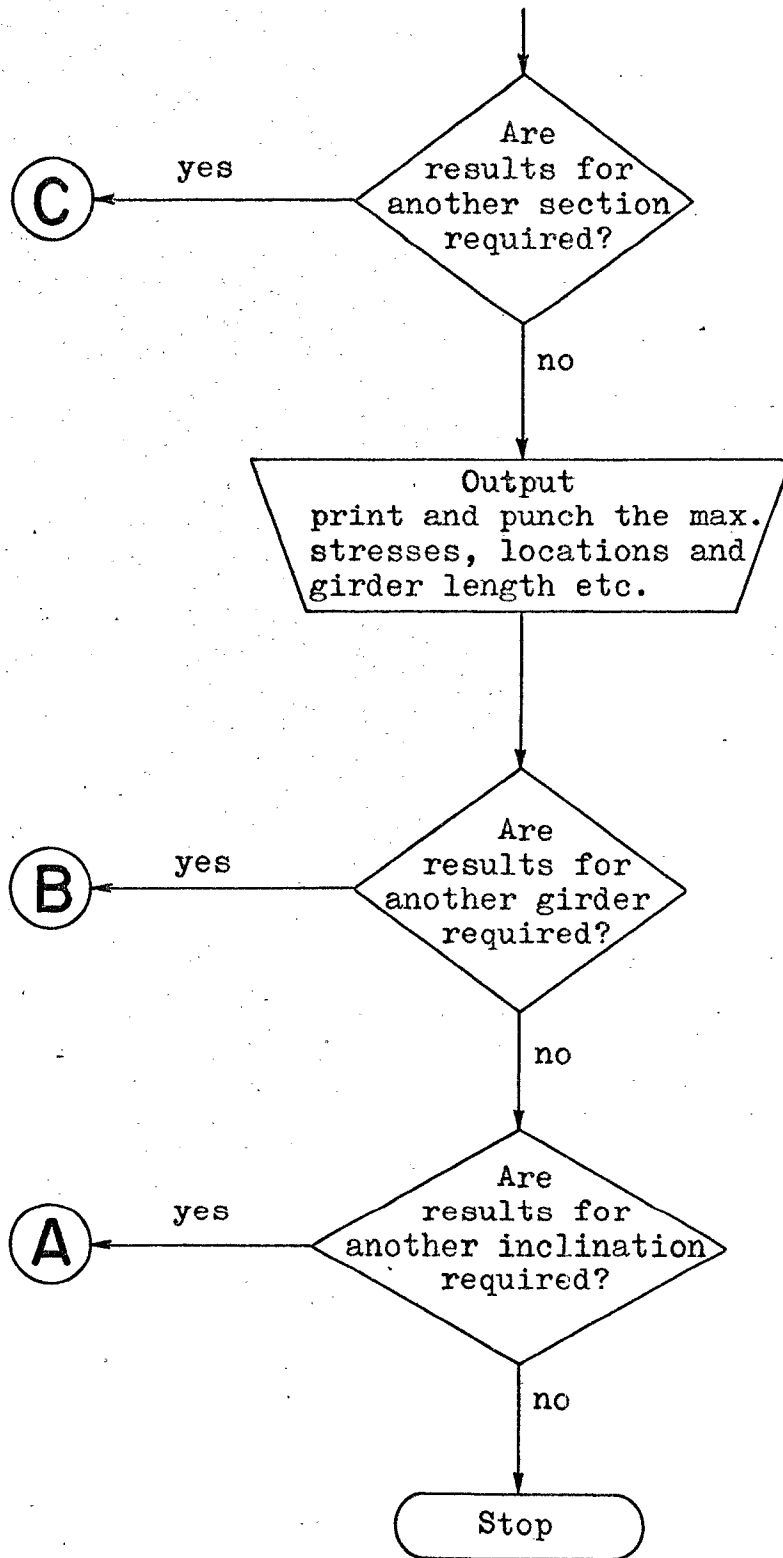
(Fig. 4 - continuation 3)

-102-
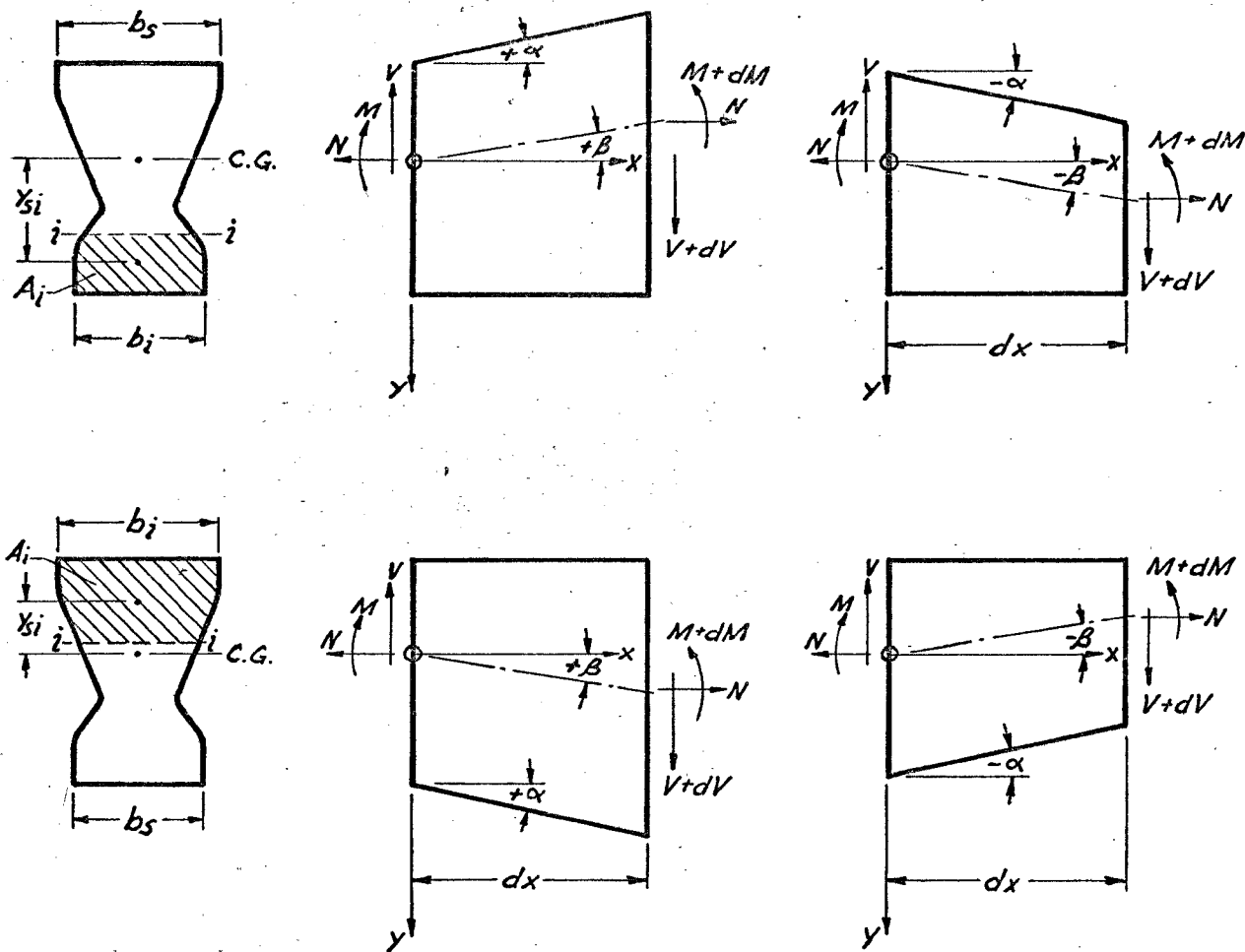
a) SECTIONS WITH VARIABLE FLANGE THICKNESS
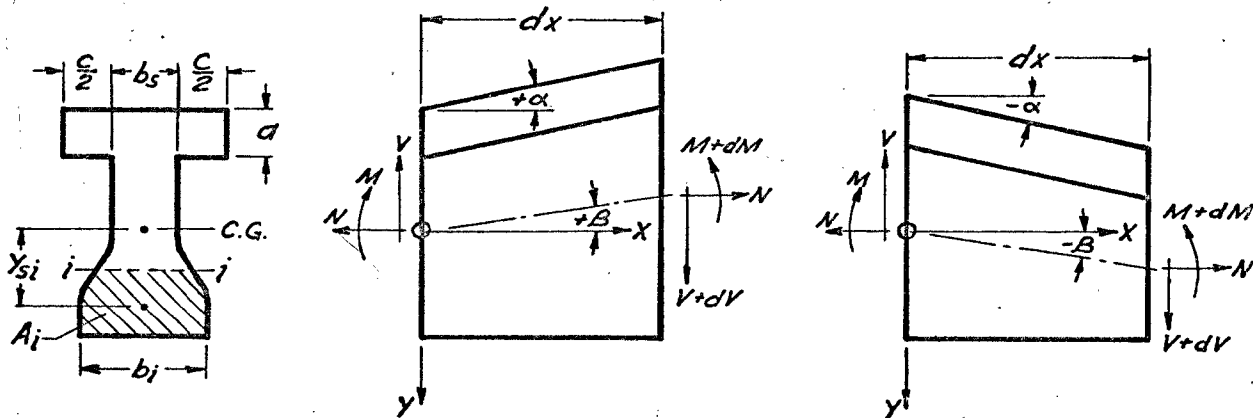


b) SECTIONS WITH CONSTANT FLANGE THICKNESS

FIGURE 5. TYPICAL FREE-BODY DIAGRAMS AND NOTATION

-103-

a) APPLIED LOADS

b) PRESTRESSING FORCE

c) COMBINED FORCE DIAGRAM
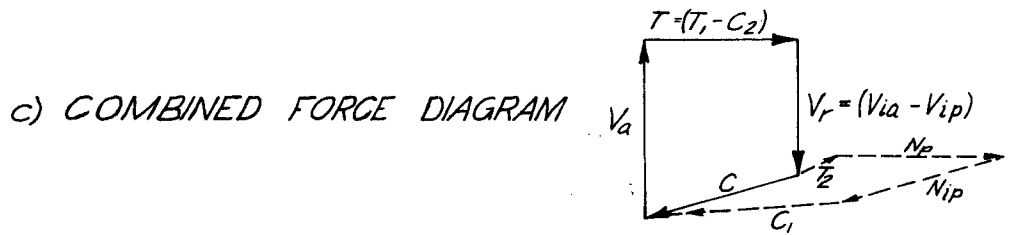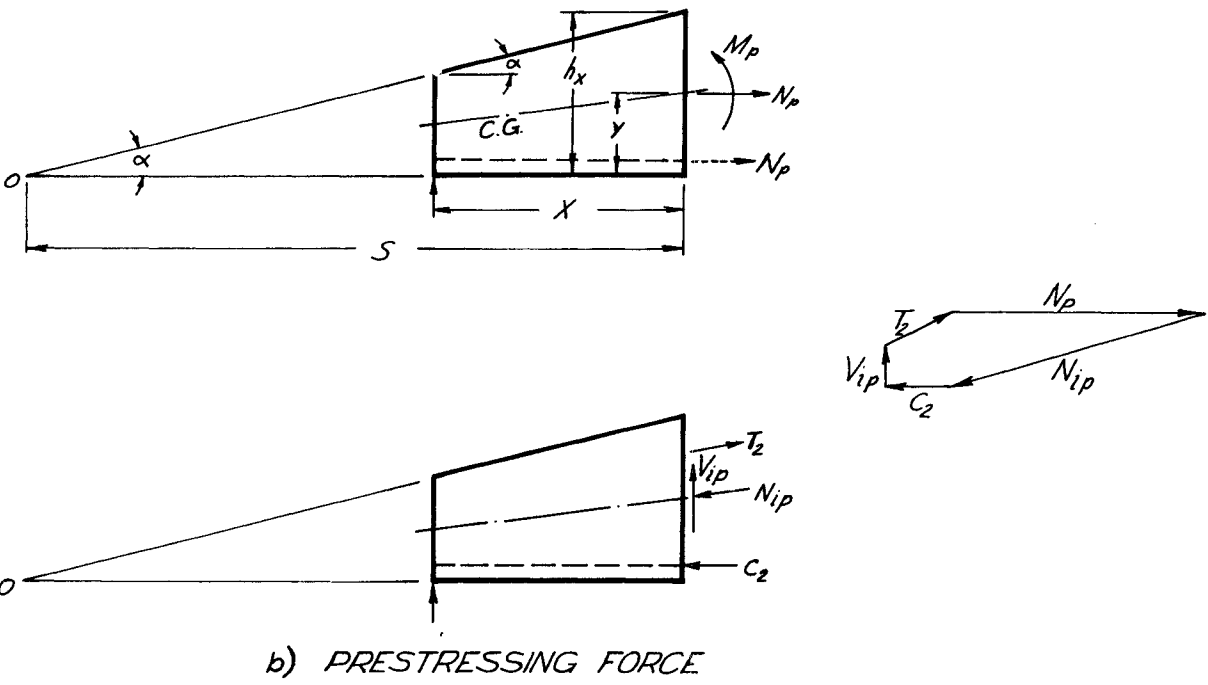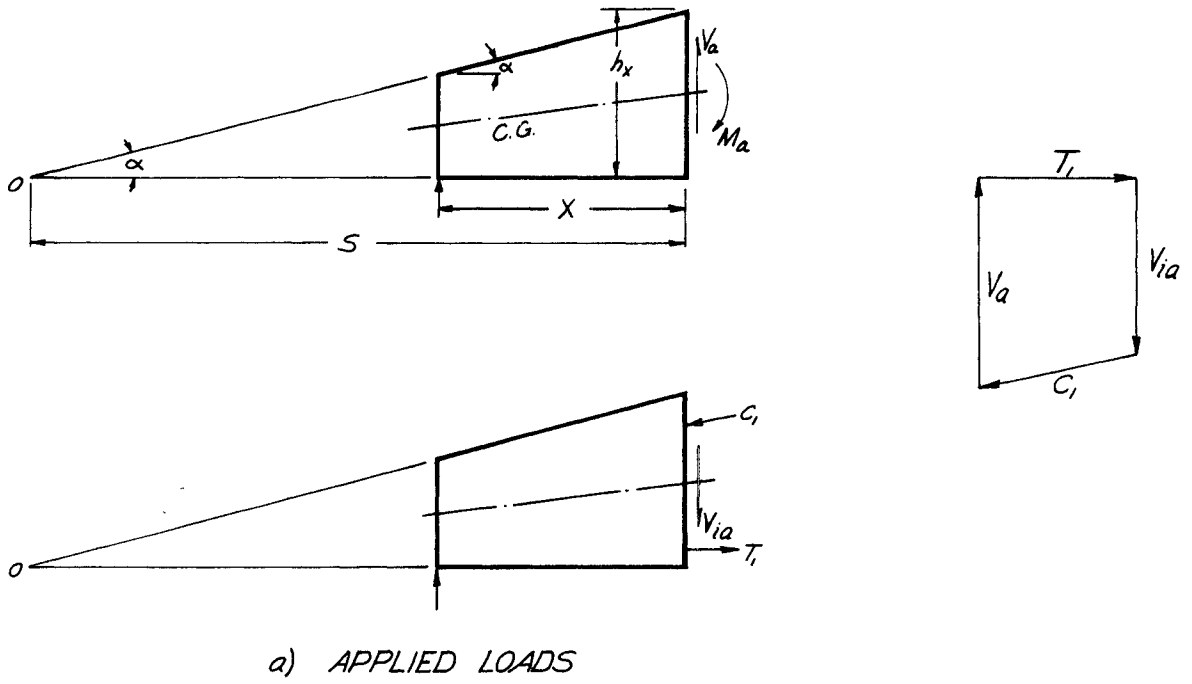
FIGURE 6    FREE-BODY DIAGRAMS FOR SHEAR REDUCTION

-104-
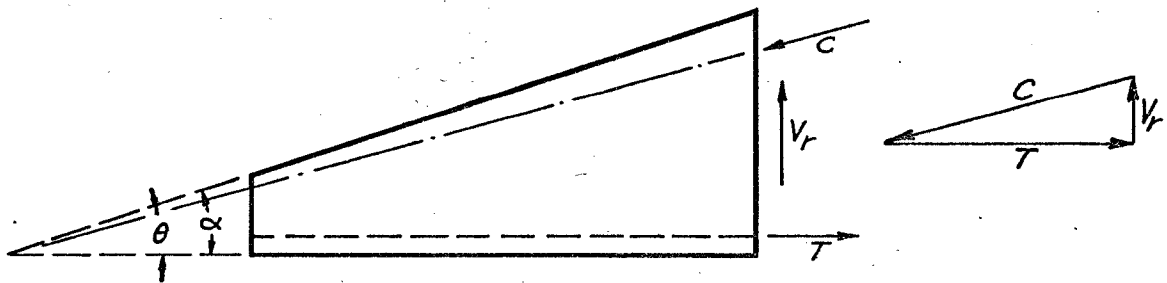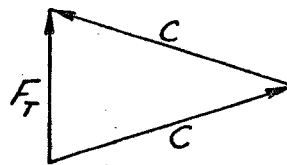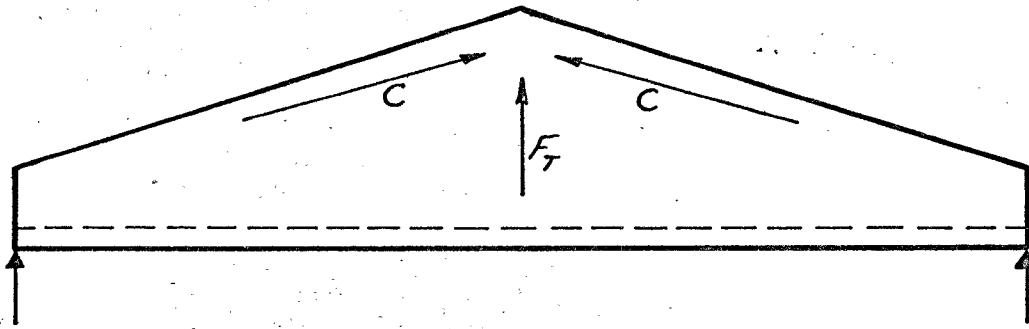
FOR CROWN AT MIDSPAN: $F_T = 2V_r$, [SEE EQS (37a) AND (38a)]

FIGURE 7.   TENSILE FORCE AT CROWN

-105-
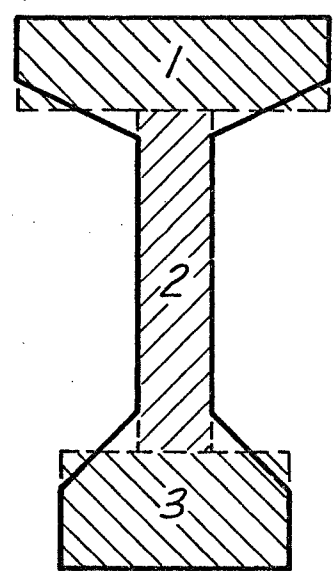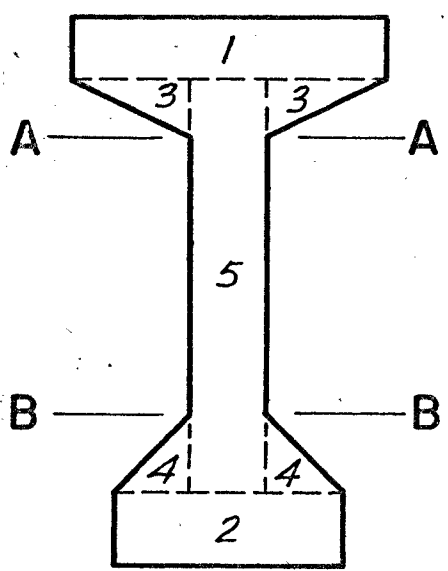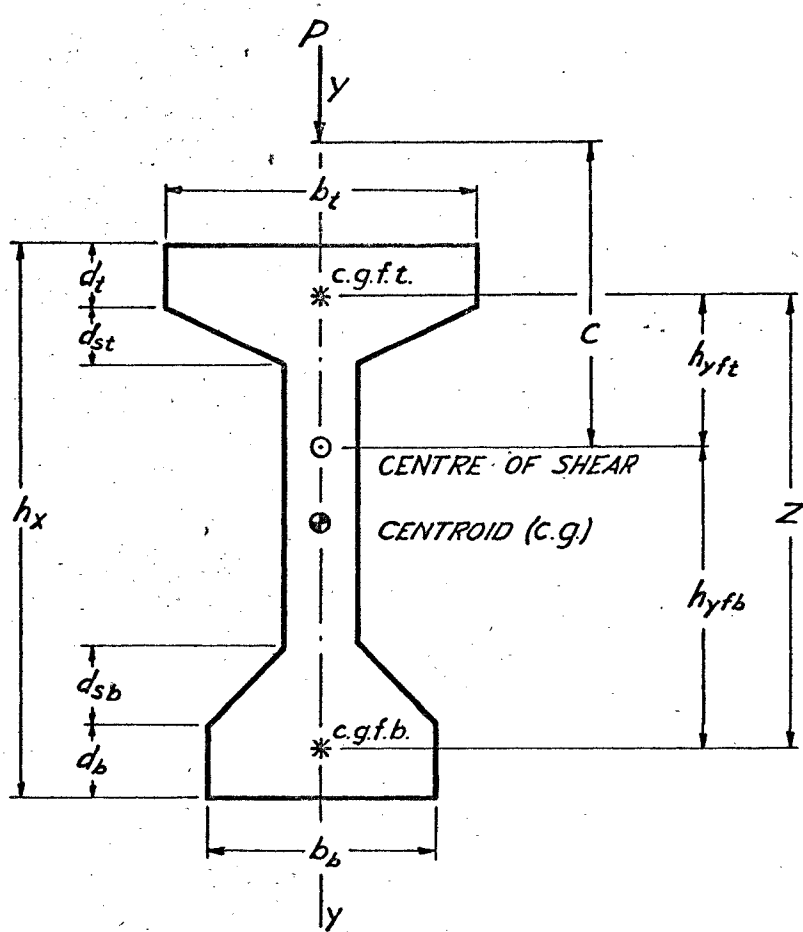
FIGURE 8. PARTITIONING OF CROSS-SECTION FOR FINDING TORSIONAL AND FLEXURAL RIGIDITIES

-106-

CROSS-SECTION   LONGITUDINAL SECTION   STRAIN DISTRIBUTION
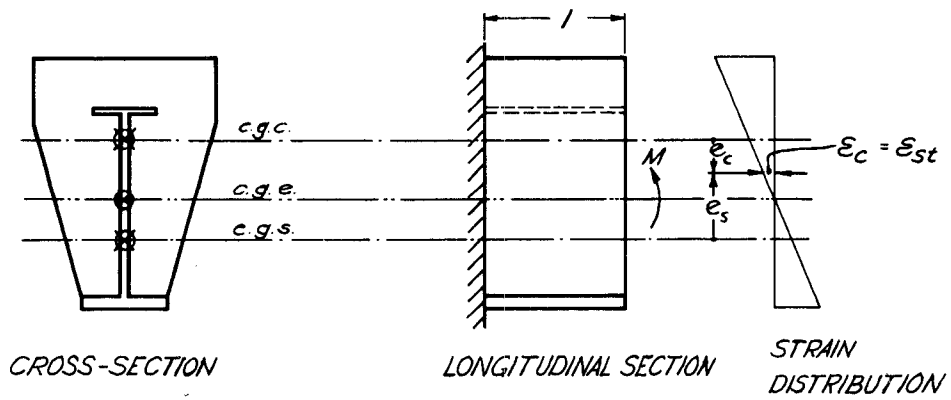
a) COMPOSITE SECTION OF CONCRETE BONDED TO STEEL

CONCRETE PART   STRAIN DISTRIBUTION   STEEL PART   STRAIN DISTRIBUTION
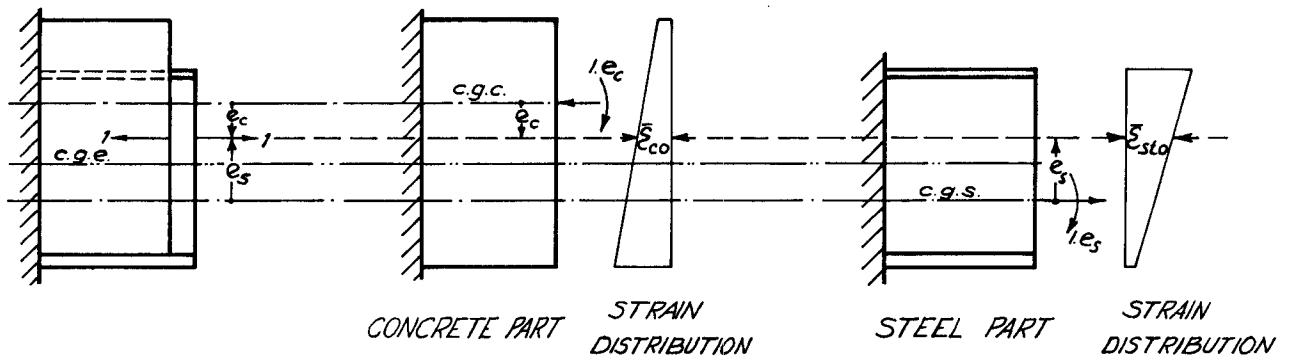
b) UNIT LOADS APPLIED TO CONCRETE AND STEEL PARTS

PRESTRESSING TENDON
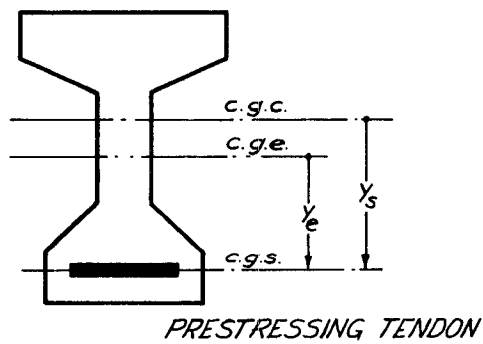
c) PRESTRESSED CONCRETE CROSS-SECTION

FIGURE 9.

-107-

# LEGEND

| CRITICAL SECTIONS FOR FLEXURE | CRITICAL SECTIONS FOR PRINCIPAL TENSILE STRESSES |

—————————— : LOCATION OF CRITICAL SEC-
TION ACCORDING TO FORMULA
DERIVED FROM GEOMETRICAL
CONSIDERATION, EQ. (9a)

□———□———□ (I) : LOCATION OF CRITICAL SECTION
UNDER WORKING LOADS WITH
MAXIMUM CREEP AND SHRINK-
AGE EFFECTS

×———×———× : LOCATION OF MAXIMUM COM-
PRESSIVE STRESS IN TOP
CONCRETE FIBRE

——Δ———Δ—— (2) : LOCATION OF CRITICAL SECTION
UNDER WORKING LOADS WITH
MINIMUM CREEP AND SHRINK-
AGE EFFECTS

○———○———○ : LOCATION OF MAXIMUM TEN-
SILE STRESS (OR MINIMUM
COMPRESSIVE STRESS) IN
BOTTOM CONCRETE FIBRE

———..———..—— (3) : LOCATION OF CRITICAL SECTION
UNDER ULTIMATE LOADS WITH
MAXIMUM CREEP AND SHRINK-
AGE EFFECTS

○——─○——─○ : LOCATION OF MAXIMUM
STRESS IN BOTTOM LAYER
OF PRESTRESSING STEEL

———·———·—— (4) : LOCATION OF CRITICAL SECTION
UNDER ULTIMATE LOADS WITH
MINIMUM CREEP AND SHRINK-
AGE EFFECTS

: FROM THE FORMULA DERIVED
BY MEANS OF CALCULUS:
(FIGS. II TO 20)

   a) LOCATION OF MINIMUM
      TENSILE STRESS IN TOP
      LAYER OF PRESTRESSING
      STEEL

— COMBINATIONS —

   b) LOCATION OF MAXIMUM
      COMPRESSIVE STRESS IN
      TOP LAYER OF CONVEN-
      TIONAL STEEL REINFOR-
      CEMENT REPLACING TOP
      LAYER OF PRESTRESSING
      STEEL

□—Δ—□—Δ—□ (5) : (I) + (2)

×———×———× {

———…———…—— (6) : (3) + (4)

: FROM THE GENERAL PRO-
GRAMME: (FIGS. 2I TO 25)

□—·Δ·—□—·Δ·—□ (7) : (I) + (2) + (3) + (4)

   LOCATION OF MAXIMUM
   TENSILE STRESS IN TOP
   LAYER OF PRESTRESSING
   STEEL

**CASE I** : FLEXURAL TENSILE STRESSES
CARRIED BY CONCRETE; SEE
SECTIONS 2.I.3.I AND 2.I.3.2

IN FIGS. I7, I8, I9 & 20

—————— : LOCATION OF CRITICAL SECTION
ACCORDING TO FORMULA
DERIVED FROM GEOMETRICAL
CONSIDERATION, EQ. (9a)

**CASE II** : FLEXURAL TENSILE STRESSES
ASSUMED TO BE CARRIED BY
ADEQUATE STEEL REINFOR-
CEMENTS; SEE SECTIONS
2.I.4.I AND 2.I.4.2

—·— : LOCATION OF CRITICAL SEC-
TIONS ACCORDING TO FOR-
MULAE DERIVED BY MEANS
OF CALCULUS: EQS, (20), (23),
(26) & (29)

-108-

# LIST OF SYMBOLS USED IN THE GRAPHS

$\alpha$      Angle between top and bottom edges of an inclined roof girder (inclination angle of the top flange)

$L$      Length of girder

$x$      Distance of any arbitrary section from the support

$\frac{1}{2}\xi = x/L$

$x_{cr}$      Distance of the critical section from the support

$\frac{1}{2}\xi_{cr} = x_{cr}/L$

$f_{ct}$      Stress in extreme top concrete fibre

$f_{cb}$      Stress in extreme bottom concrete fibre

$f_{s1}$      Stress in bottom layer of prestressing steel

$f_{s2}$      Stress in top steel layer (prestressing steel tendons or conventional steel reinforcements)

$f_{so1}$      Initial stress in the bottom layer of the prestressing steel

$f_{so2}$      Initial stress in top steel layer (for non-tensioned top steel layer $f_{so2} = 0.0$)

$y_{cr}$      Position of maximum principal tensile stress relative to the soffit of the girder at the critical section

$h_{cr}$      Total height of the girder at the critical section

$\zeta_{cr} = y_{cr}/h_{cr}$

$\gamma_{cr}$      Angle between the direction of the maximum principal tensile stress and the horizontal axis at the critical section

-109-
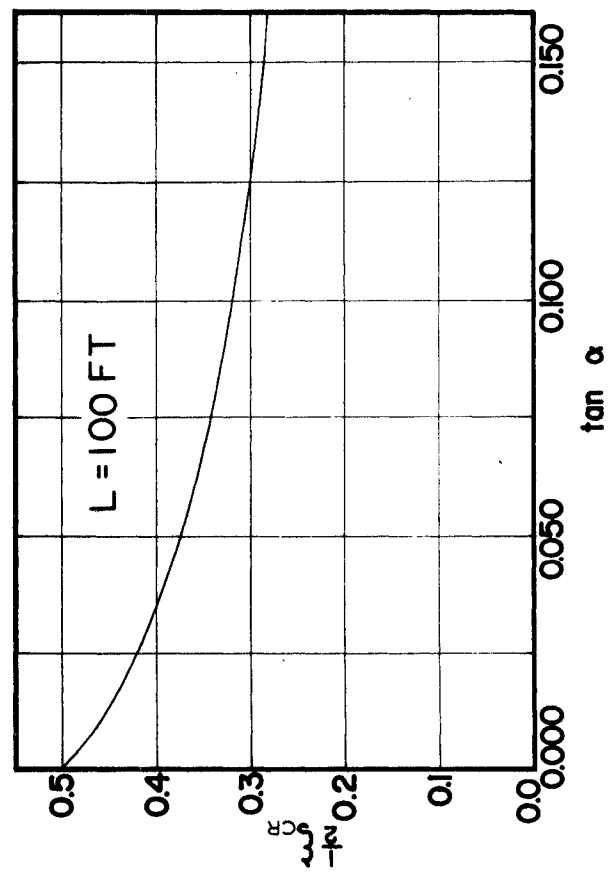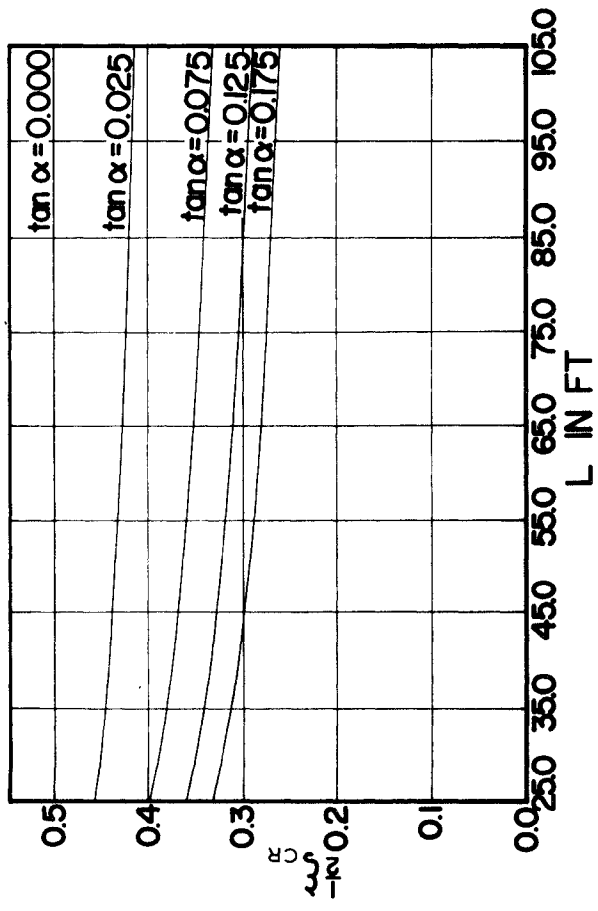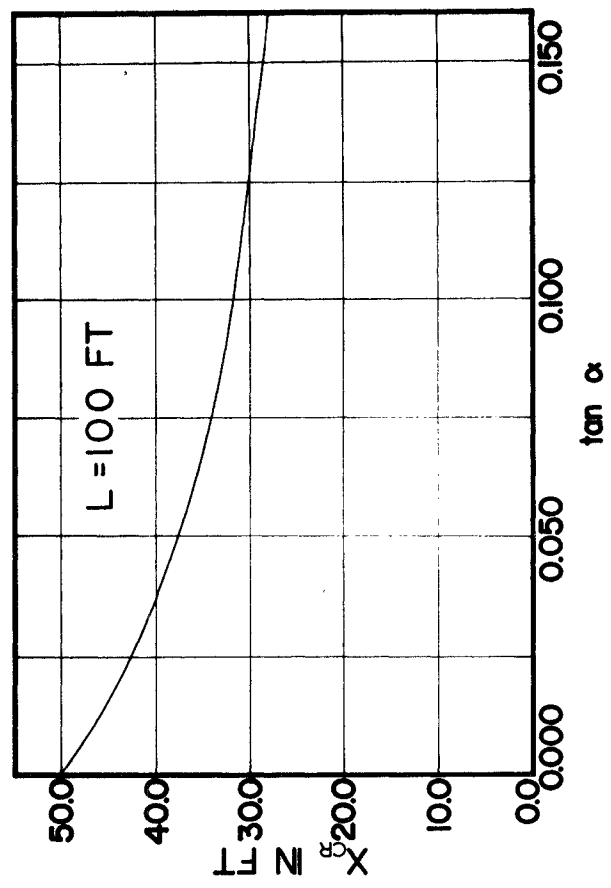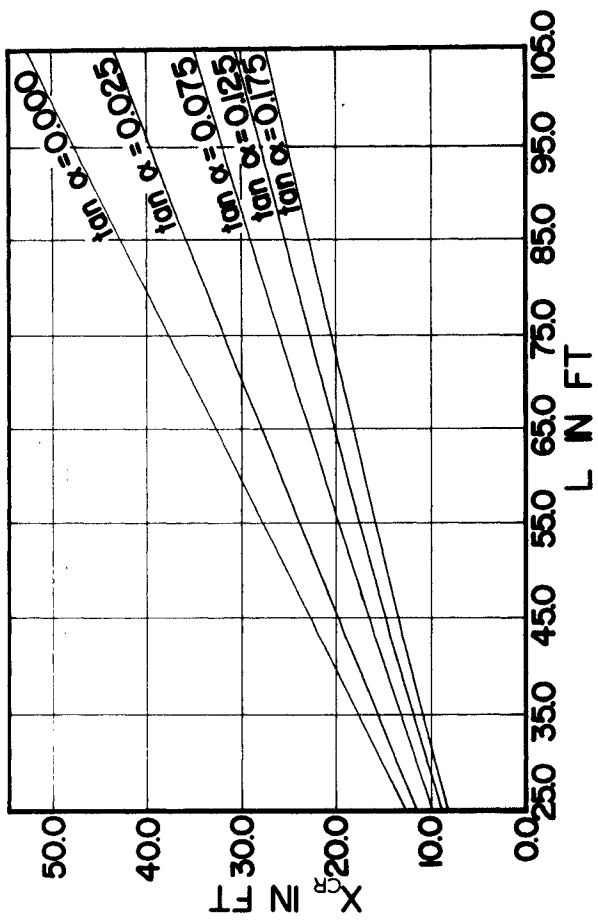
FIGURE 10

CRITICAL SECTION LOCATIONS FOR FLEXURE BASED ON EQS. (9a) & (15a)

-110-
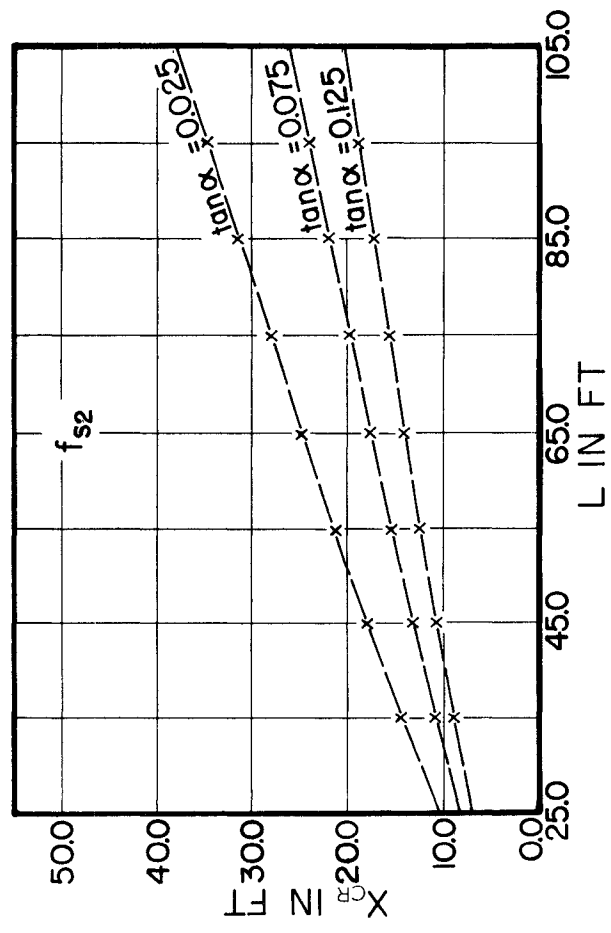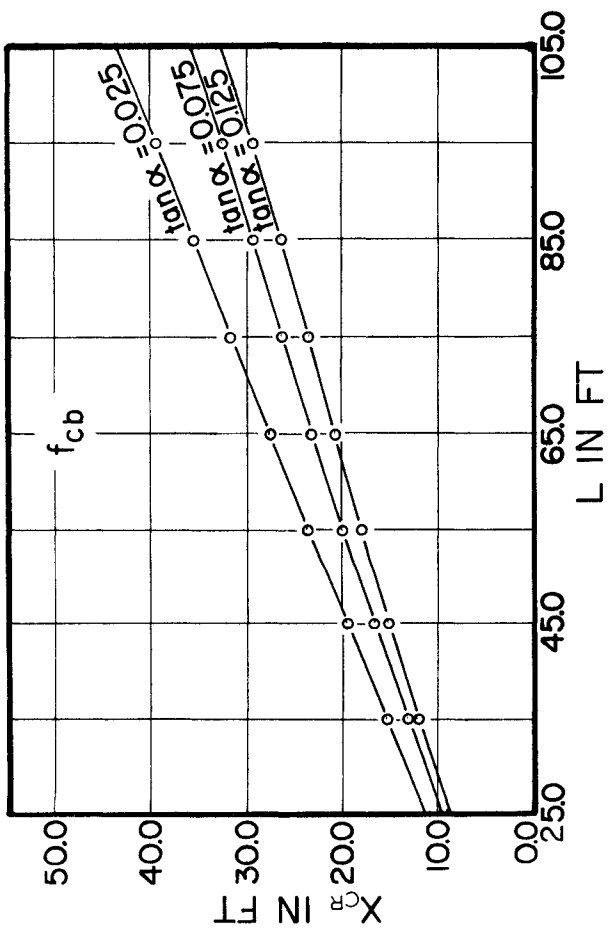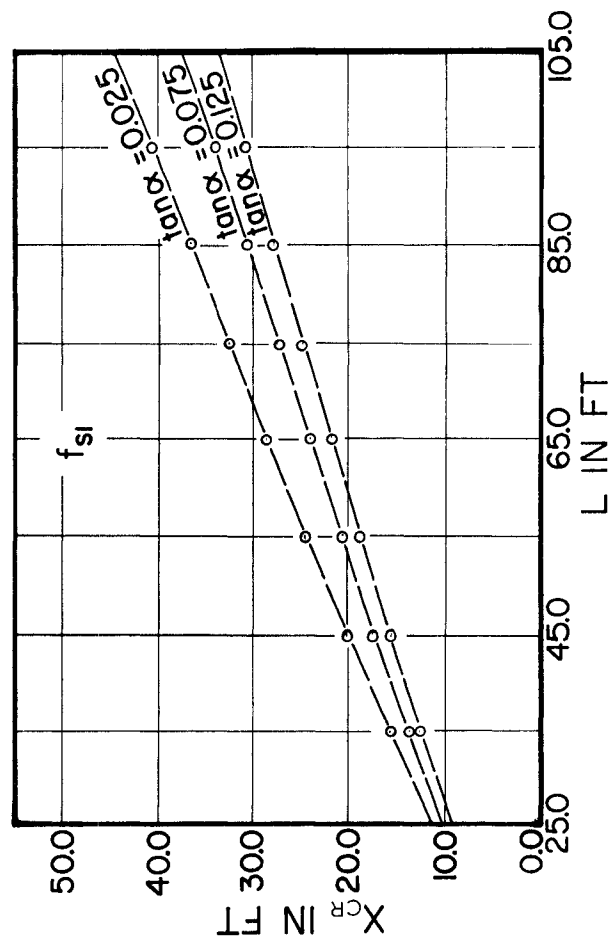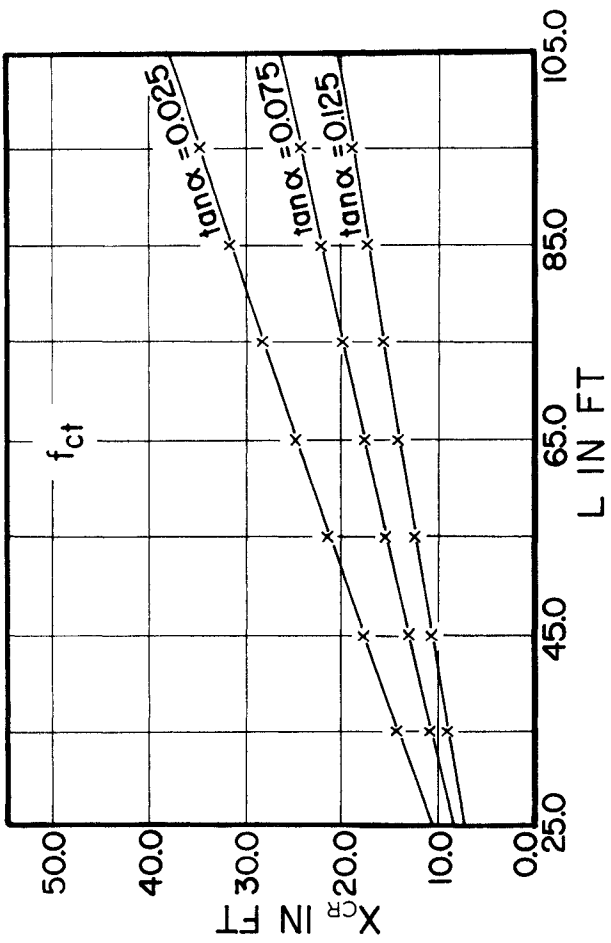
FIGURE 11

CRITICAL SECTION LOCATIONS FOR FLEXURE BASED ON EQS. (20), (23), (26) & (29)

FULLY PRESTRESSED
$f_{SO2} = 100.0$ KSI
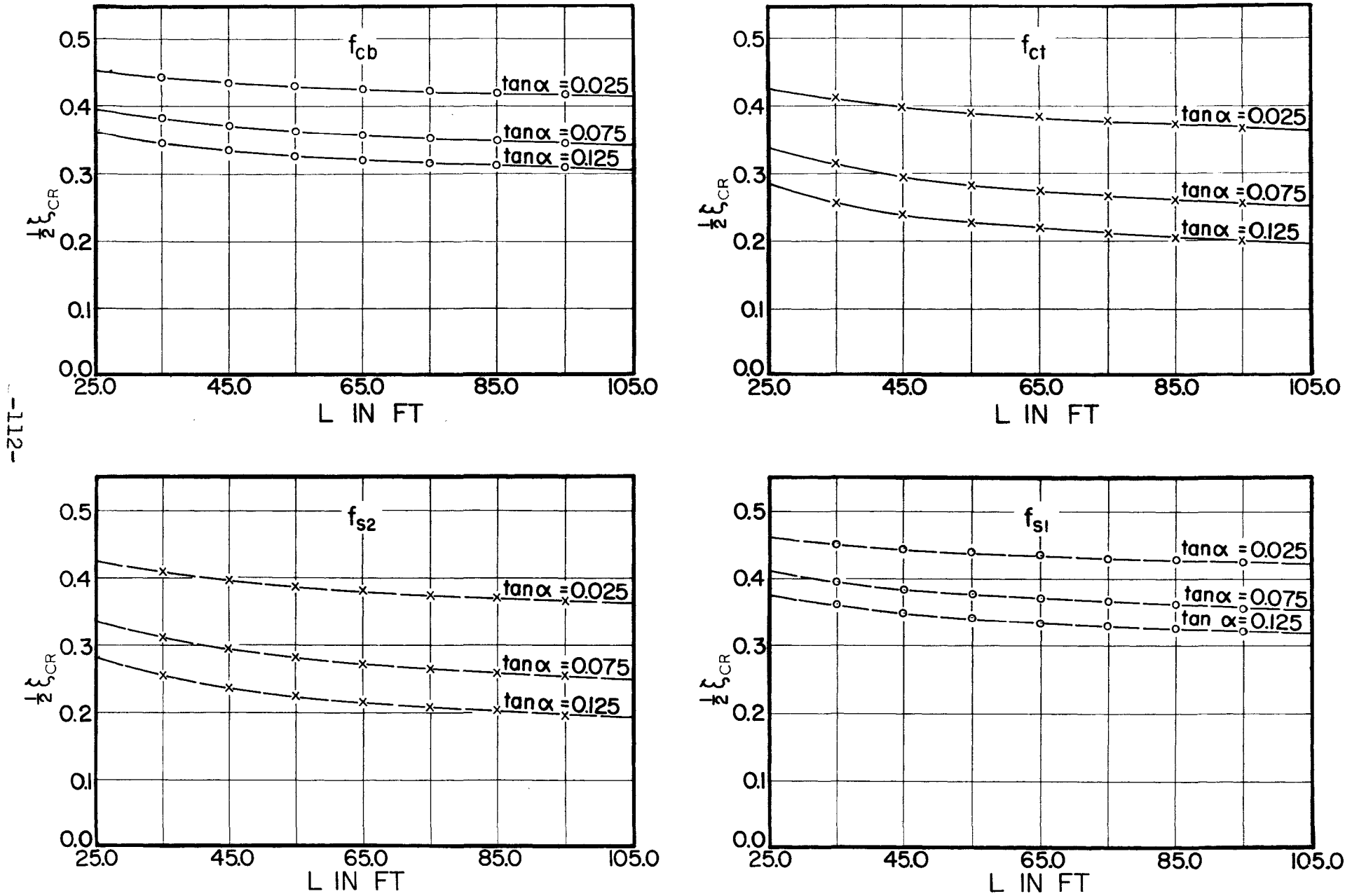
FIGURE 12

DIMENSIONLESS LOCATIONS OF CRITICAL SECTIONS FOR FLEXURE BASED ON EQS. (20), (23), (26) & (29)

FULLY PRESTRESSED
$f_{SO2} = 100.0$ KSI
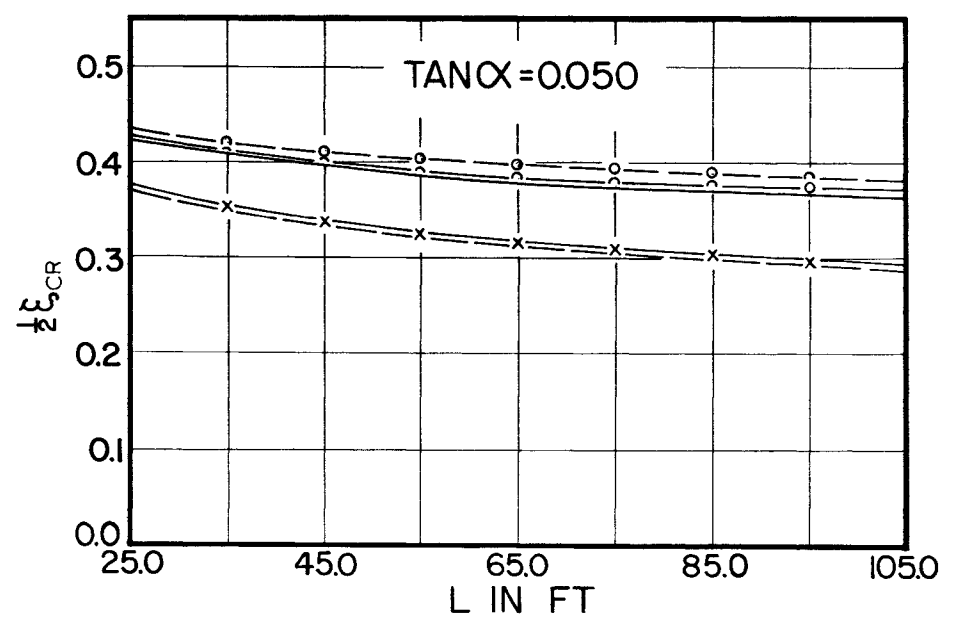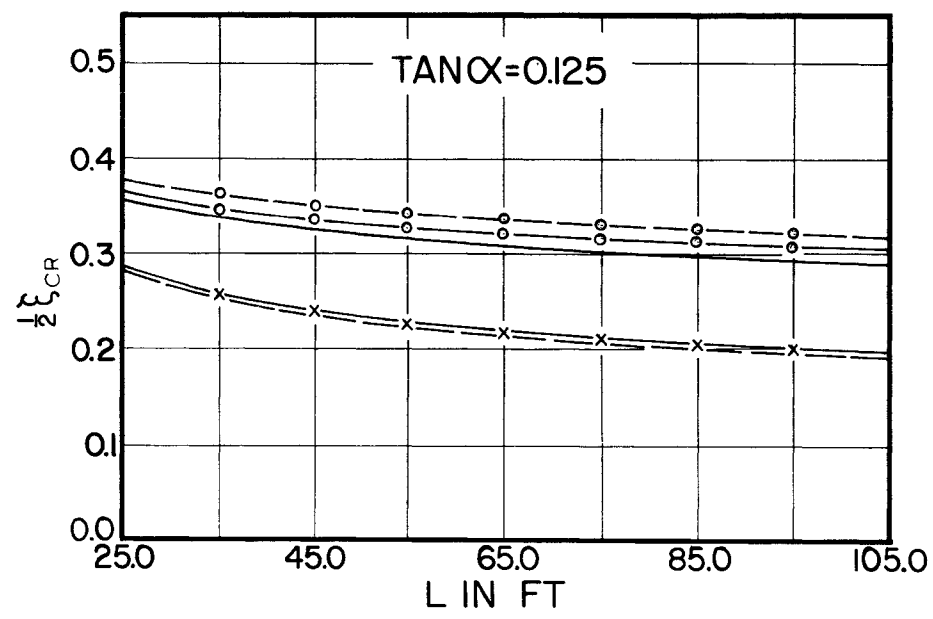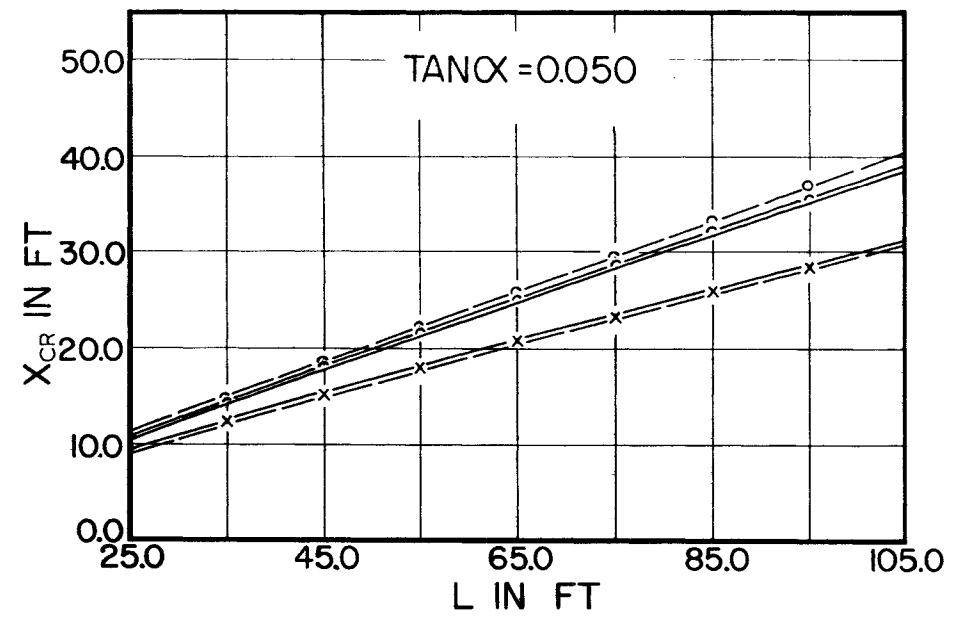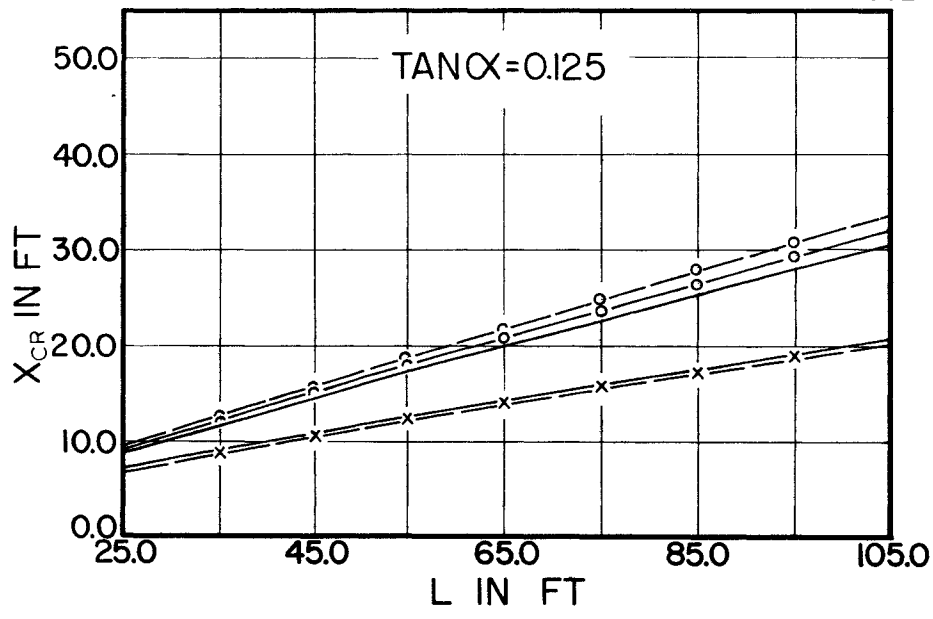


FIGURE 13

COMPARISON OF CRITICAL SECTION LOCATIONS FOR FLEXURE BASED ON EQS. (9a), (15a), (20), (23), (26) & (29)

FULLY PRESTRESSED
$f_{SO2} = 0.0$ KSI
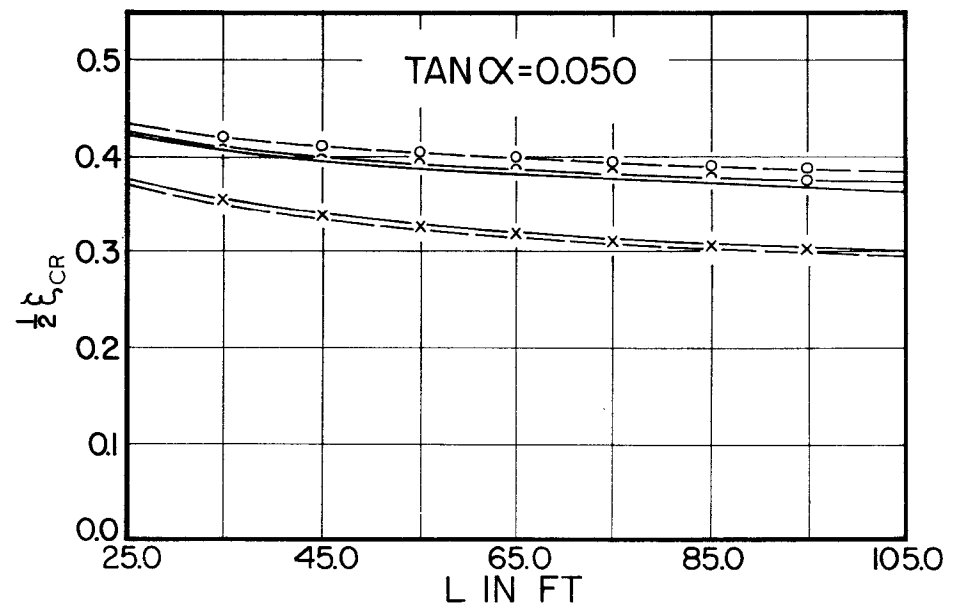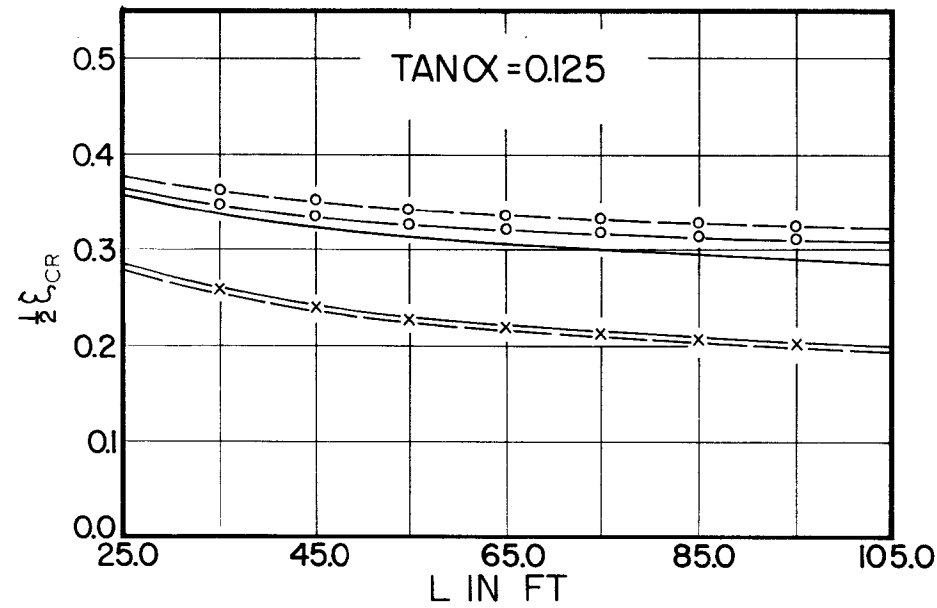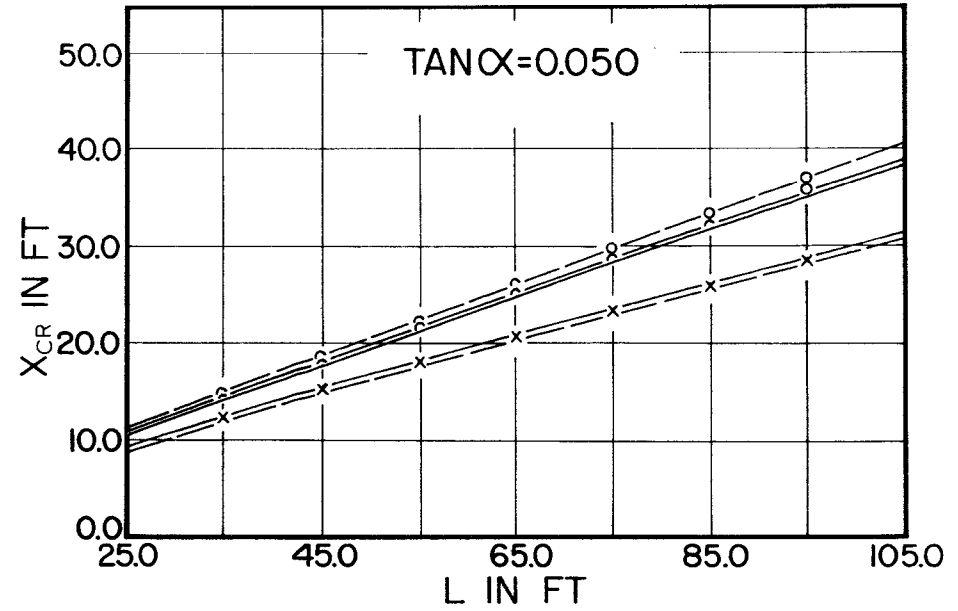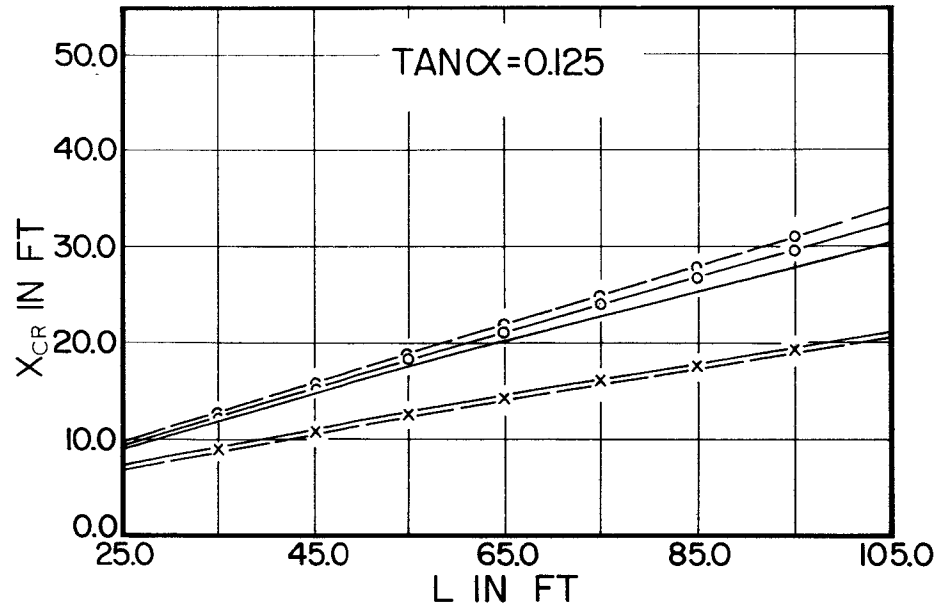
FIGURE 14

COMPARISON OF CRITICAL SECTION LOCATIONS FOR FLEXURE BASED ON EQS. (9a), (15a), (20), (23), (26) & (29)

-115-

PARTIALLY PRESTRESSED
$f_{SO2} = 100.0$ KSI
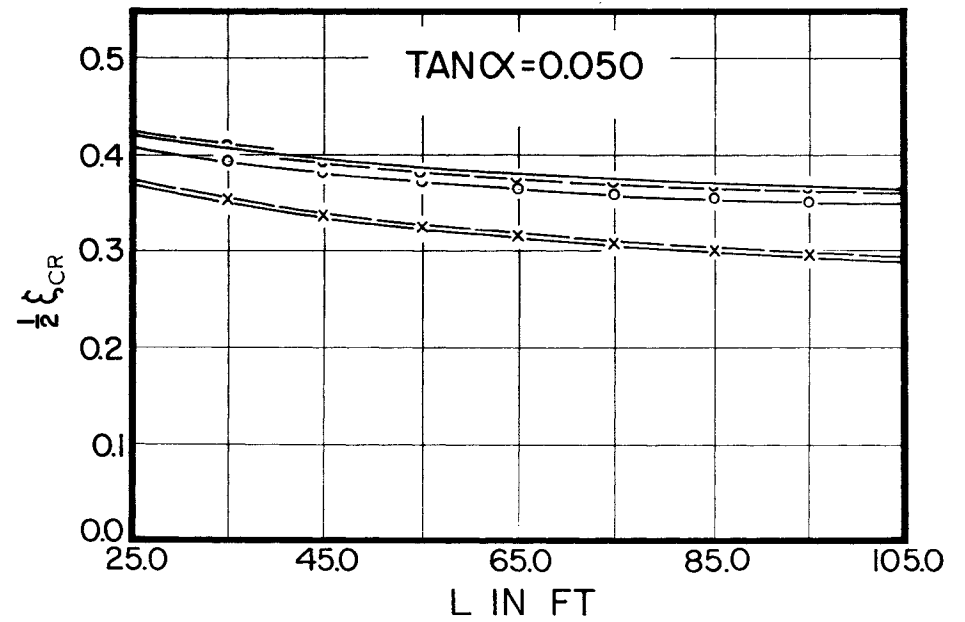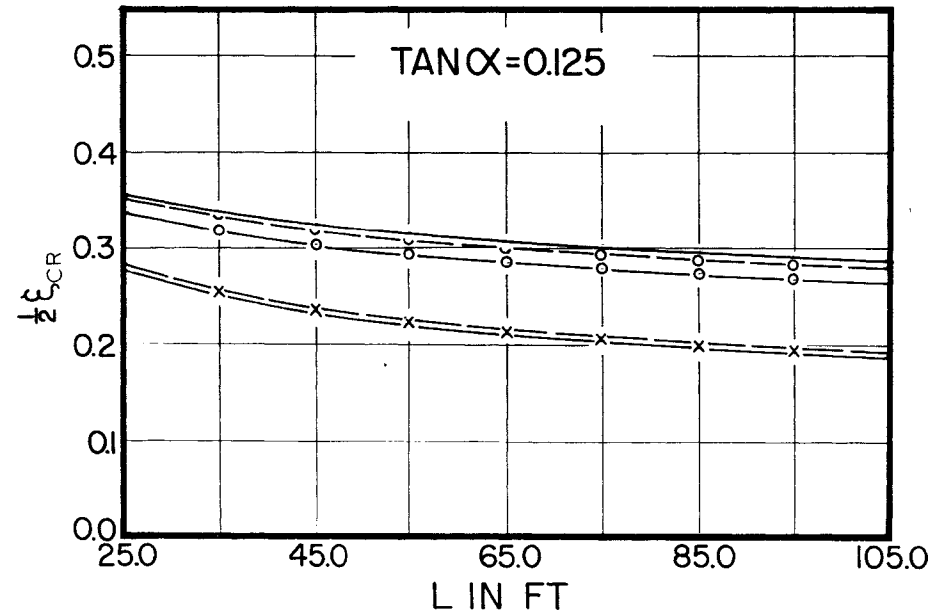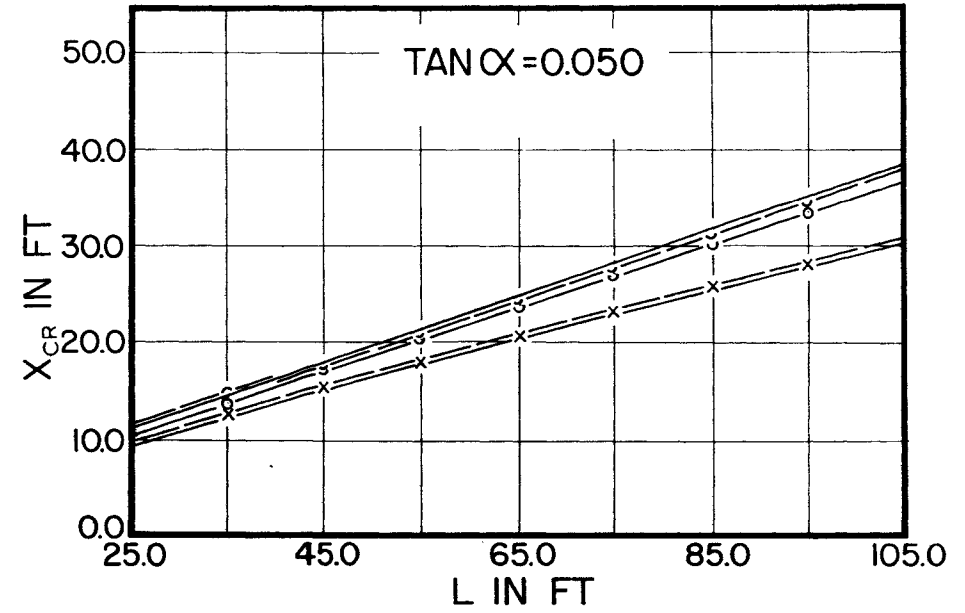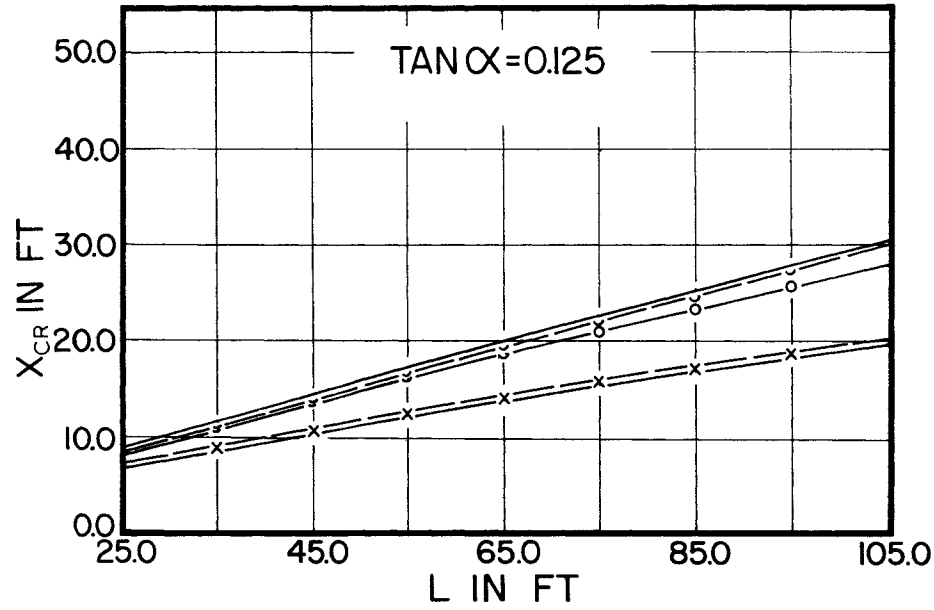
FIGURE 15

COMPARISON OF CRITICAL SECTION LOCATIONS FOR FLEXURE BASED ON EQS. (9a), (15a), (20), (23), (26) & (29)

$f_{SO2} = 100.0$ KSI
FULLY PRESTRESSED
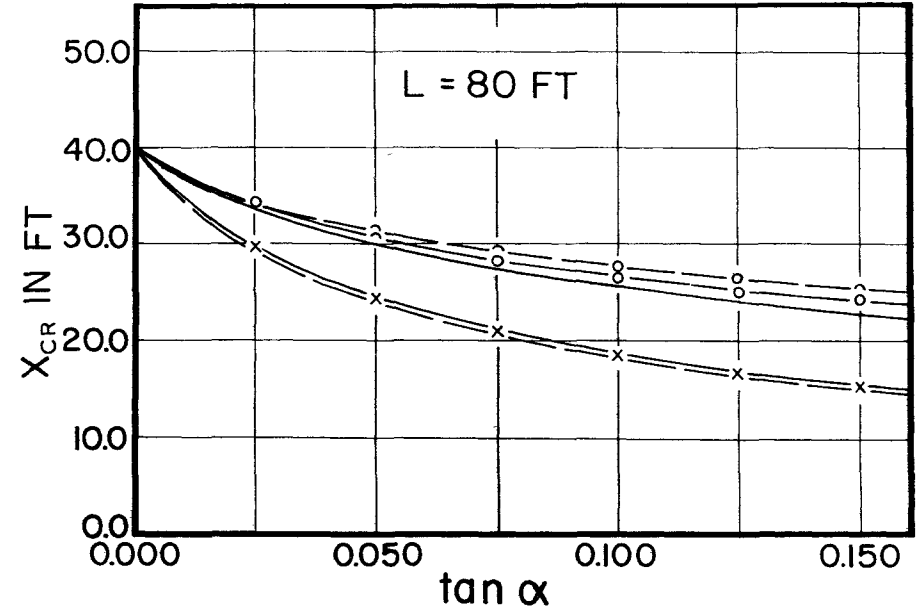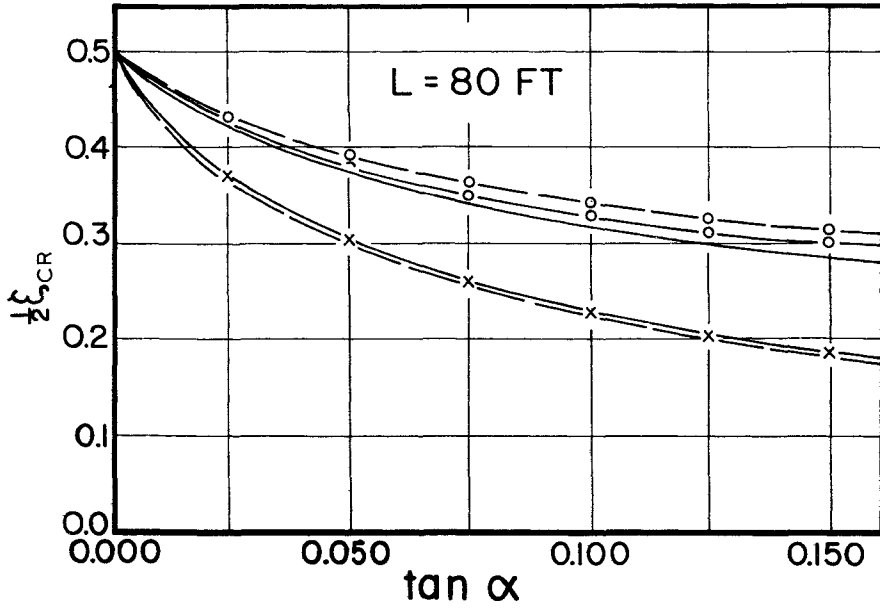


PARTIALLY PRESTRESSED
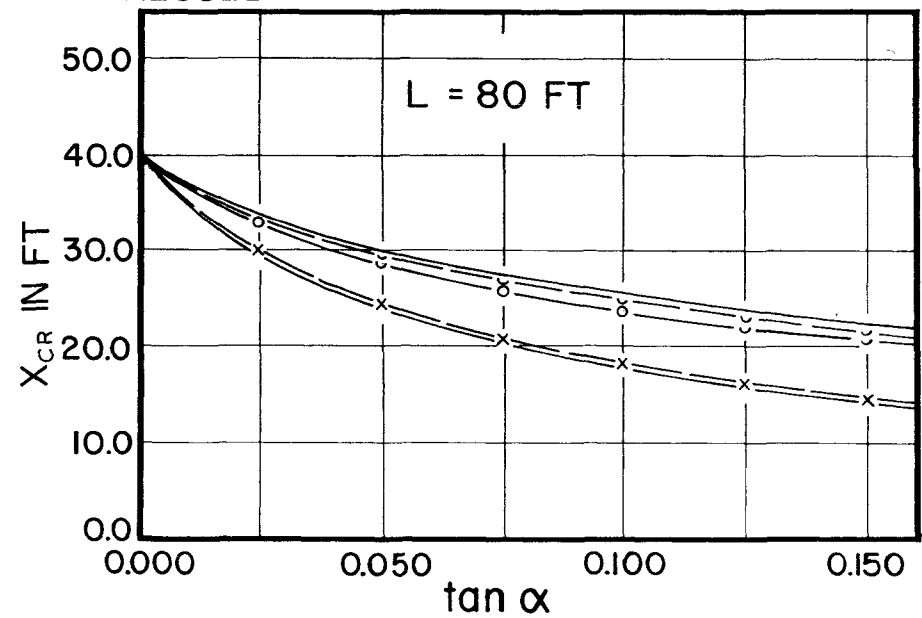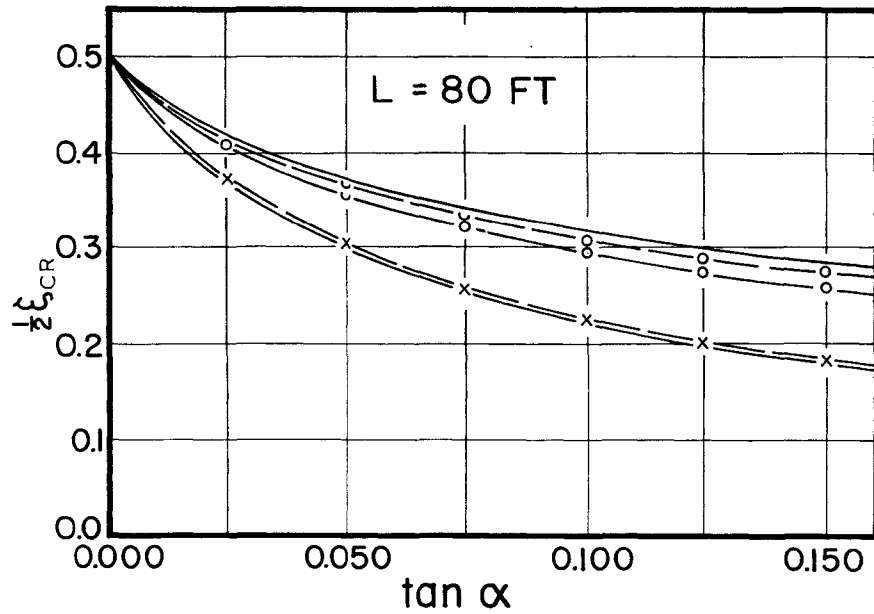


FIGURE 16

COMPARISON OF CRITICAL SECTION LOCATIONS FOR FLEXURE BASED ON EQS. (9a), (15a), (20), (23), (26) & (29) FOR 80 FT SPAN GIRDER

## FULLY PRESTRESSED
## $\tan \alpha = 0.050$
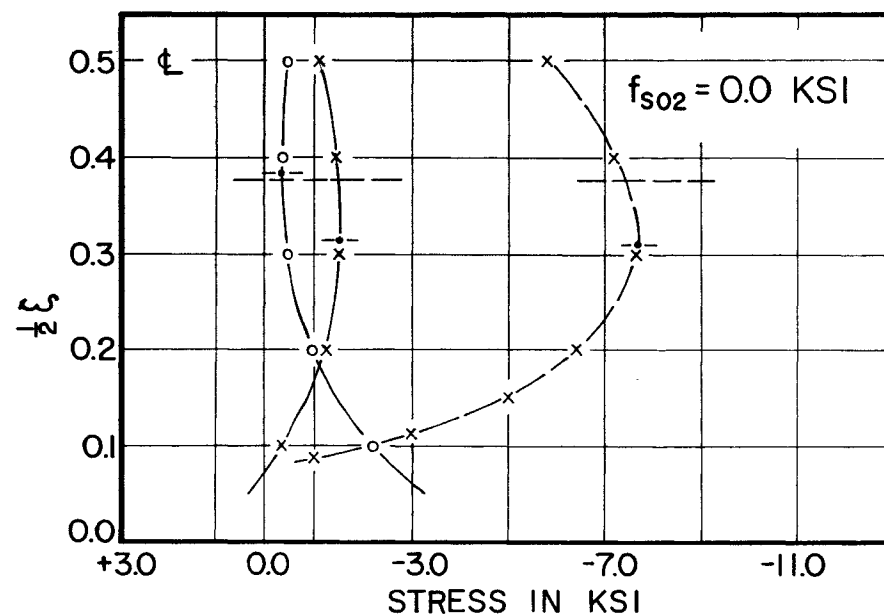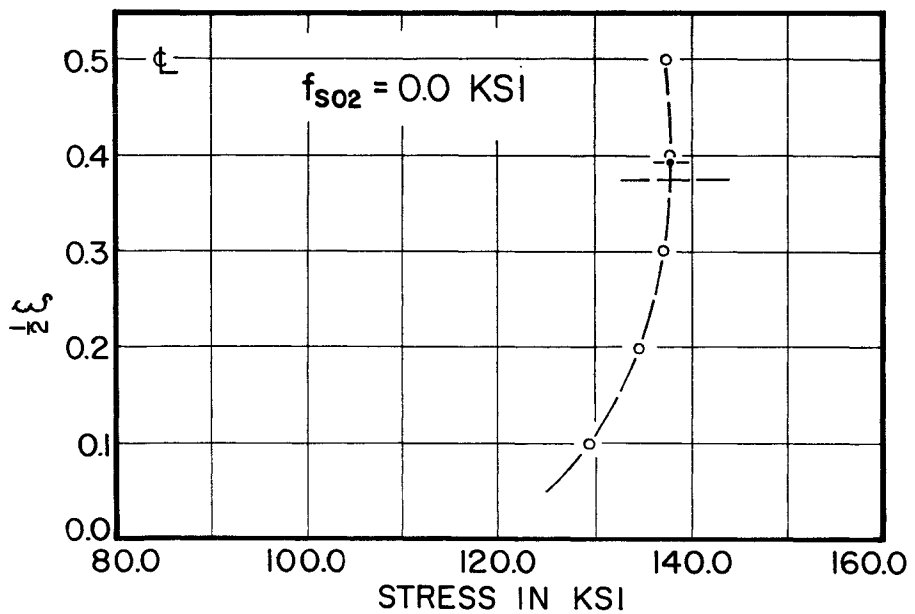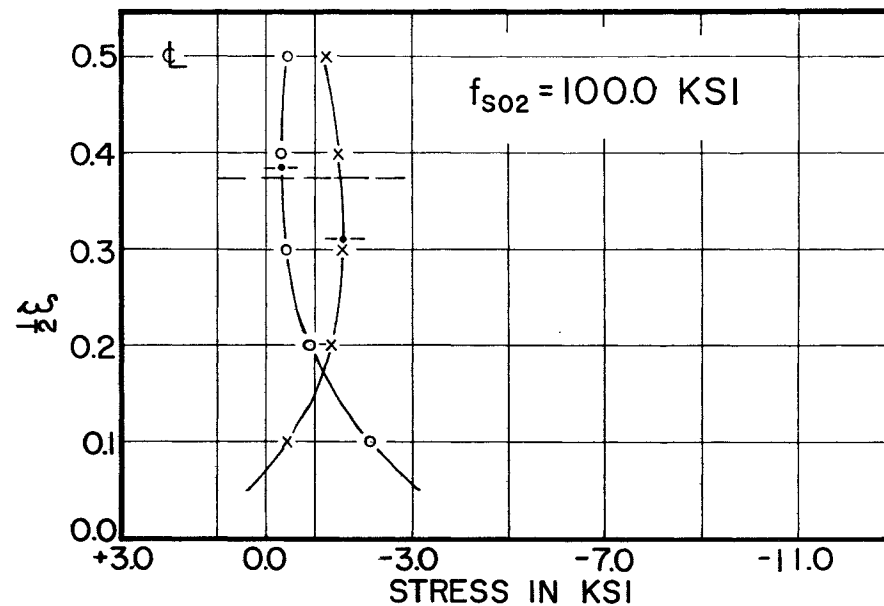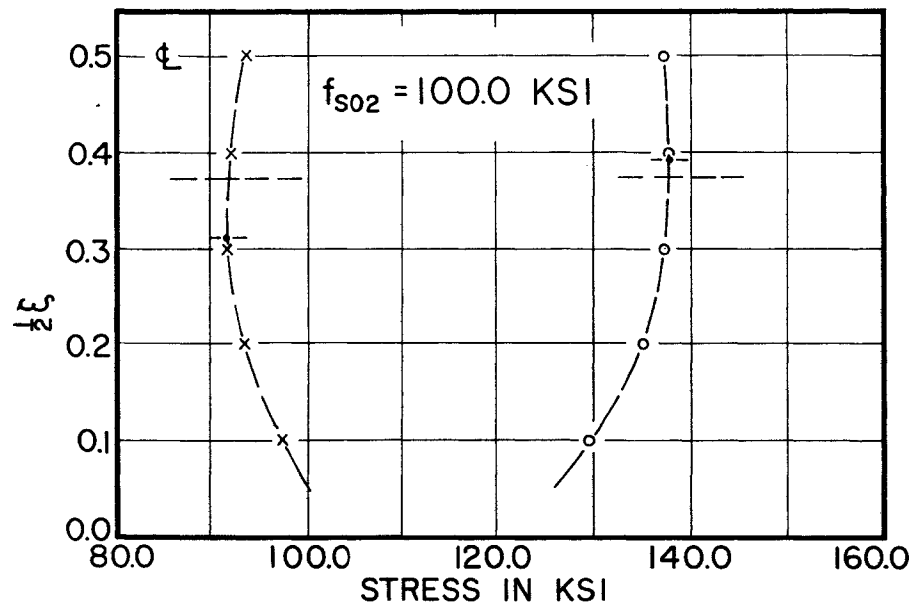


FIGURE 17

COMPARISON OF STRESS DISTRIBUTION BASED ON EQS. (18), (20), (21), (23), (24), (26), (27) & (29)

(DATA FOR 80 FT SPAN GIRDER)

## FULLY PRESTRESSED
### $\tan \alpha = 0.125$
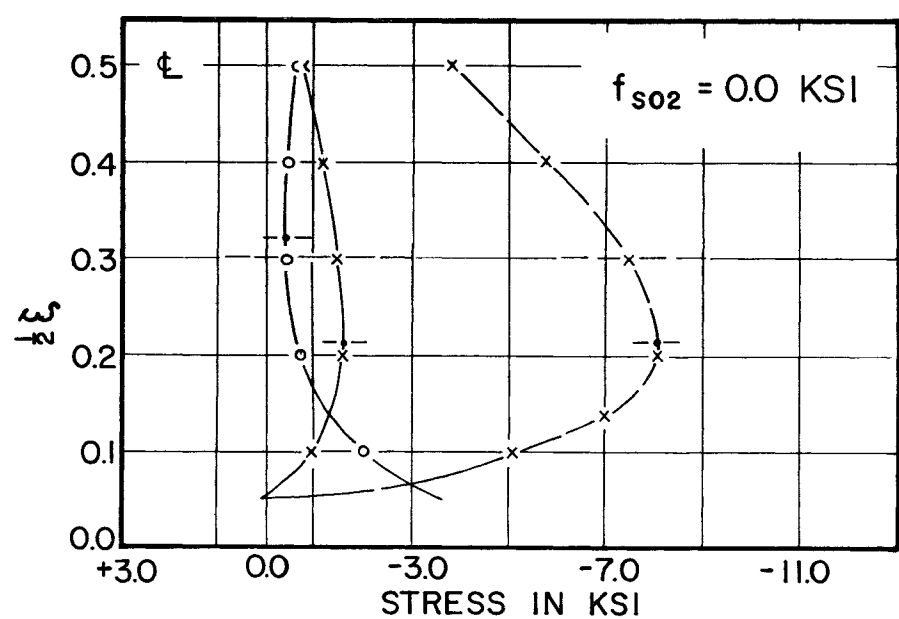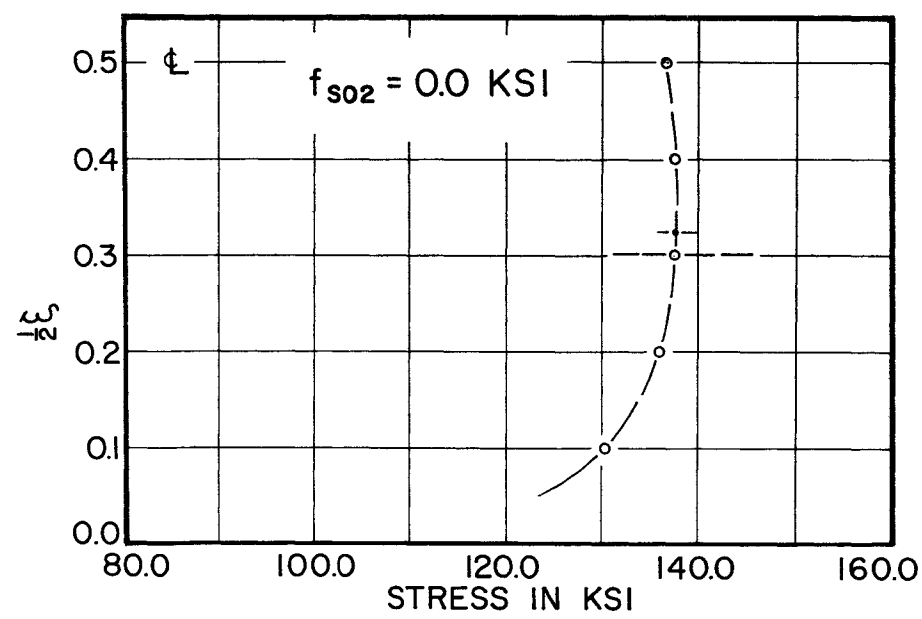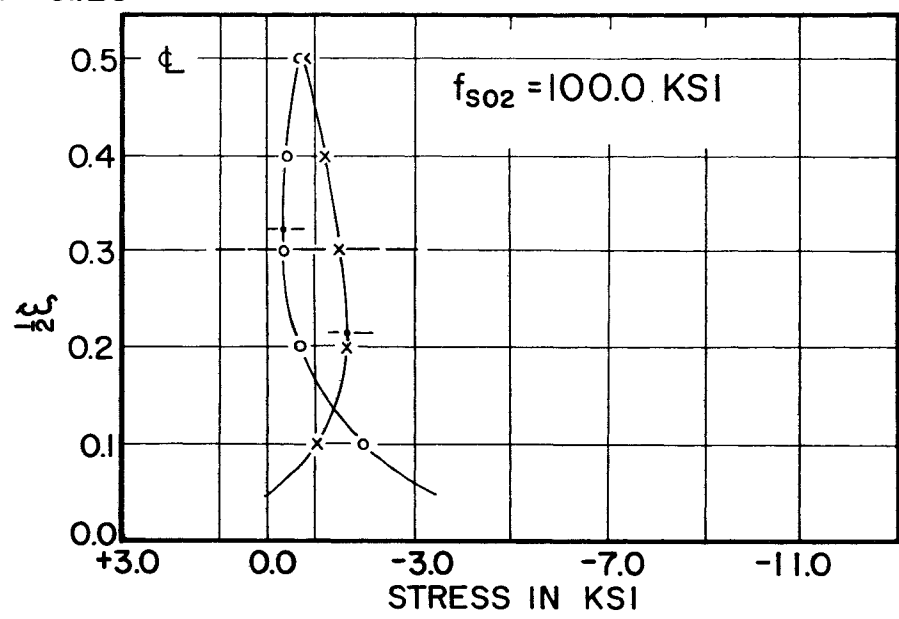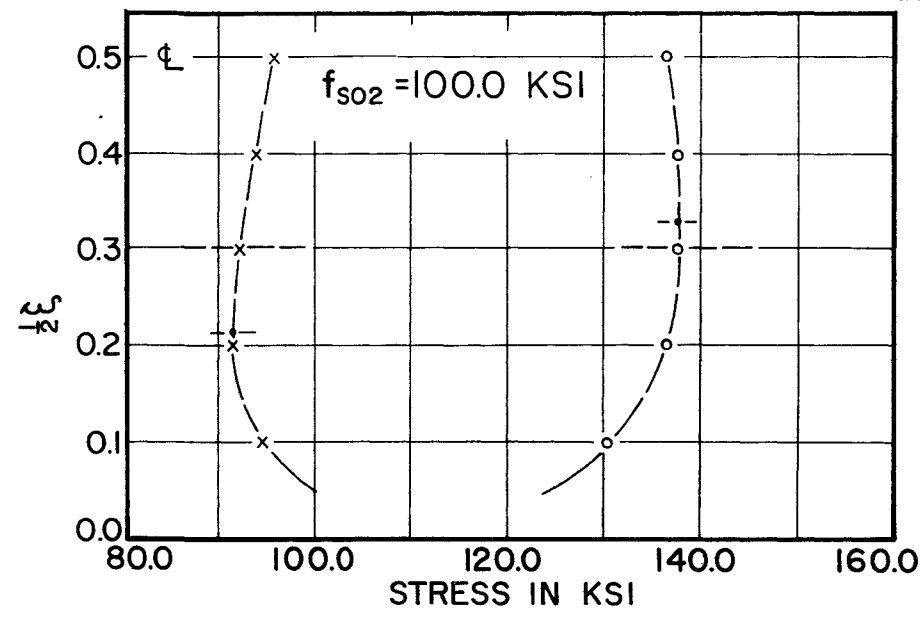


FIGURE 18

COMPARISON OF STRESS DISTRIBUTION BASED ON EQS. (18), (20), (21), (23), (24), (26), (27) & (29)

(DATA FOR 80 FT SPAN GIRDER)

# PARTIALLY PRESTRESSED
## $\tan \alpha = 0.050$
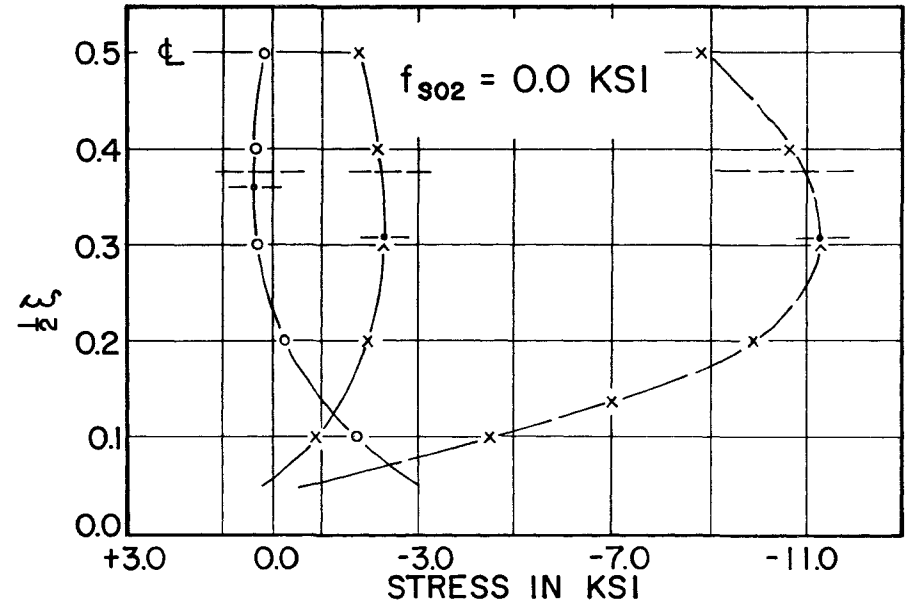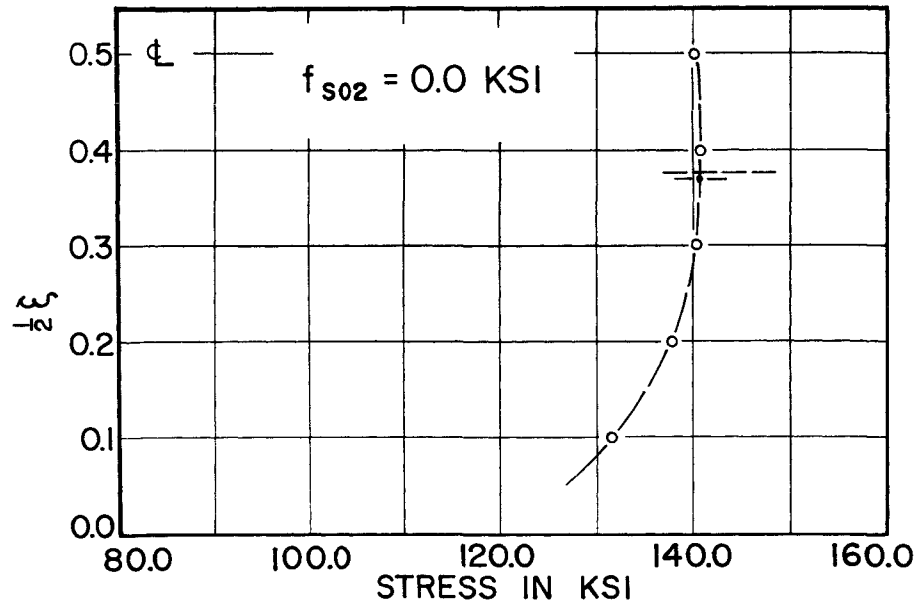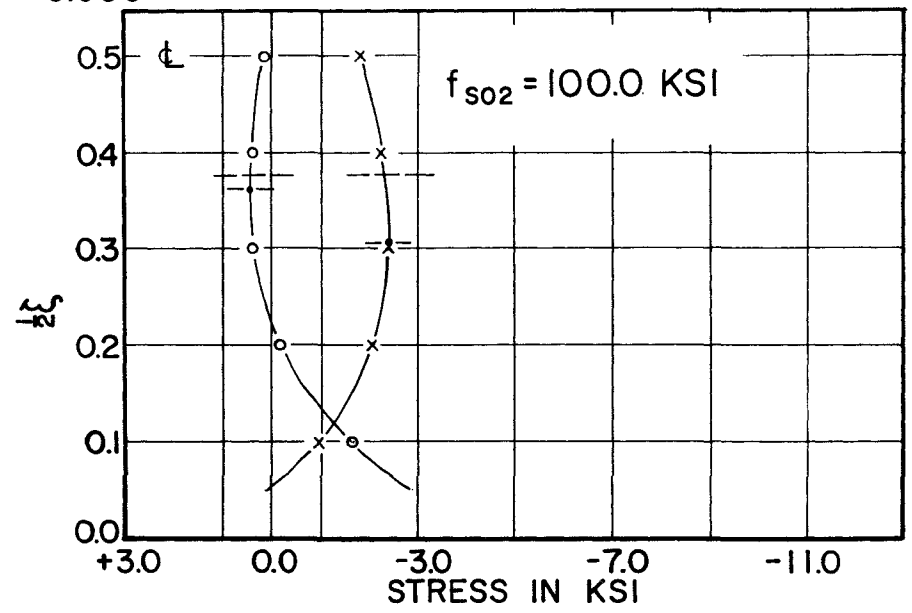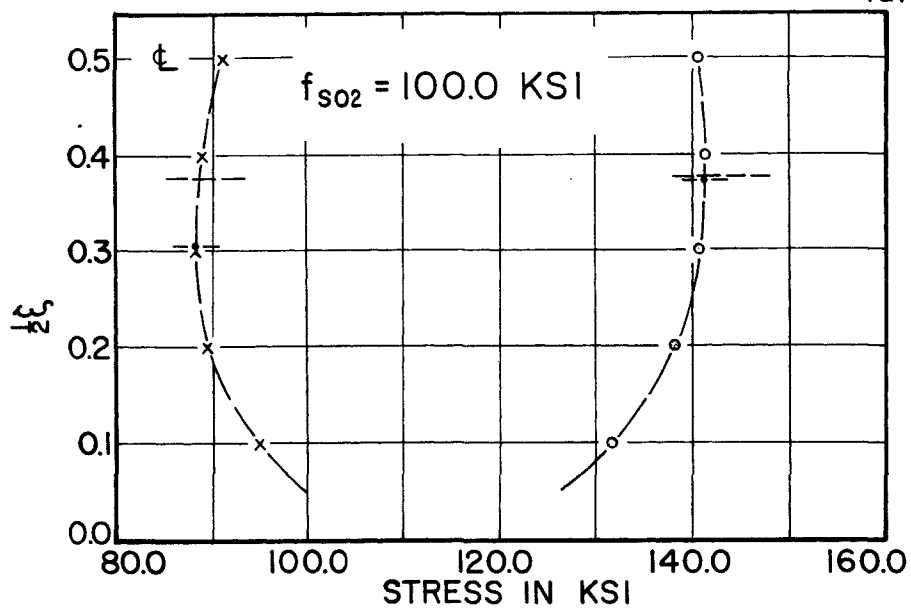


FIGURE 19

COMPARISON OF STRESS DISTRIBUTION BASED ON EQS. (18), (20), (21), (23), (24), (26), (27) & (29)

(DATA FOR 80 FT SPAN GIRDER)

PARTIALLY PRESTRESSED
tan α = 0.125
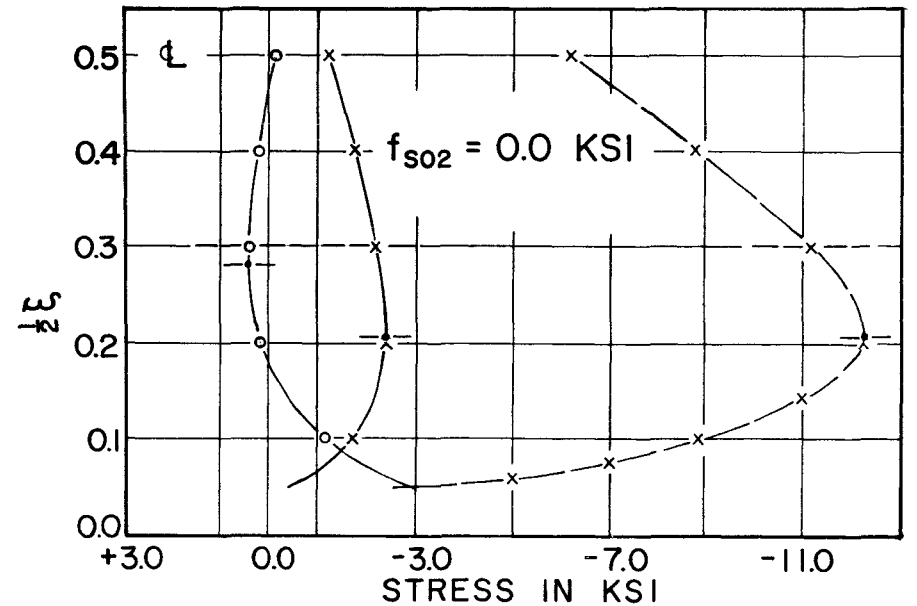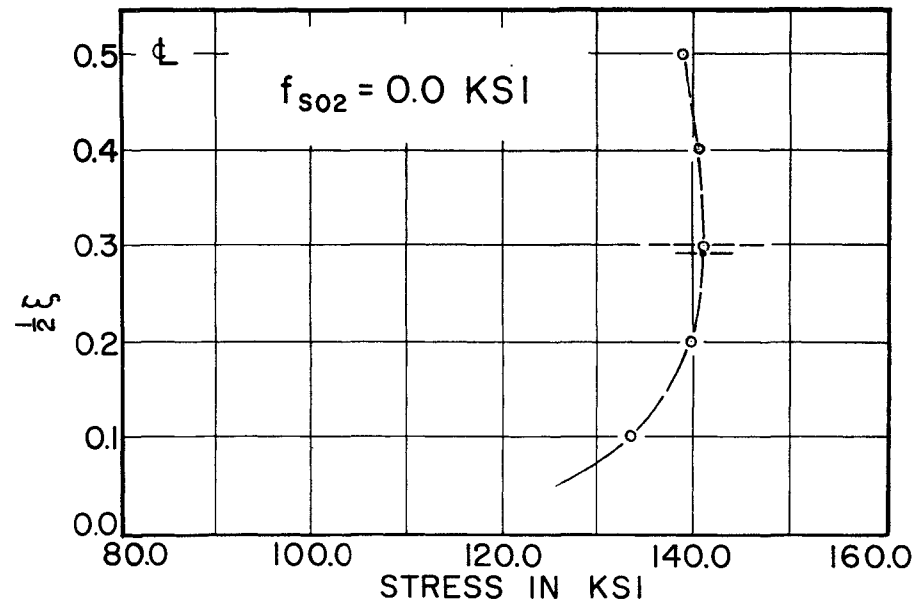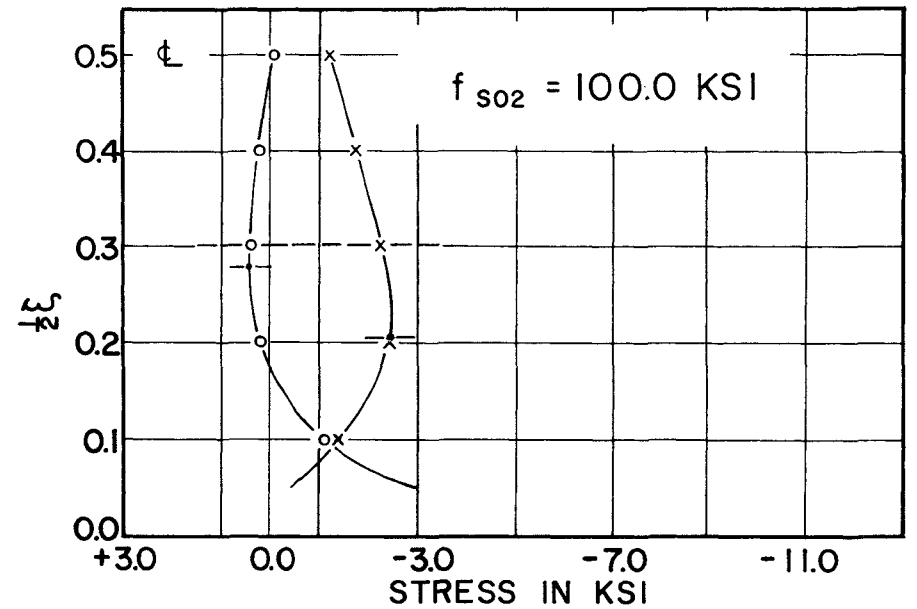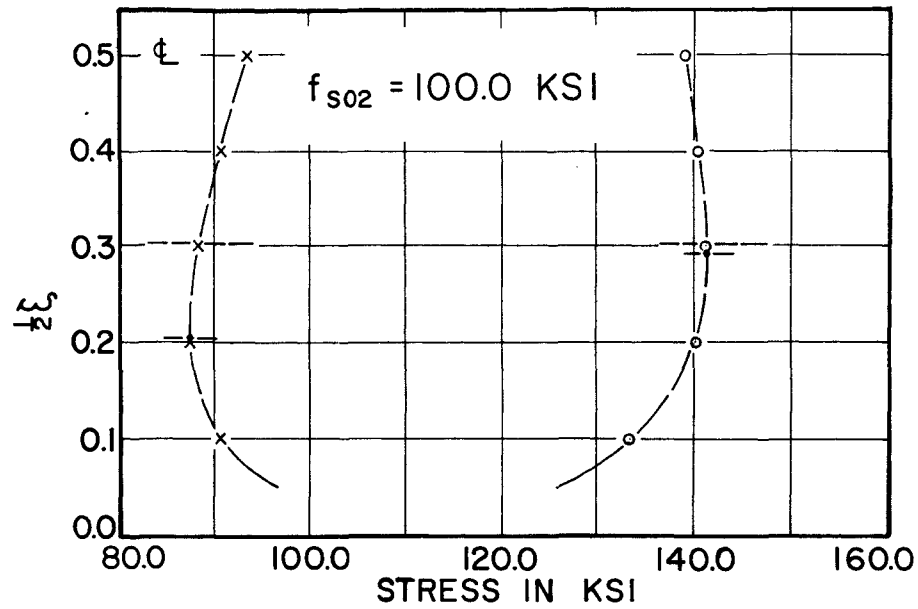
FIGURE 20

COMPARISON OF STRESS DISTRIBUTION BASED ON EQS. (18), (20), (21), (23), (24), (26), (27) & (29)

(DATA FOR 80 FT SPAN GIRDER)

MAX. CREEP & SHRINKAGE
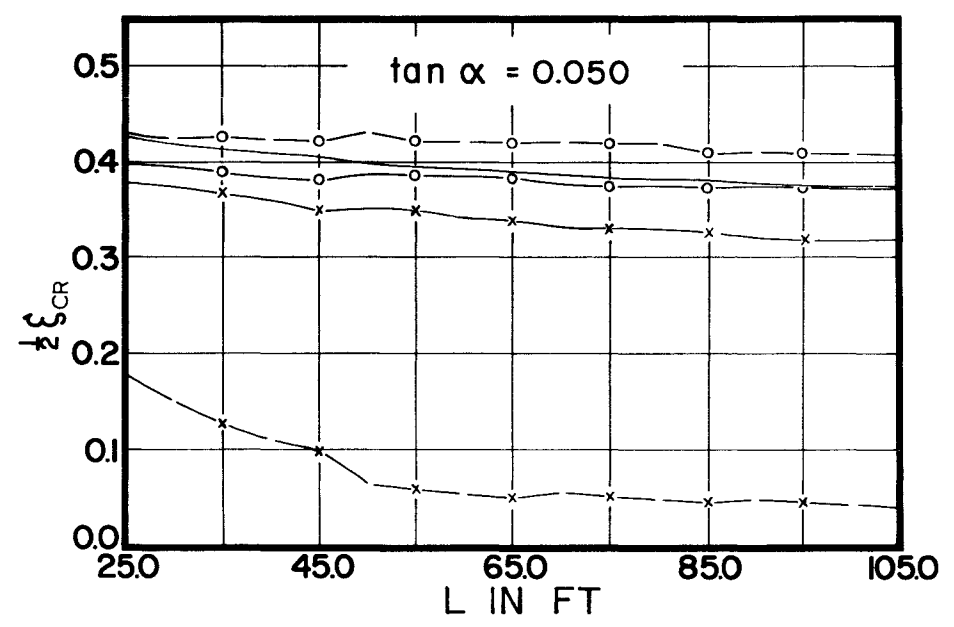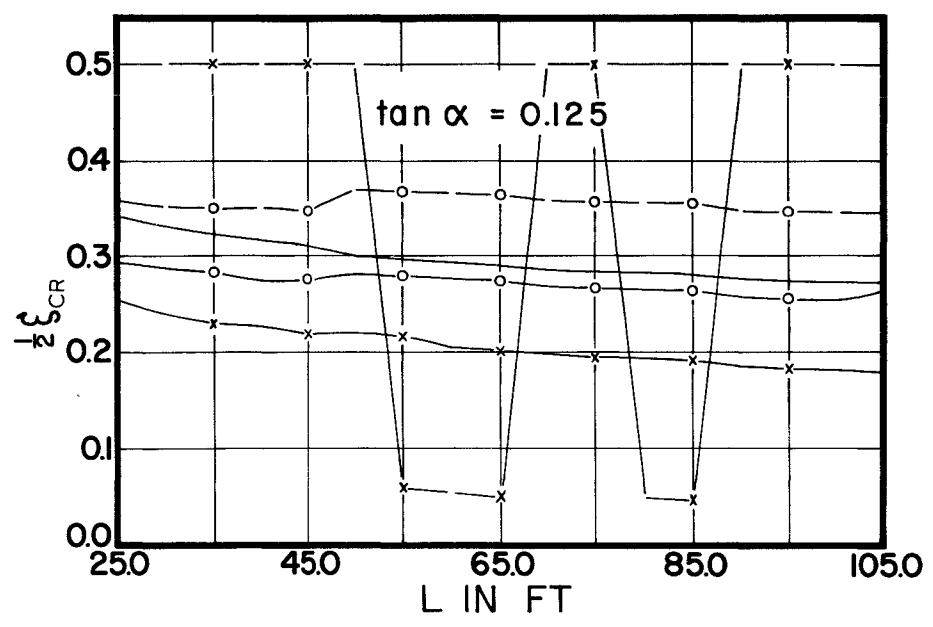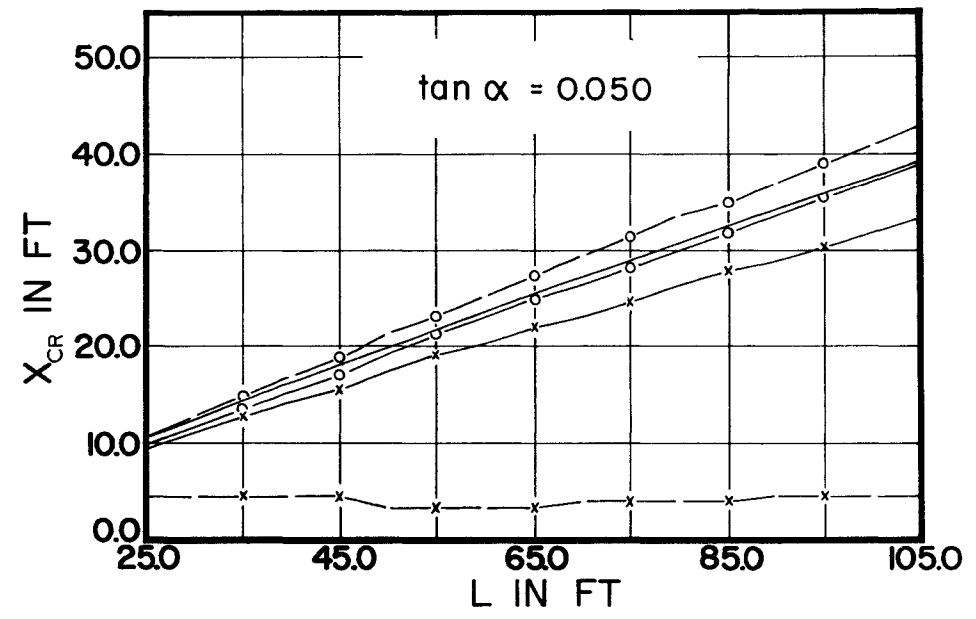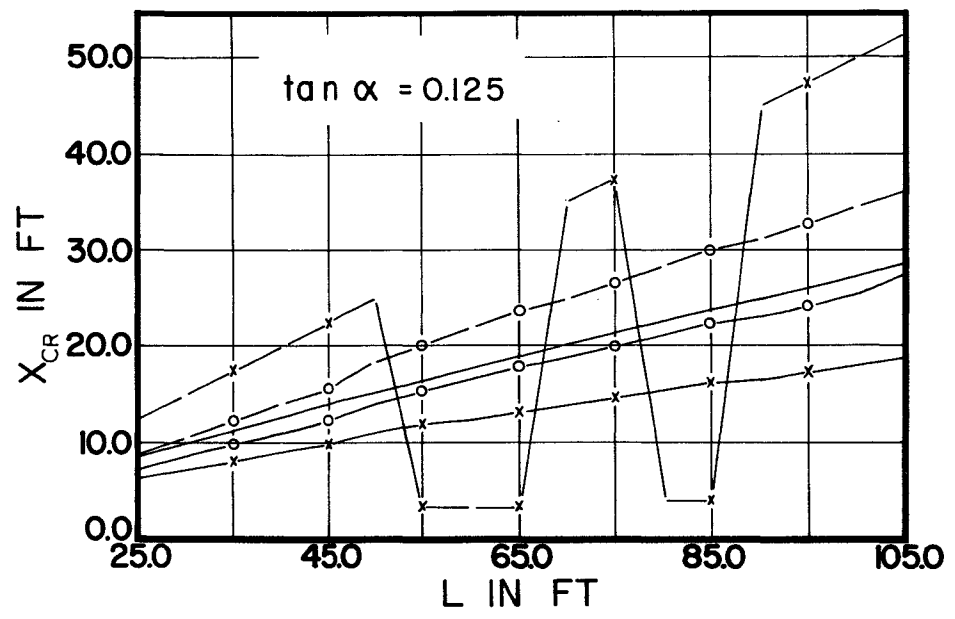


FIGURE 21

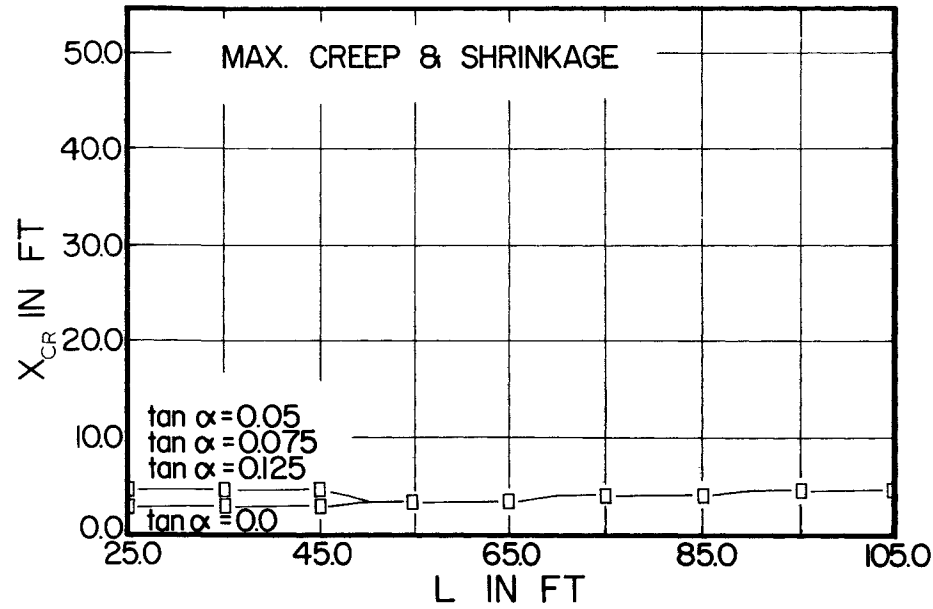CRITICAL SECTION LOCATIONS FOR FLEXURE BASED ON GENERAL COMPUTER SOLUTION PROGRAMME AND EQS. (9a) & (15a)

MAX. CREEP & SHRINKAGE
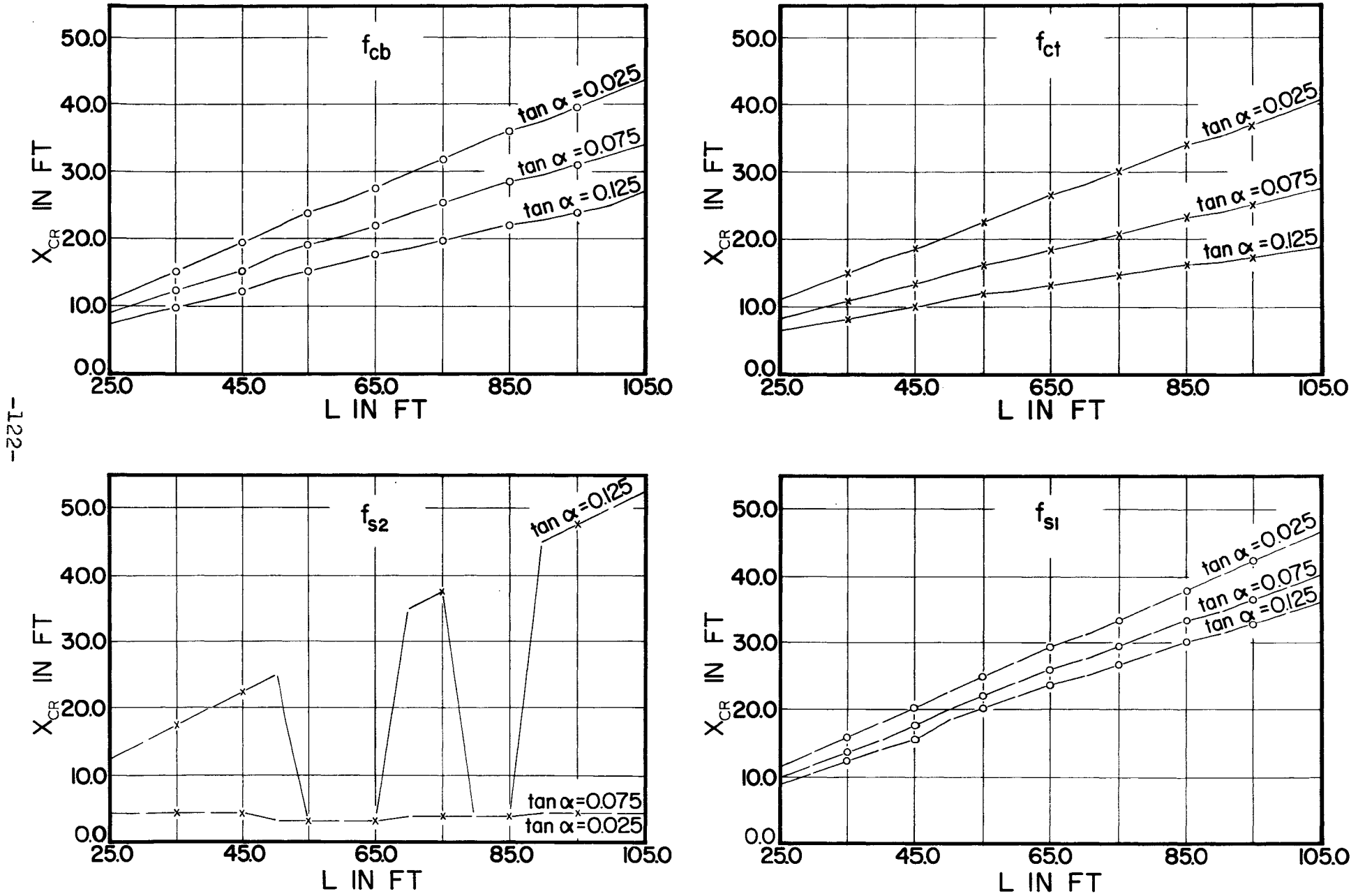
FIGURE 22

CRITICAL SECTION LOCATIONS FOR FLEXURE BASED ON GENERAL COMPUTER SOLUTION PROGRAMME FOR VARIOUS TAN α

## MAX. CREEP & SHRINKAGE
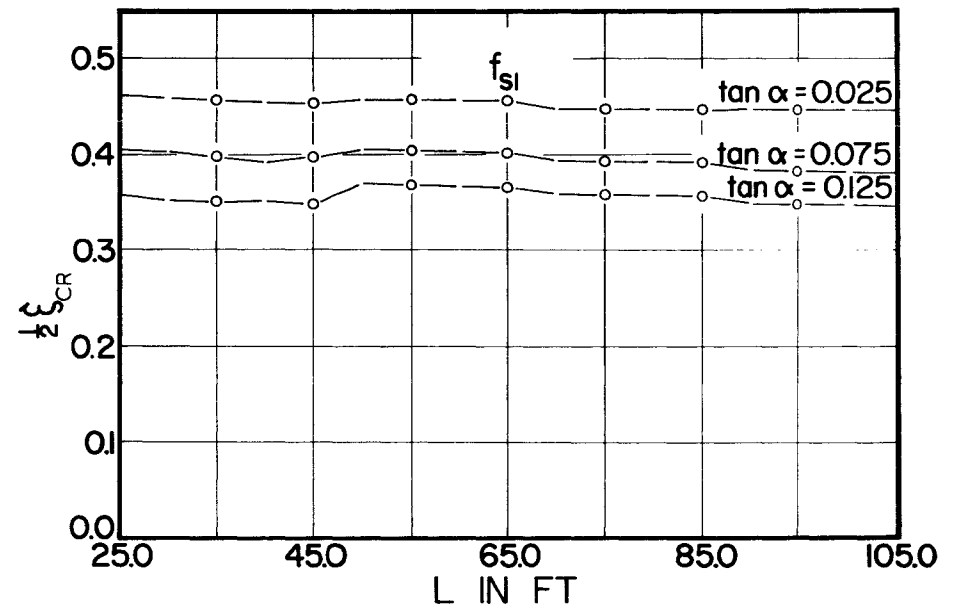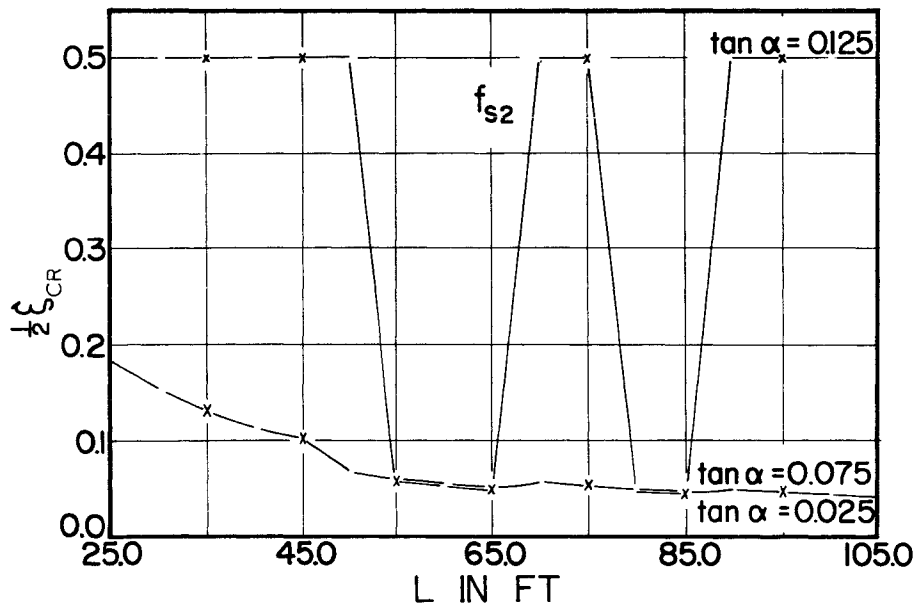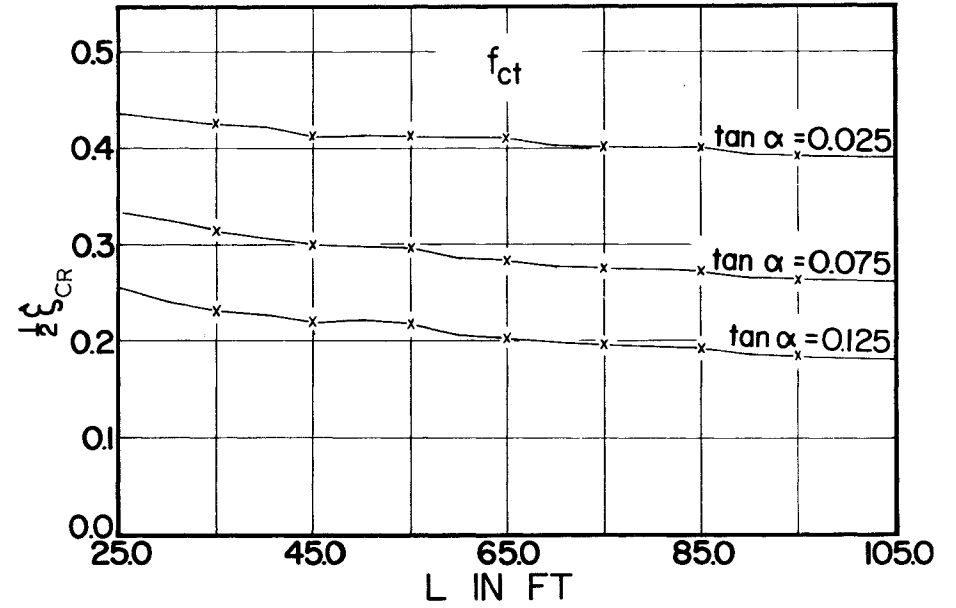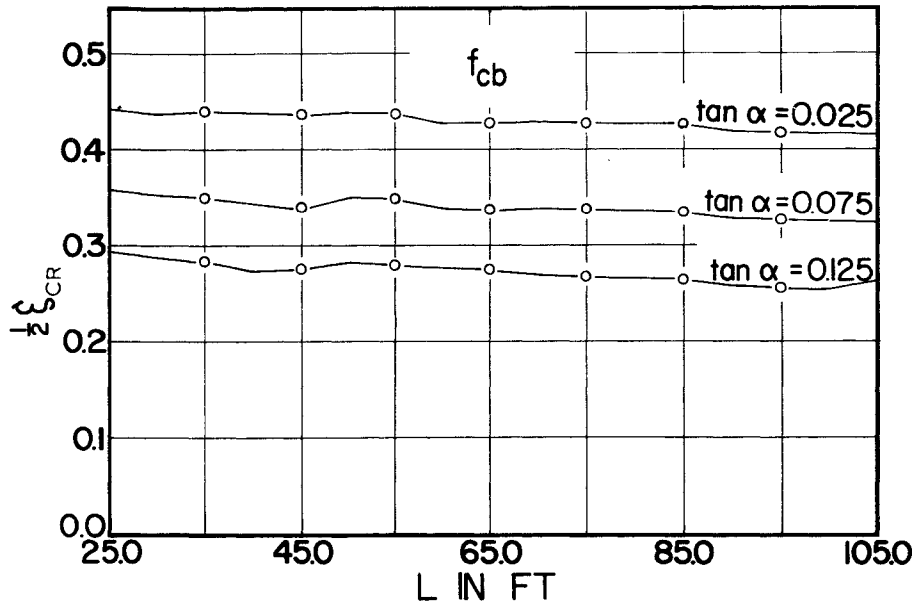
## FIGURE 23

DIMENSIONLESS LOCATIONS OF CRITICAL SECTIONS FOR FLEXURE BASED ON COMPUTER SOLUTION PROGRAMME

MIN.  CREEP  &  SHRINKAGE
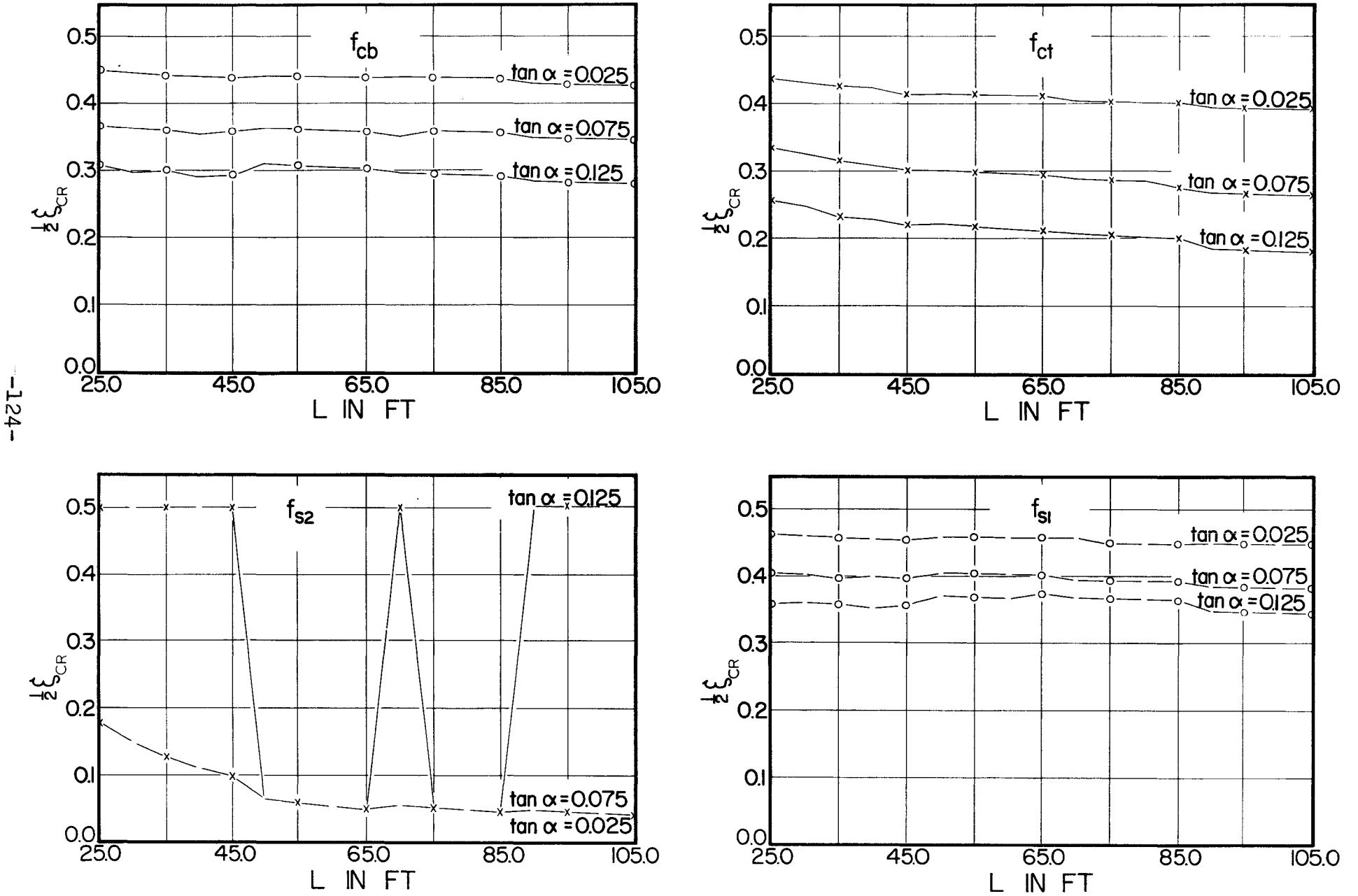


## FIGURE  24
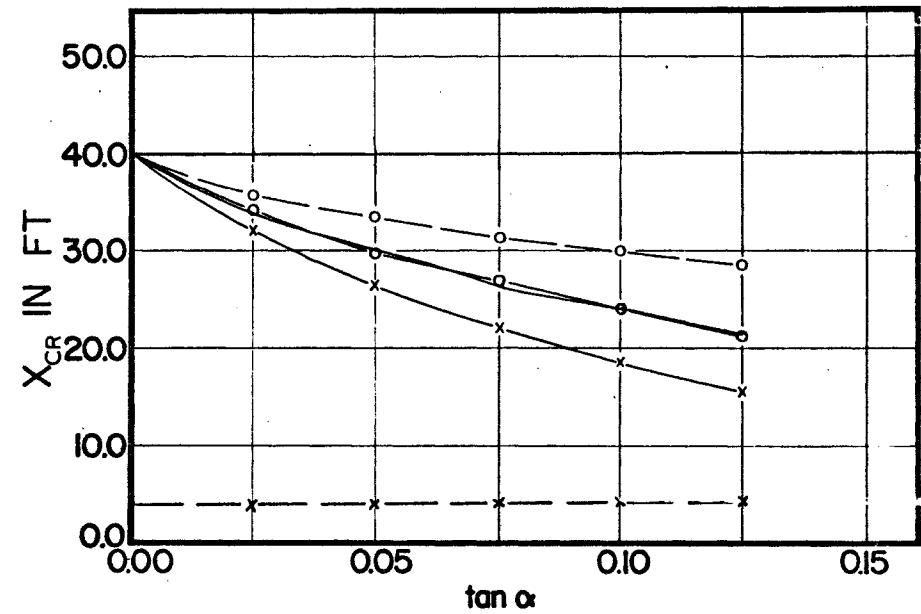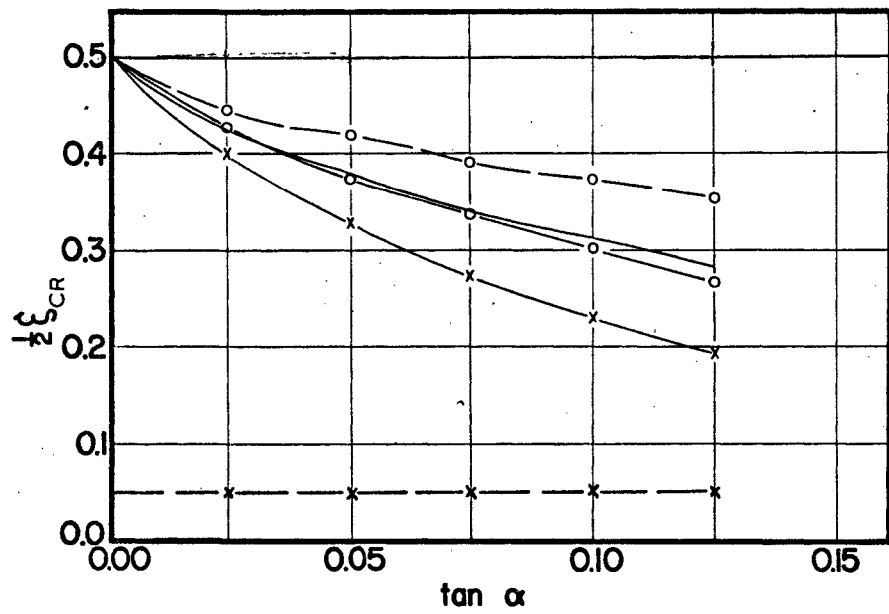
DIMENSIONLESS  LOCATIONS  OF  CRITICAL  SECTIONS  FOR  FLEXURE  BASED  ON  COMPUTER  SOLUTION  PROGRAMME
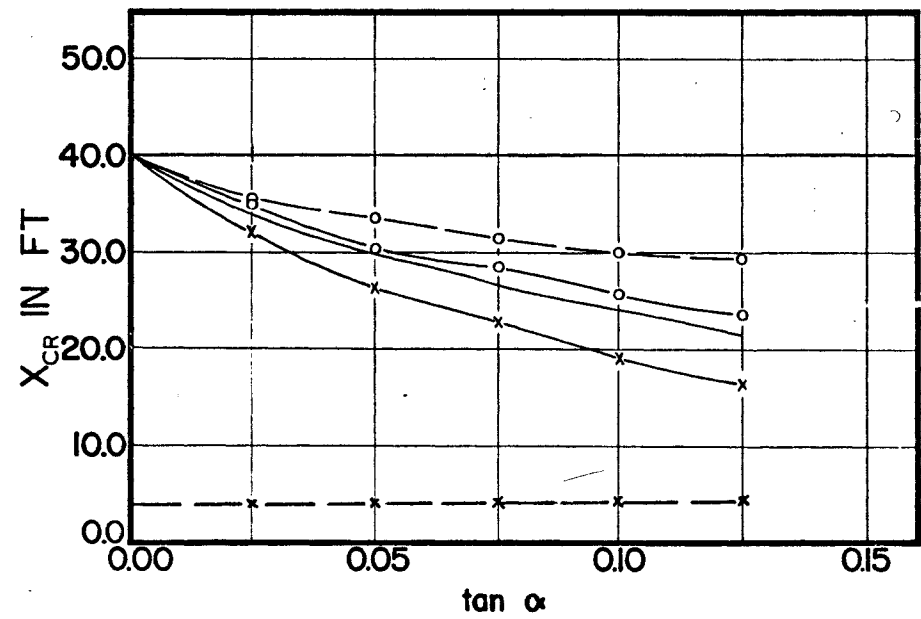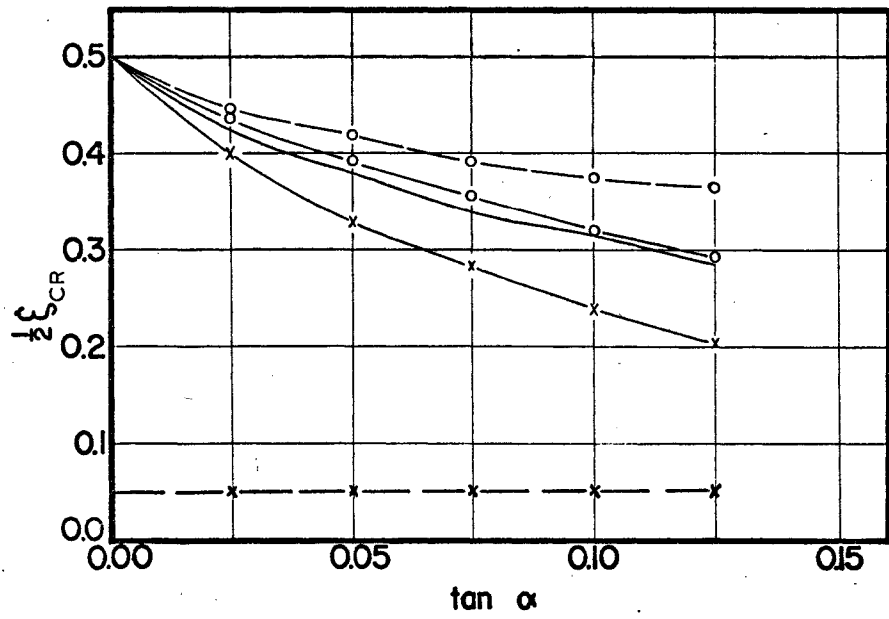
FIGURE 25

COMPARISON OF CRITICAL SECTION LOCATIONS FOR FLEXURE BASED ON COMPUTER SOLUTION PROGRAMME FOR 80 FT SPAN GIRDER

tan α = 0.0
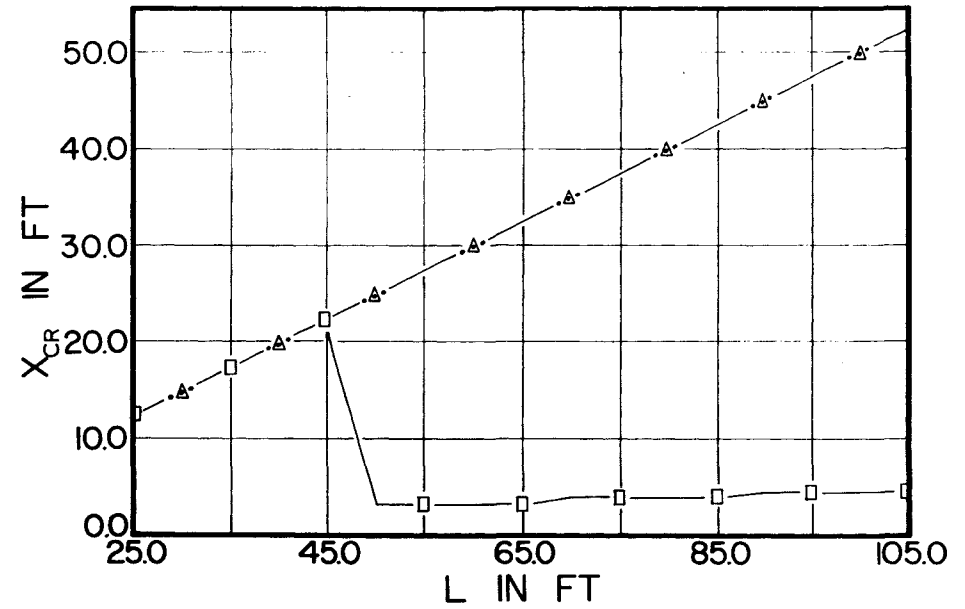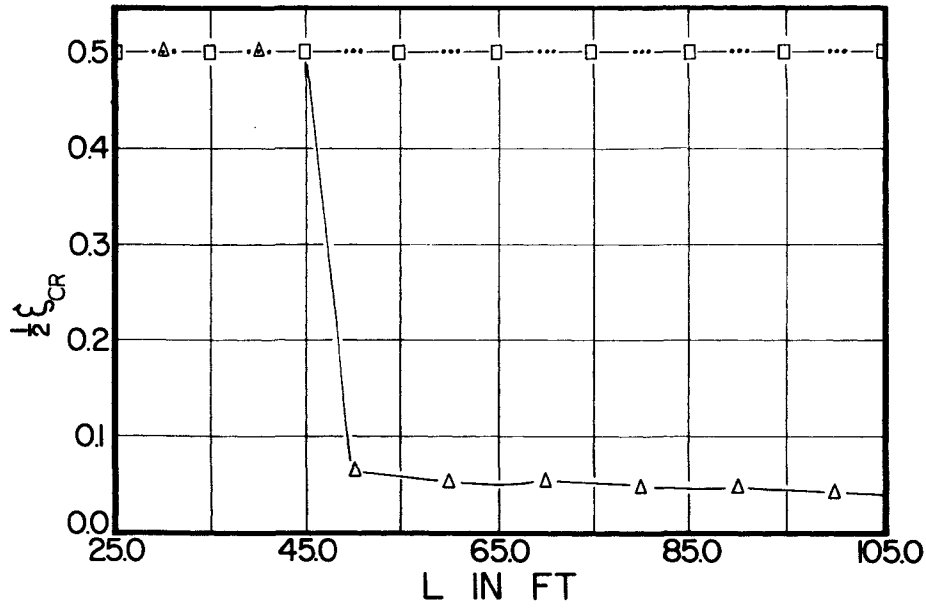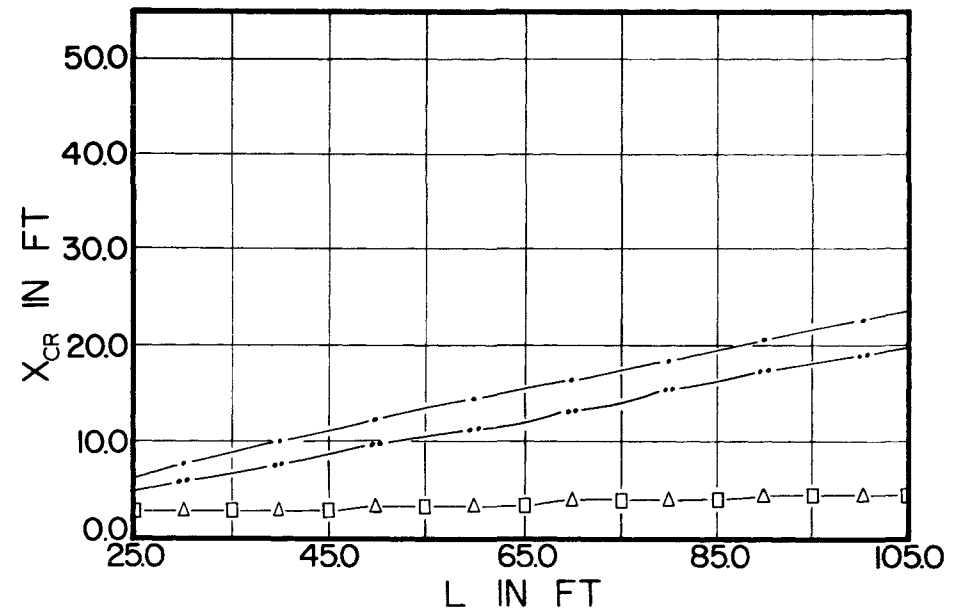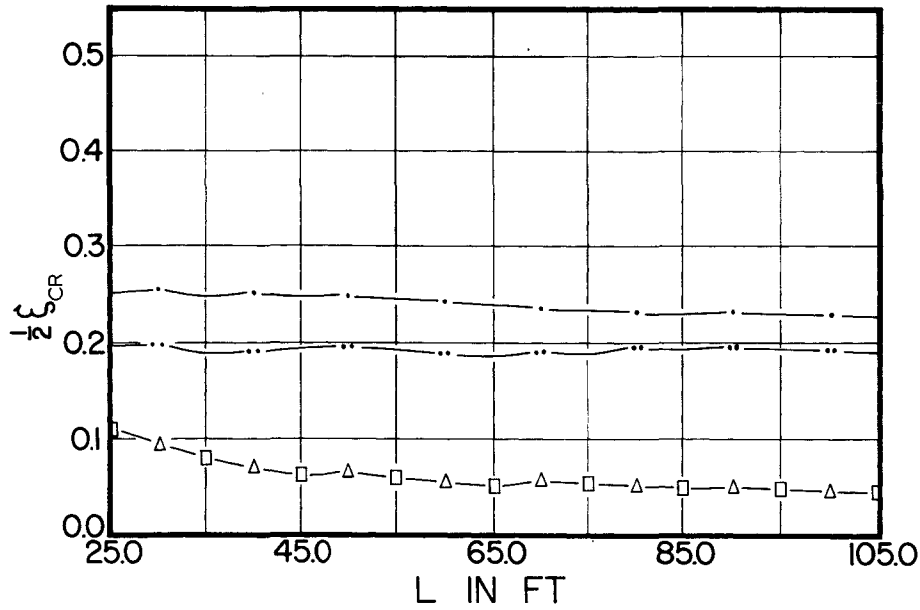
CASE I



CASE II



FIGURE 26

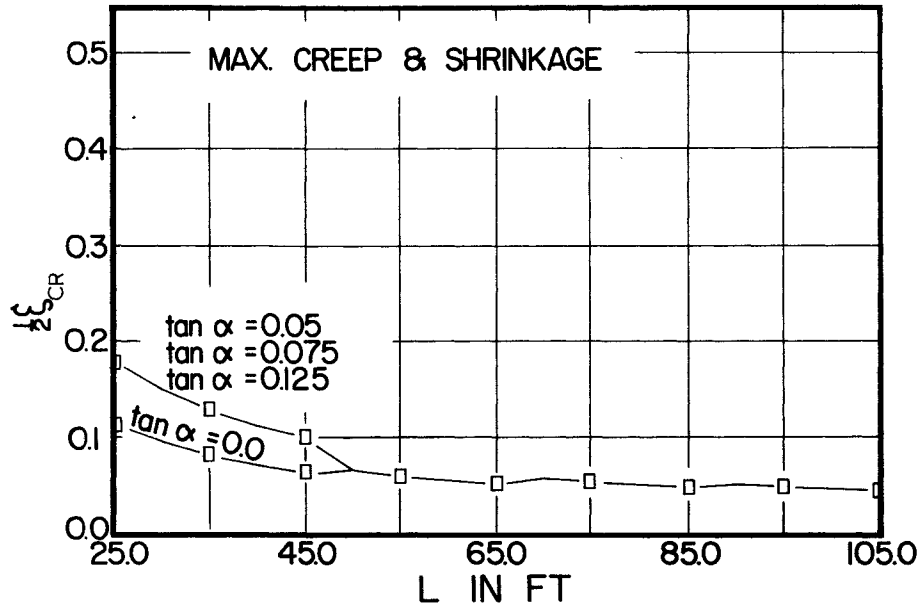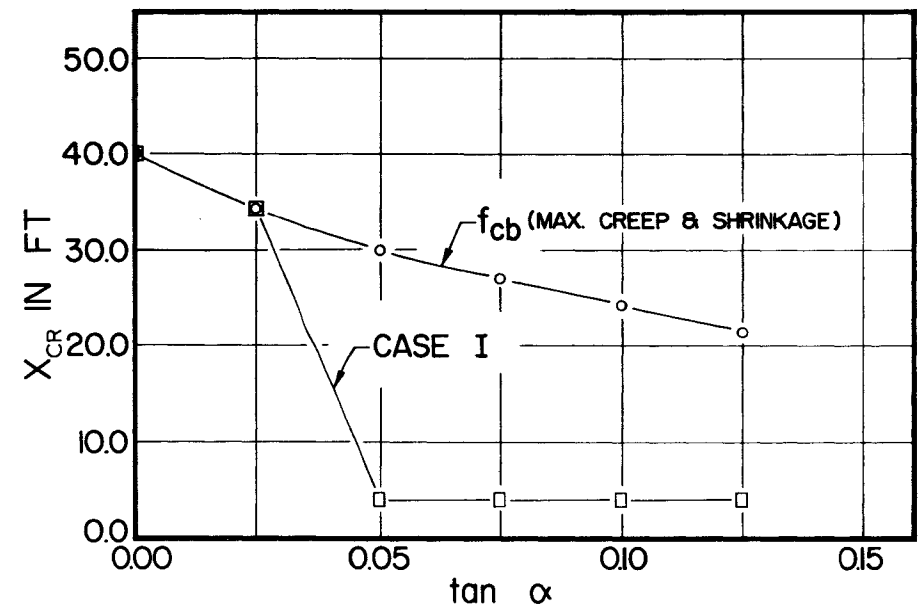COMPARISON OF CRITICAL SECTION LOCATIONS FOR PRINCIPAL TENSILE STRESS BASED ON GENERAL COMPUTER SOLUTION PROGRAMME
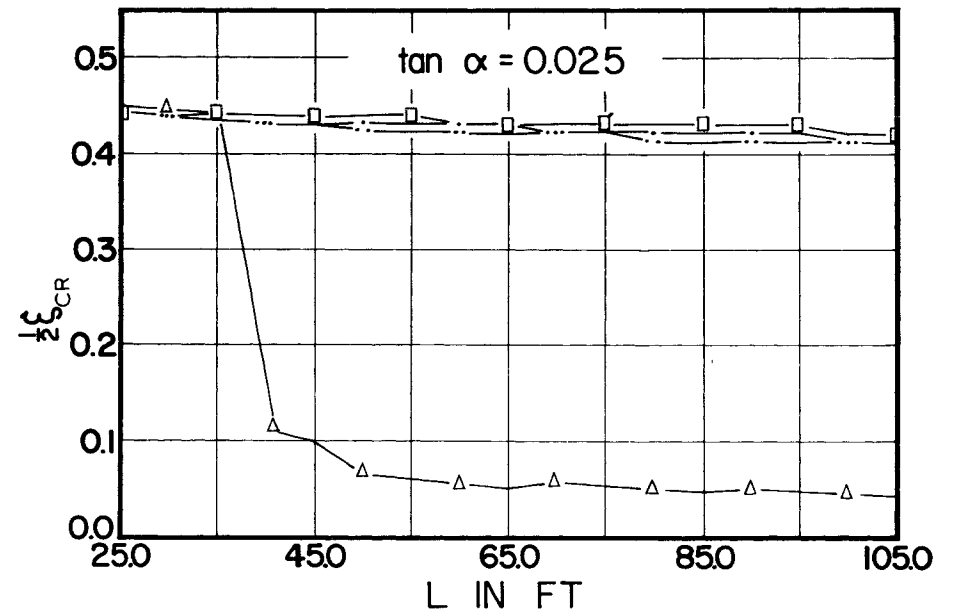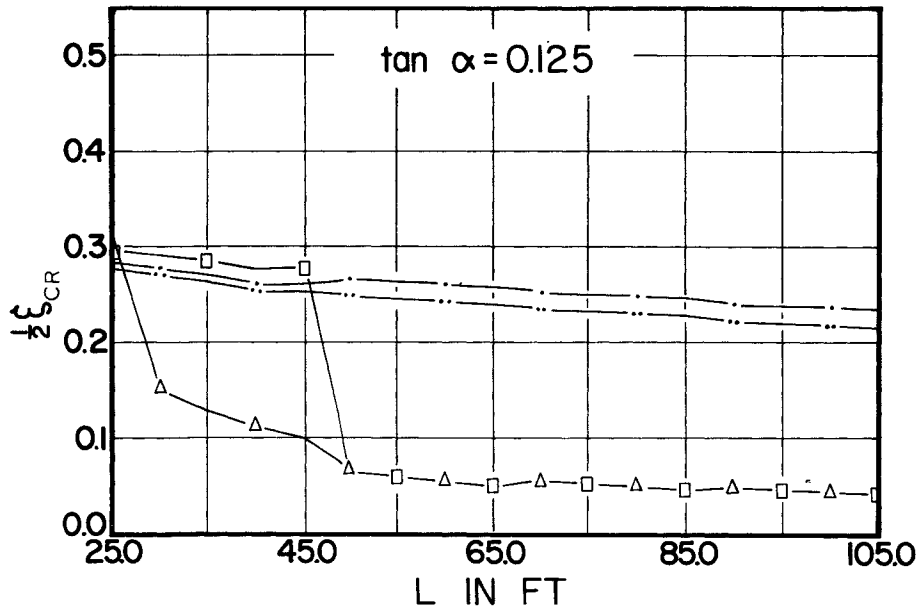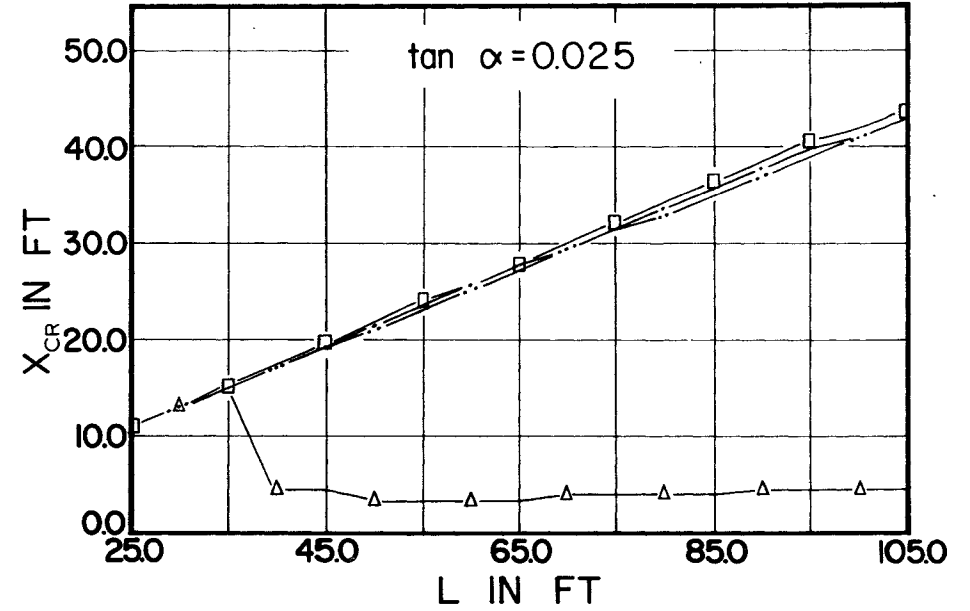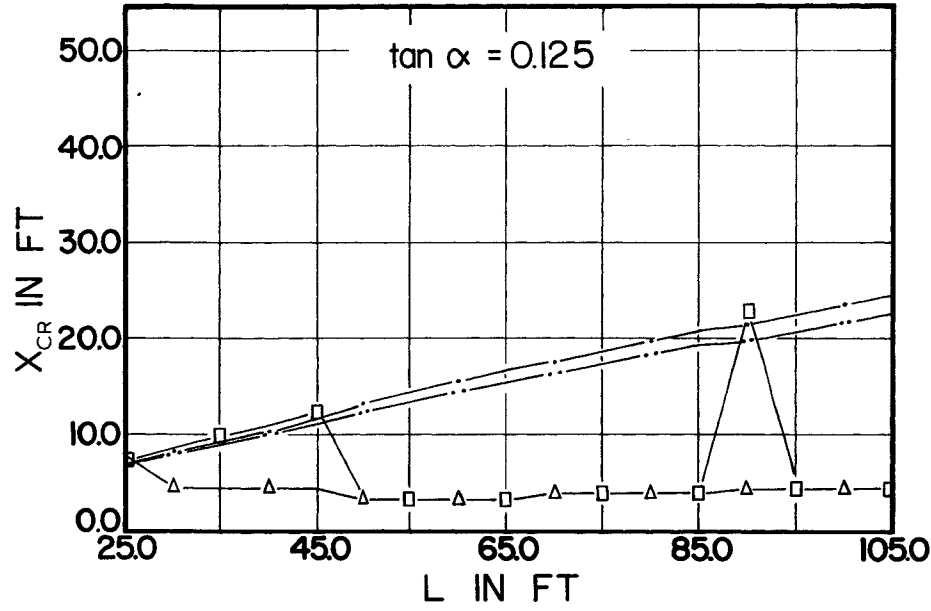
CASE I



FIGURE 27

COMPARISON OF CRITICAL SECTION LOCATIONS FOR PRINCIPAL TENSILE STRESS BASED ON GENERAL COMPUTER SOLUTION PROGRAMME
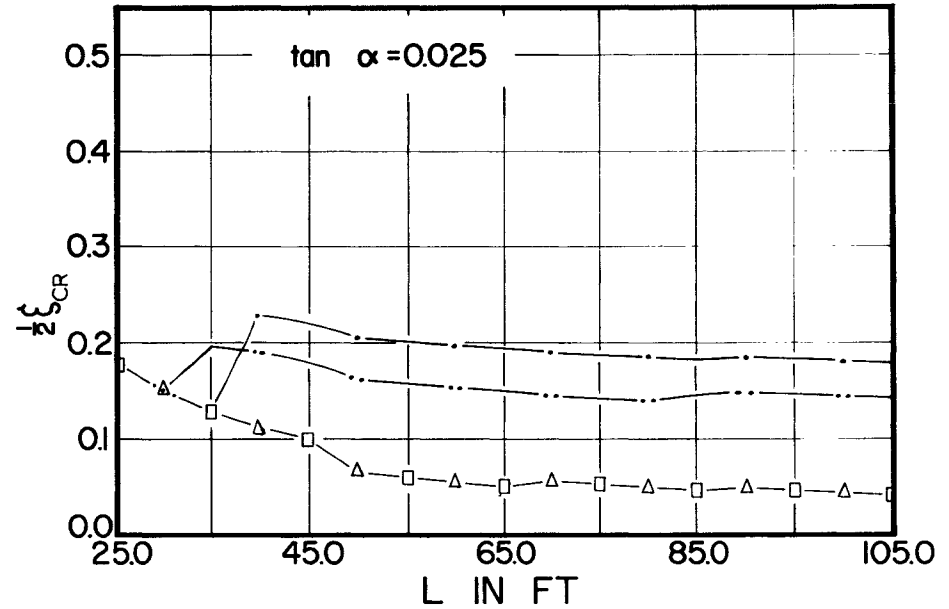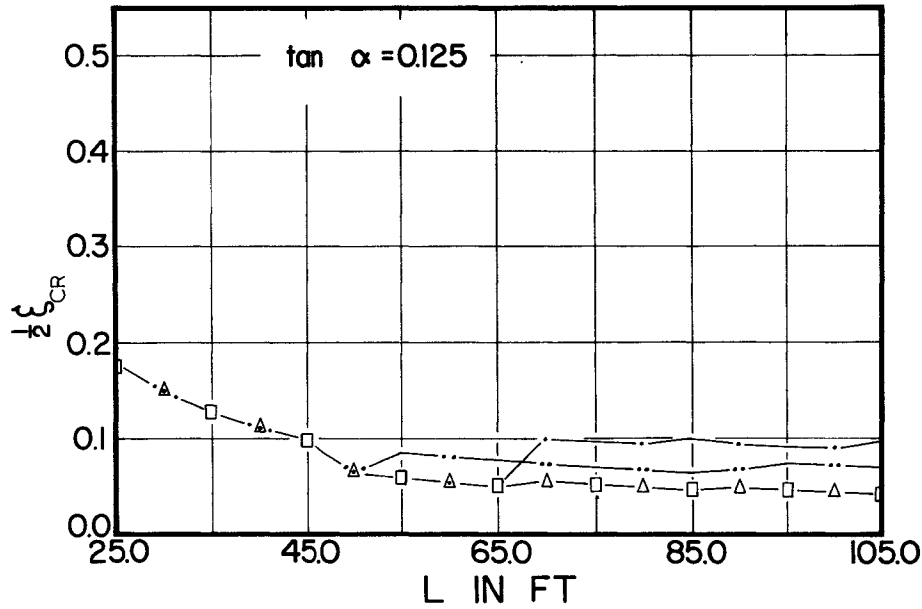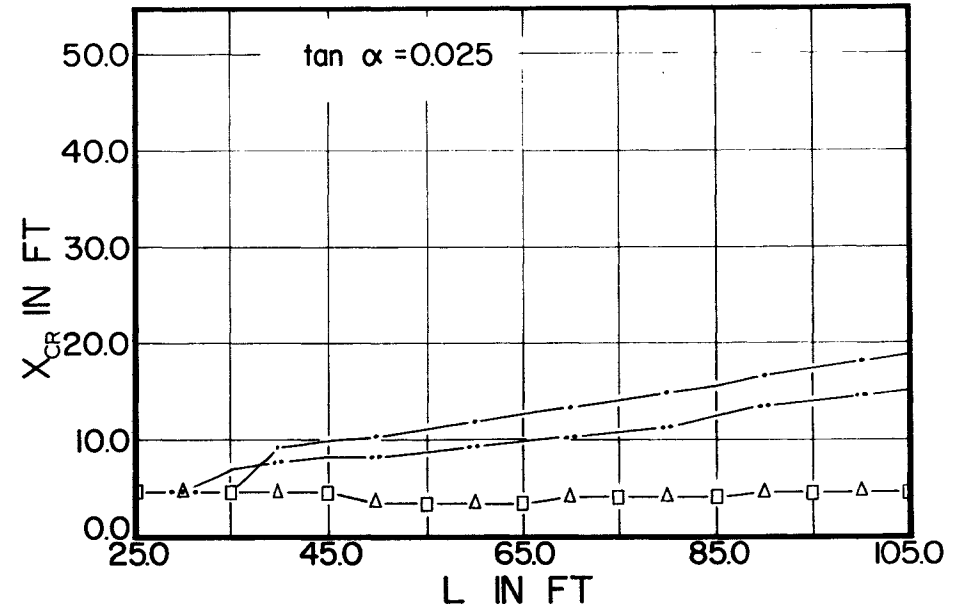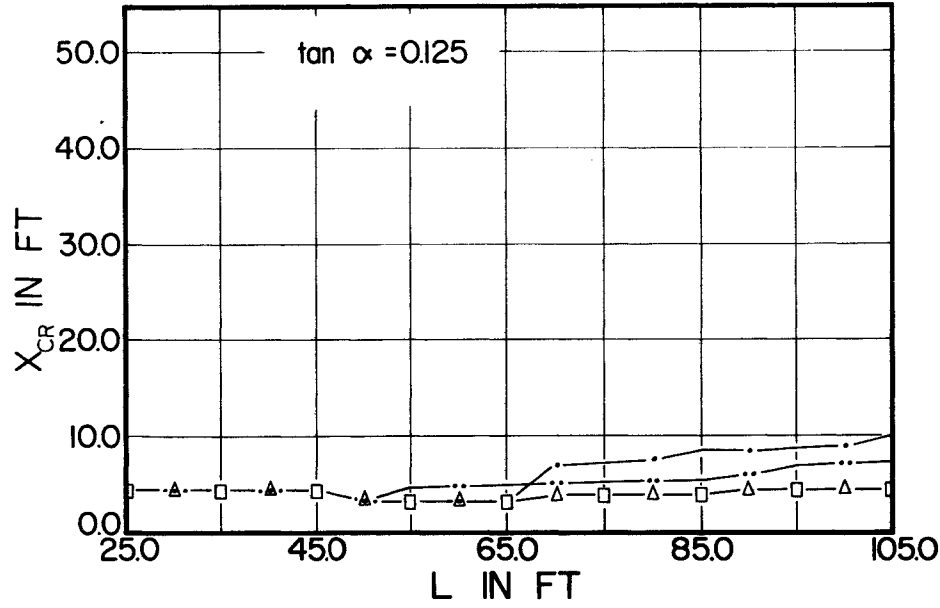
CASE Ⅱ

FIGURE 28

COMPARISON OF CRITICAL SECTION LOCATIONS FOR PRINCIPAL TENSILE STRESS BASED ON GENERAL COMPUTER SOLUTION PROGRAMME
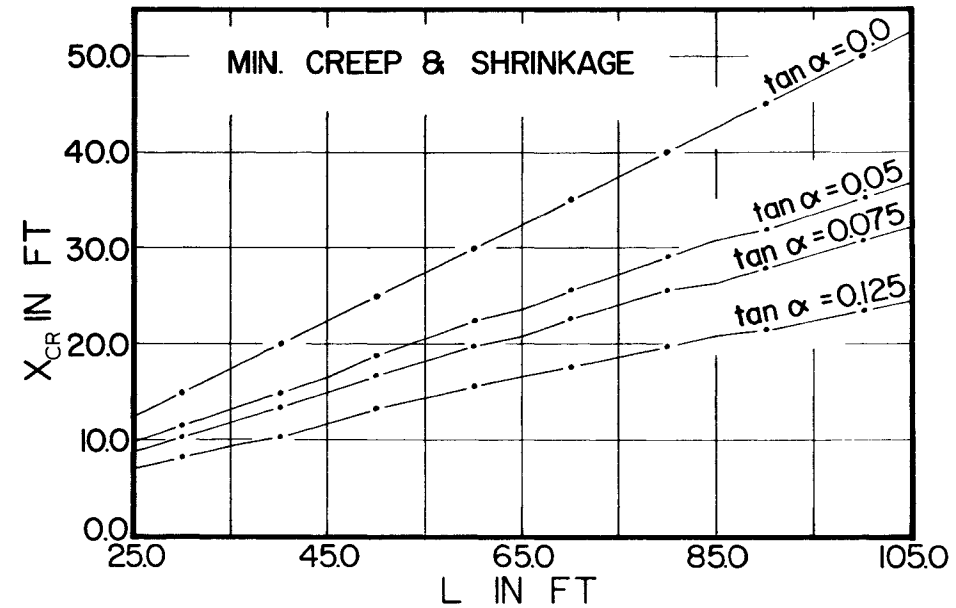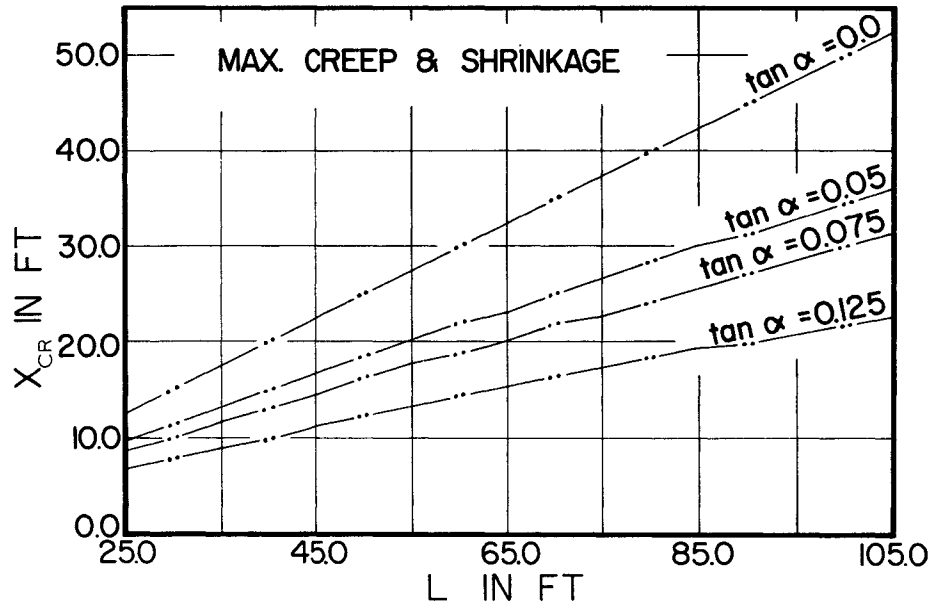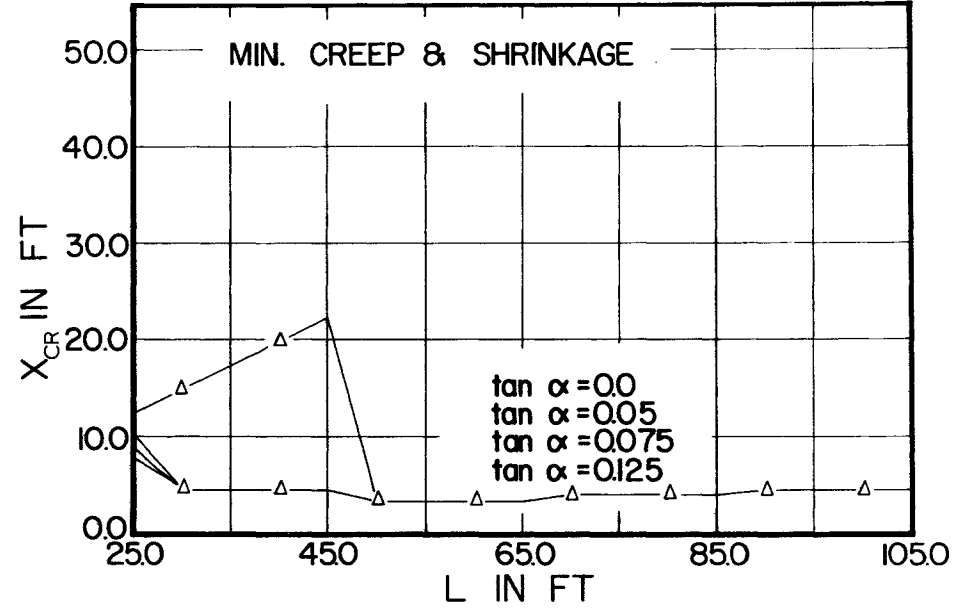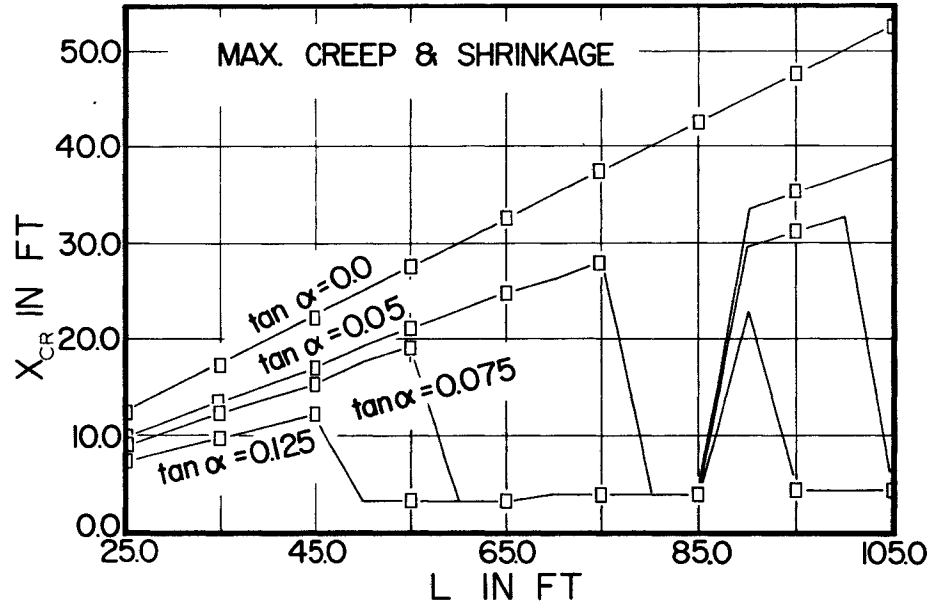
CASE I



FIGURE 29

COMPARISON OF CRITICAL SECTION LOCATIONS FOR PRINCIPAL TENSILE STRESS BASED ON GENERAL COMPUTER SOLUTION PROGRAMME
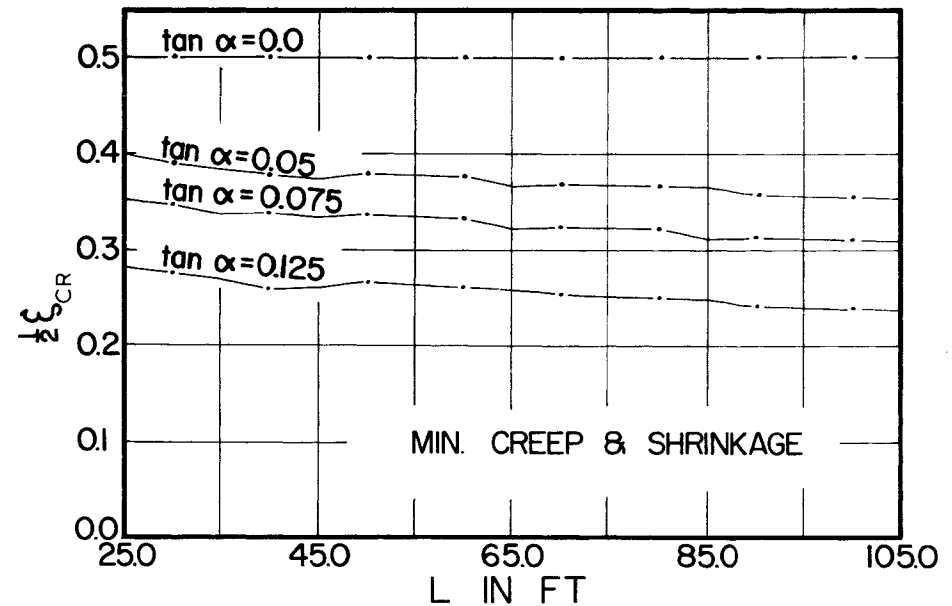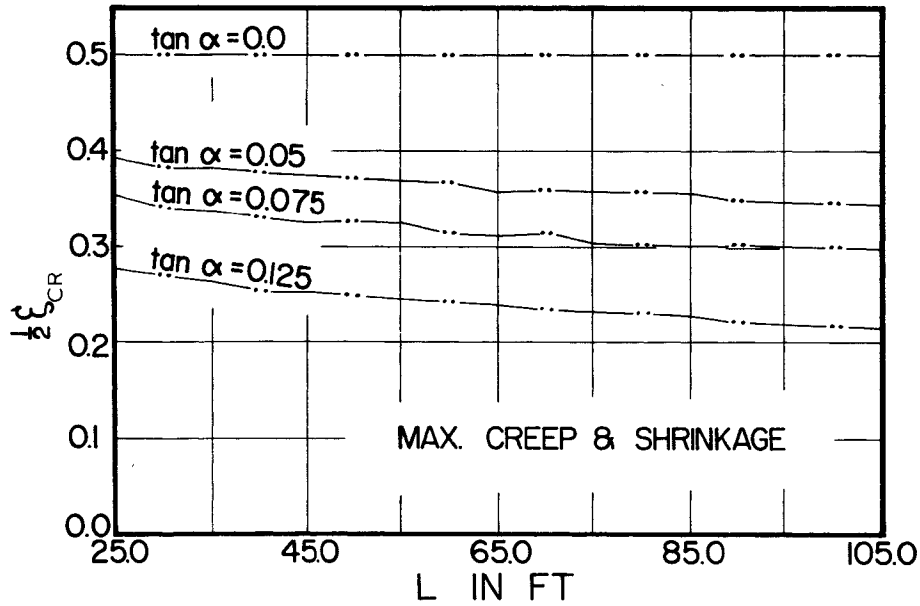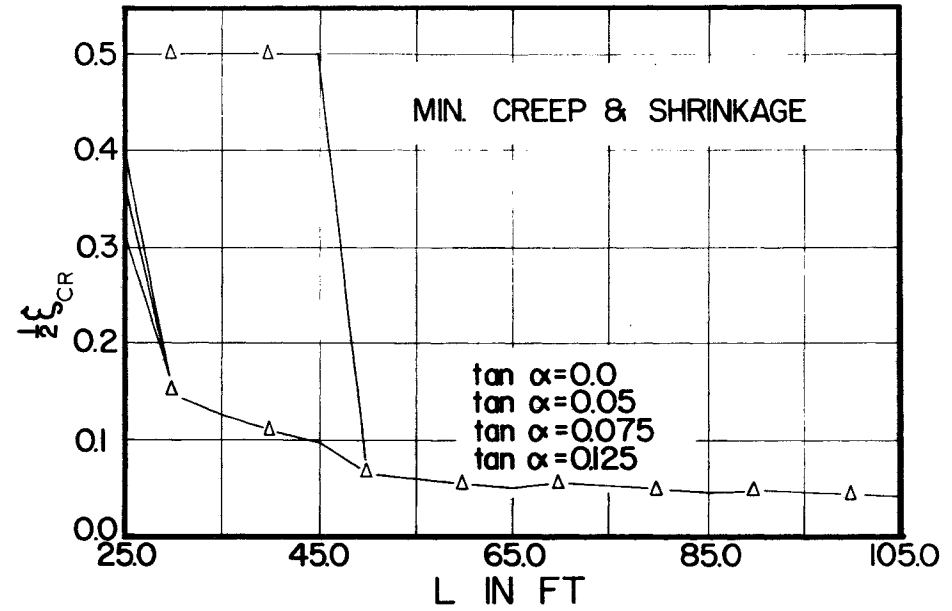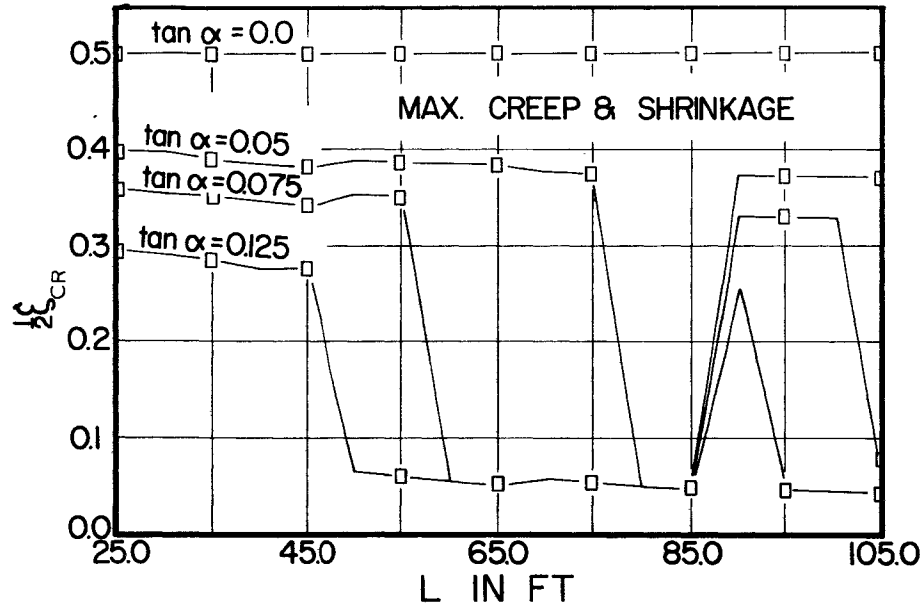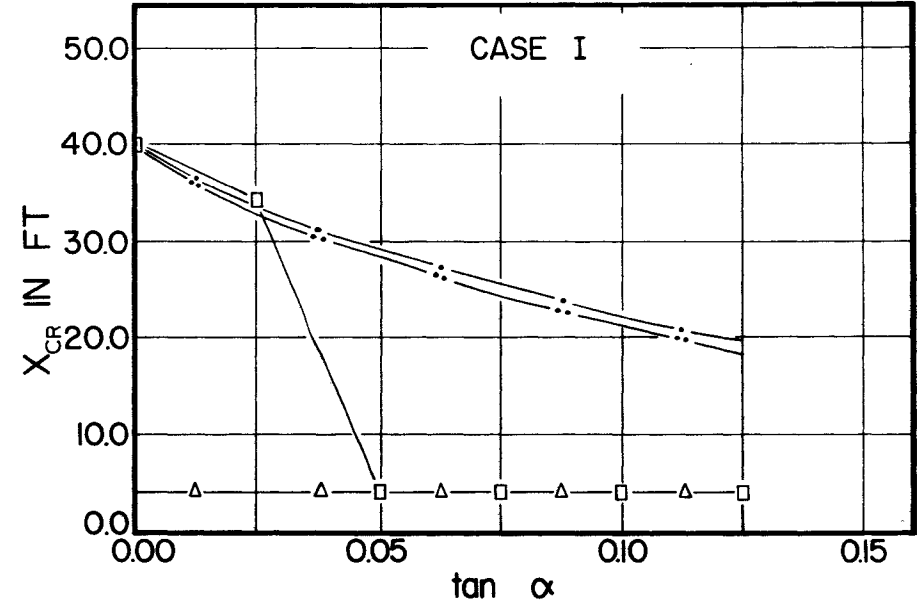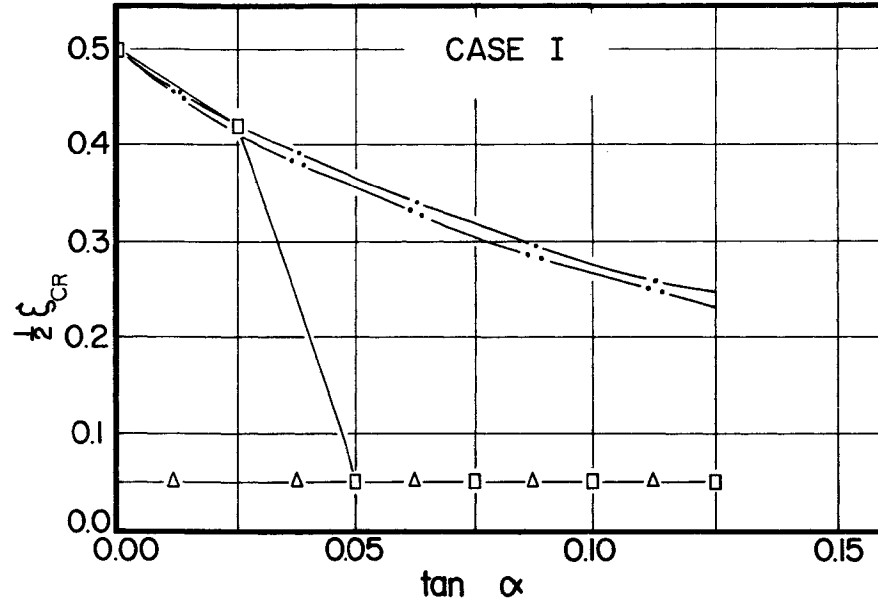
CASE I



FIGURE 30

COMPARISON OF DIMENSIONLESS LOCATIONS OF CRITICAL SECTIONS FOR PRINCIPAL TENSILE STRESS BASED ON GENERAL COMPUTER SOLUTION PROGRAMME
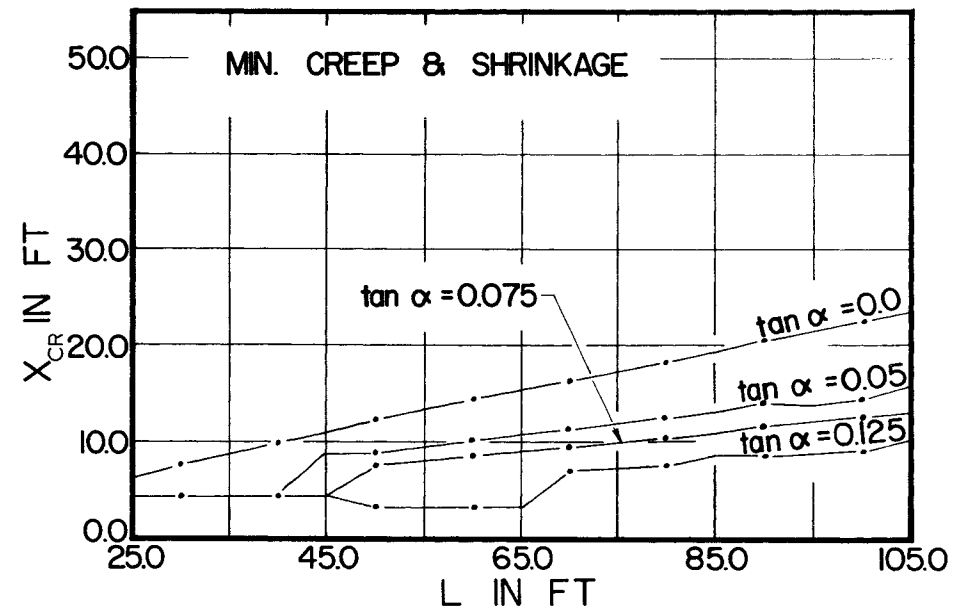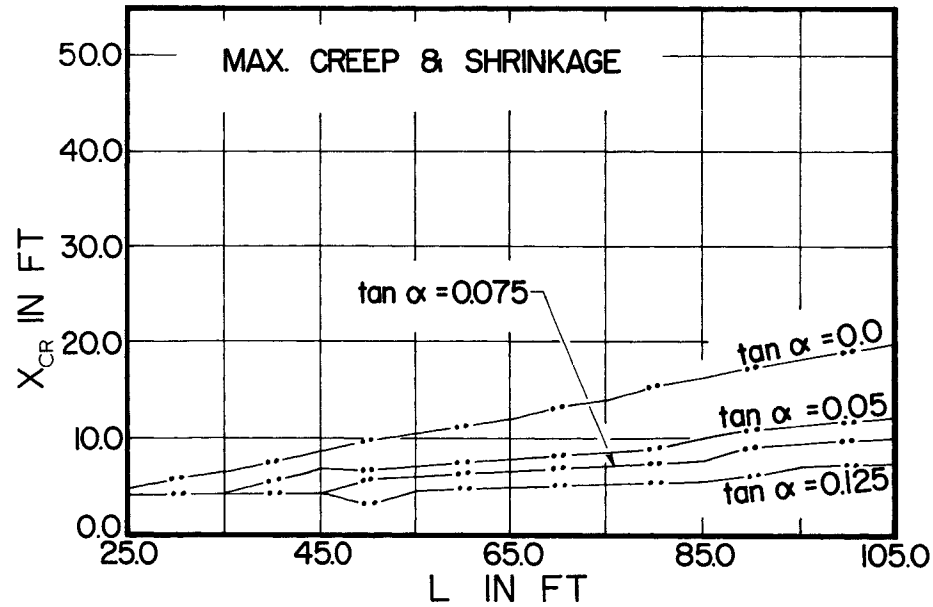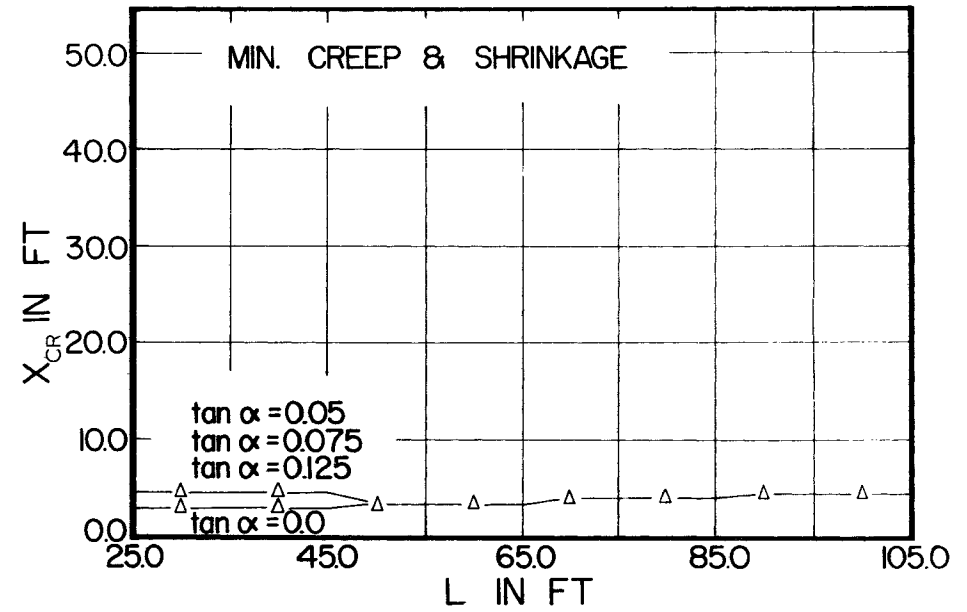
CASE II



FIGURE 31

COMPARISON OF CRITICAL SECTION LOCATIONS FOR PRINCIPAL TENSILE STRESS BASED ON GENERAL COMPUTER SOLUTION PROGRAMME

CASE II
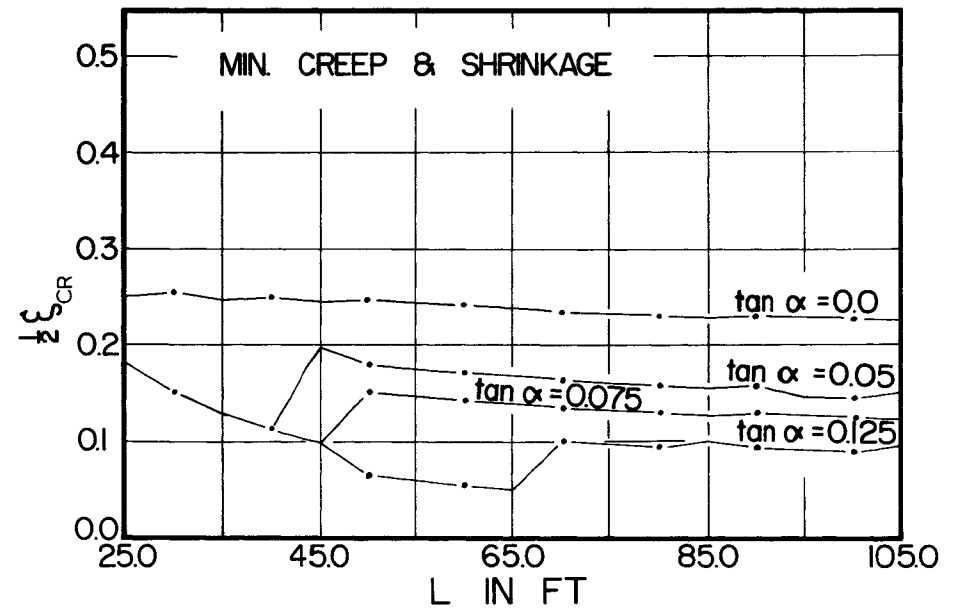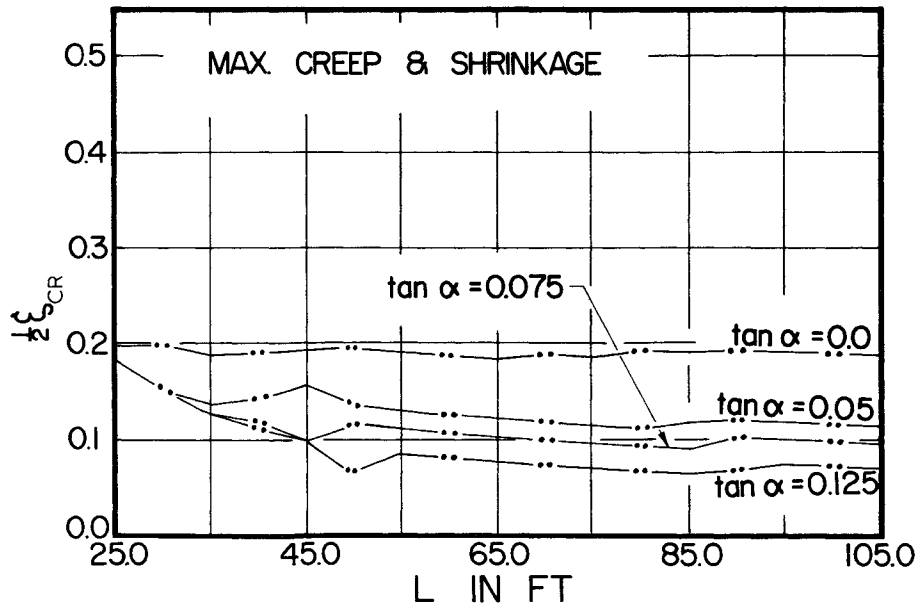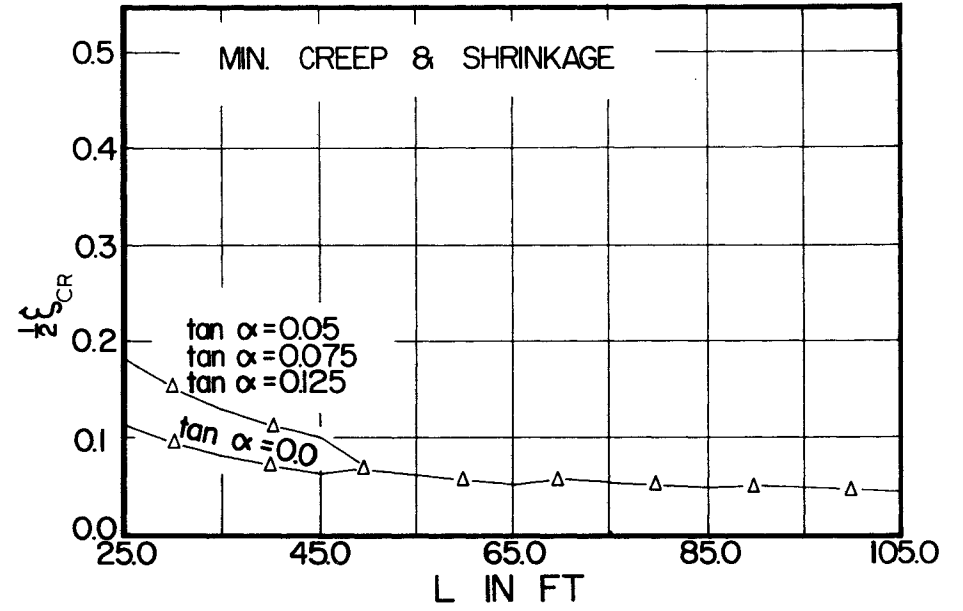


FIGURE 32

COMPARISON OF DIMENSIONLESS LOCATIONS OF CRITICAL SECTIONS FOR PRINCIPAL TENSILE STRESS
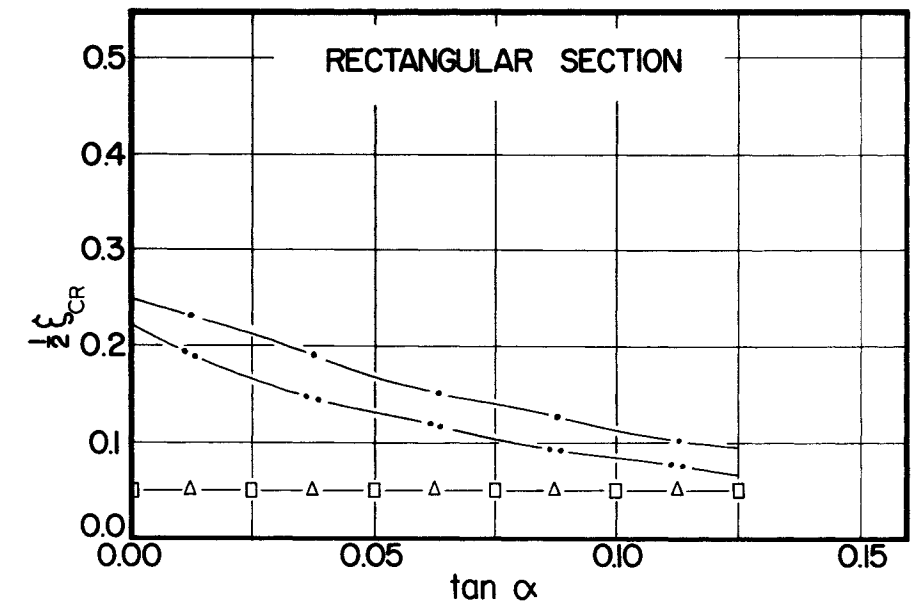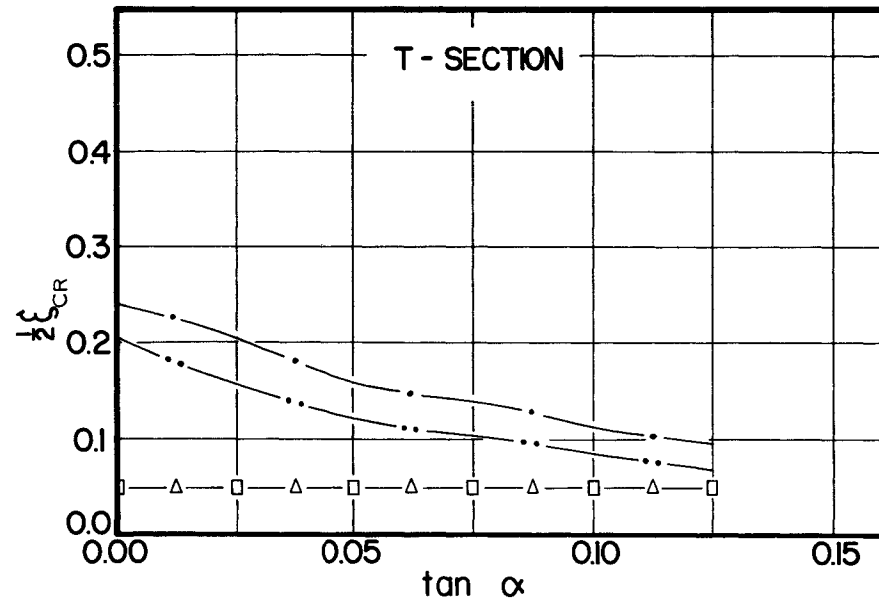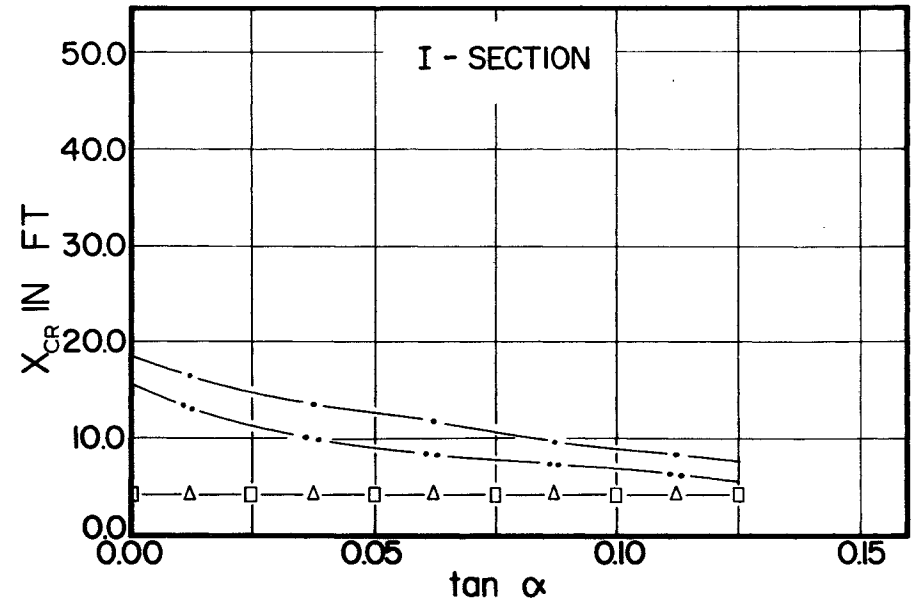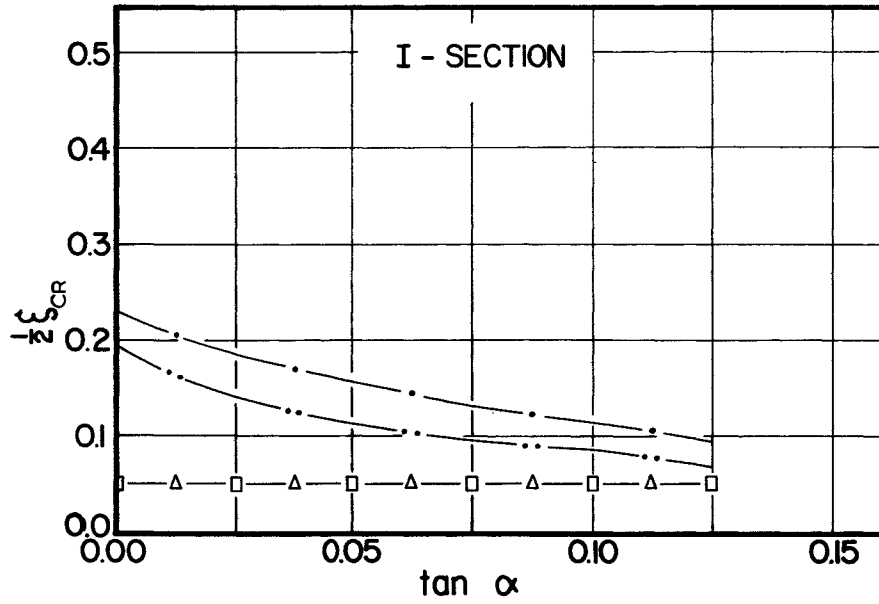BASED ON GENERAL COMPUTER SOLUTION PROGRAMME
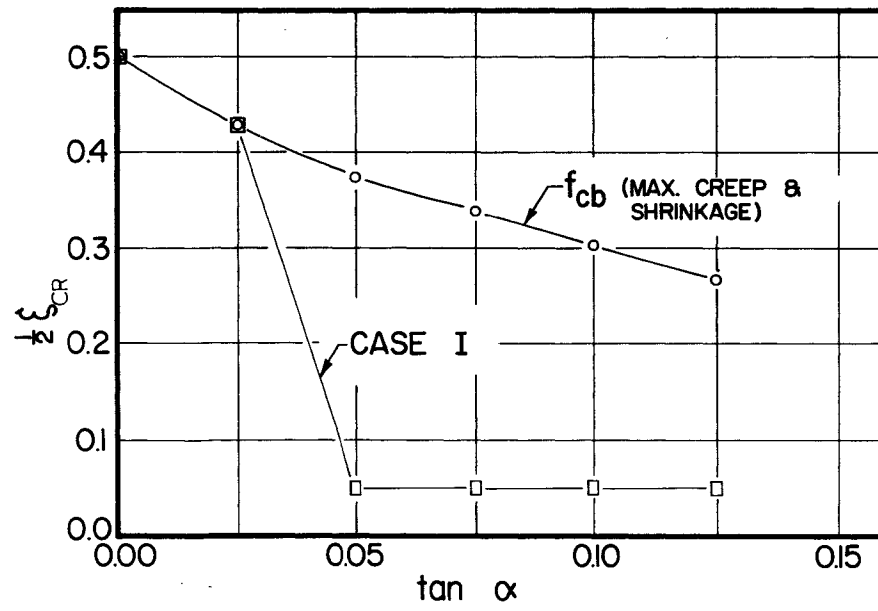
L = 80 FT



## FIGURE 33

COMPARISON OF CRITICAL SECTION LOCATIONS FOR PRINCIPAL TENSILE STRESS FOR 80 FT SPAN GIRDER BASED ON GENERAL COMPUTER SOLUTION PROGRAMME

L = 80 FT

CASE II



FIGURE 34

COMPARISON OF CRITICAL SECTION LOCATIONS FOR PRINCIPAL TENSILE STRESS FOR 80 FT SPAN GIRDER
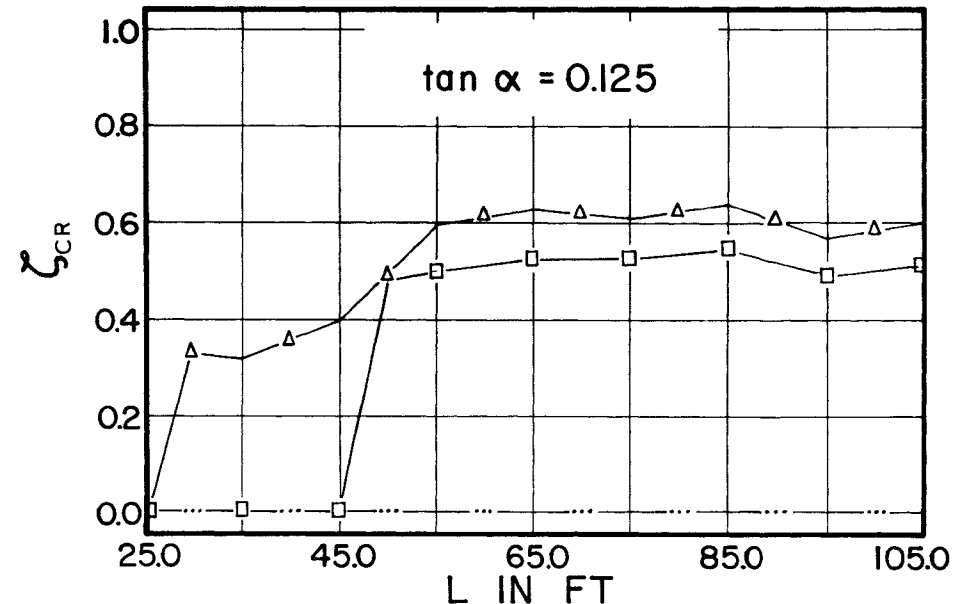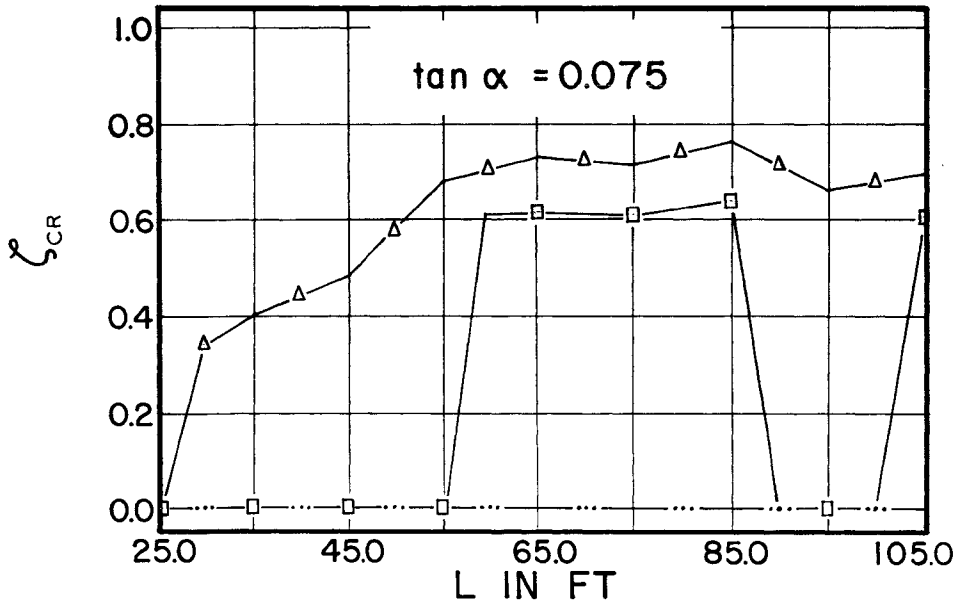BASED ON GENERAL COMPUTER SOLUTION PROGRAMME

CASE I



FIGURE 35

COMPARISON OF POSITIONS OF MAXIMUM PRINCIPAL TENSILE STRESSES RELATIVE TO SOFFIT OF GIRDER AT CRITICAL SECTIONS
BASED ON GENERAL COMPUTER SOLUTION PROGRAMME
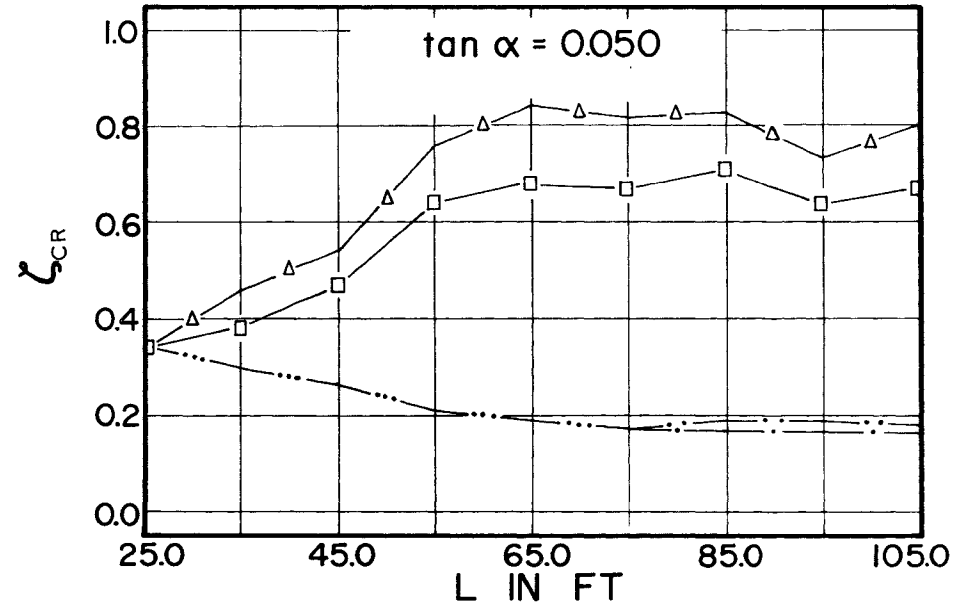
CASE II

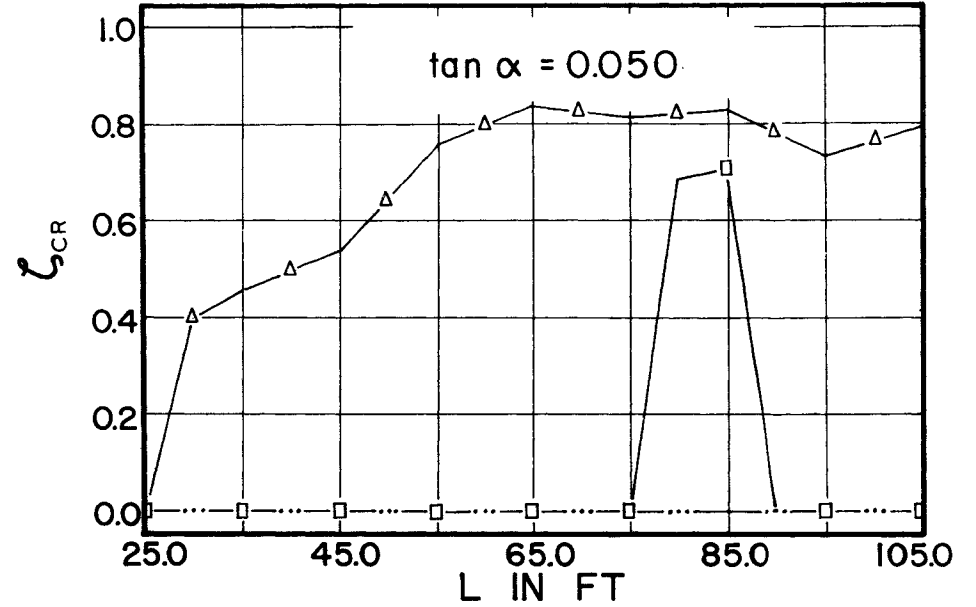## FIGURE 36

COMPARISON OF POSITION OF MAXIMUM PRINCIPAL TENSILE STRESSES RELATIVE TO SOFFIT OF GIRDER AT CRITICAL SECTIONS BASED ON GENERAL COMPUTER SOLUTION PROGRAMME
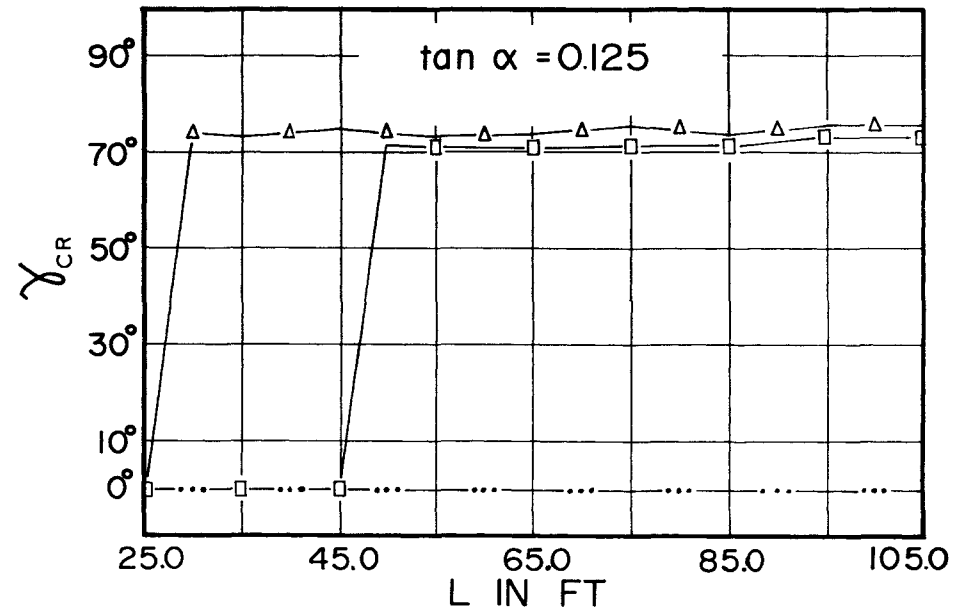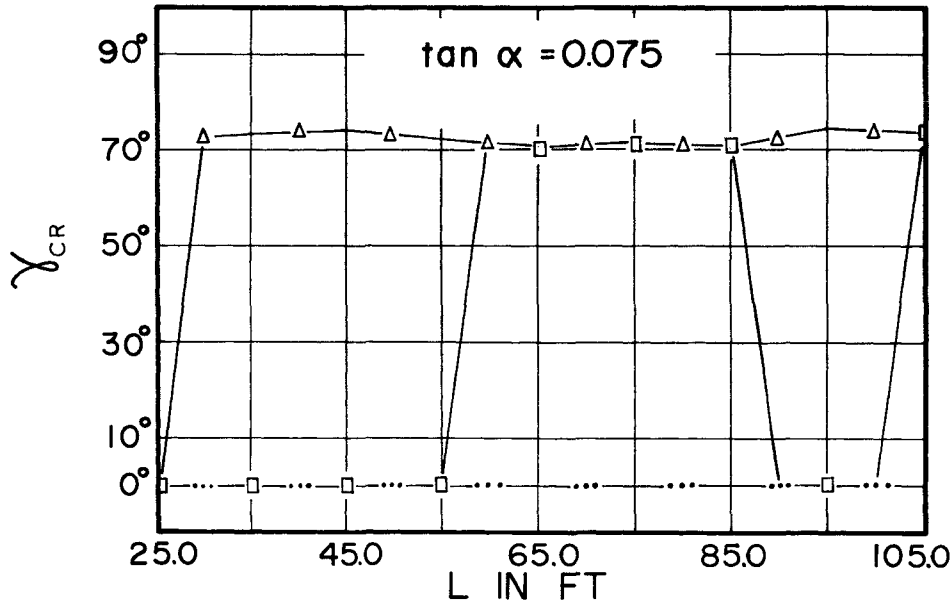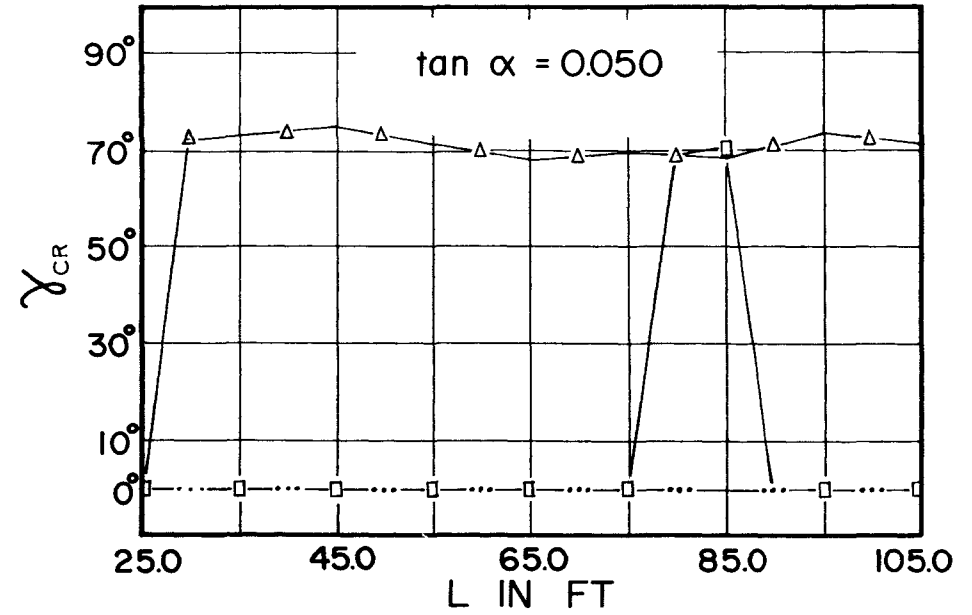
CASE I



FIGURE 37

COMPARISON OF INCLINATIONS OF MAXIMUM PRINCIPAL TENSILE STRESSES WITH HORIZONTAL AXIS AT CRITICAL SECTIONS
BASED ON GENERAL COMPUTER SOLUTION PROGRAMME
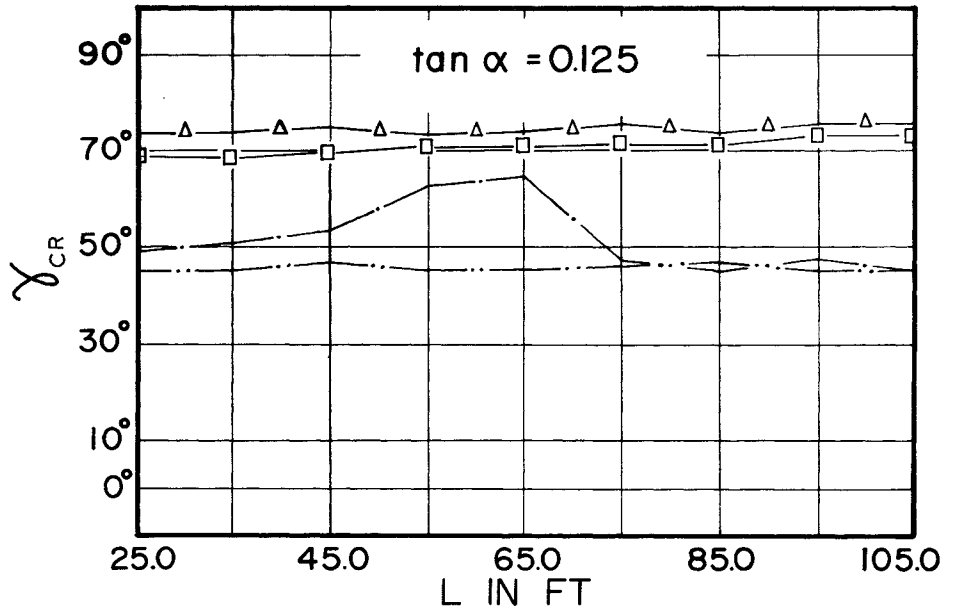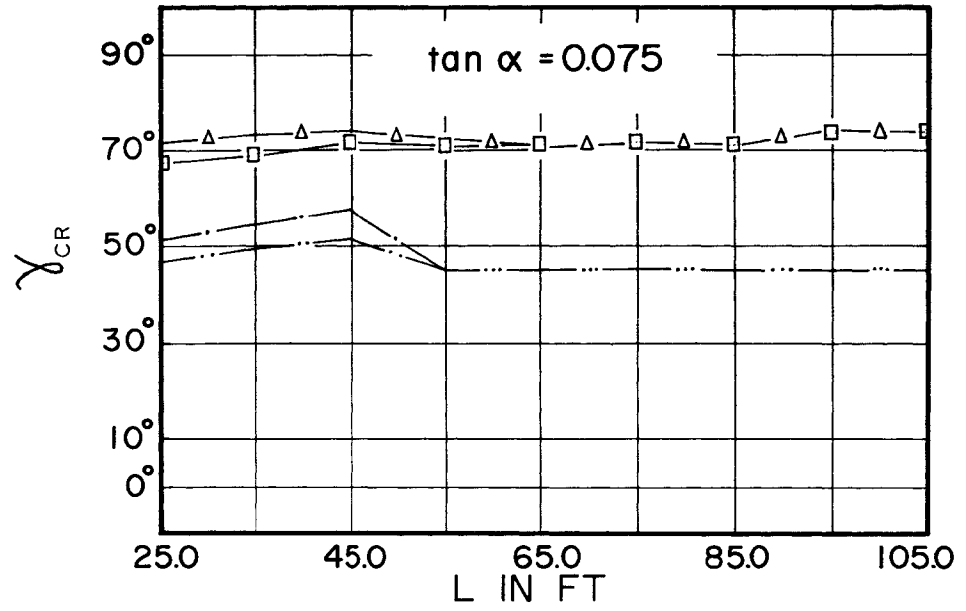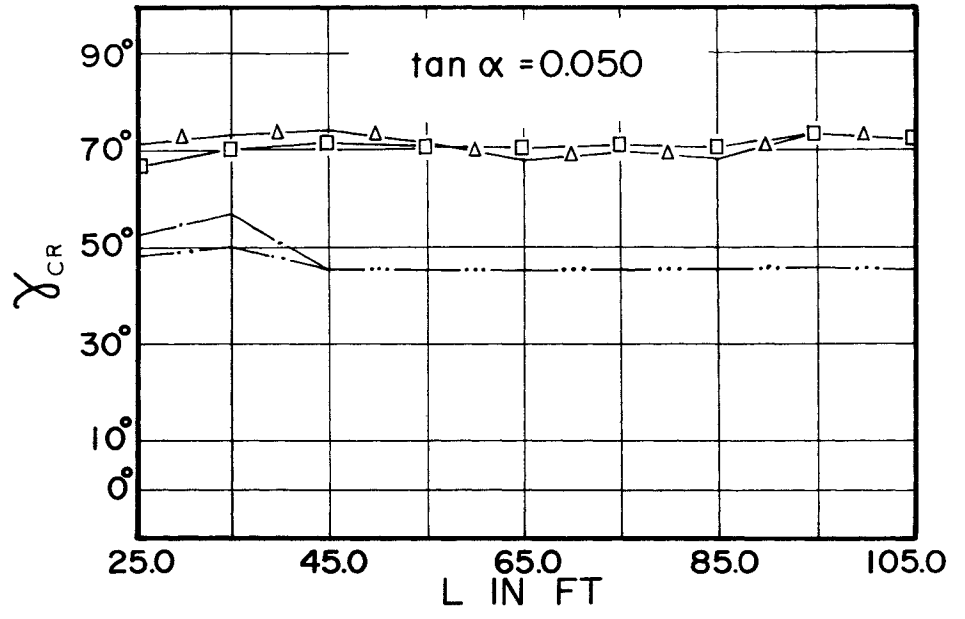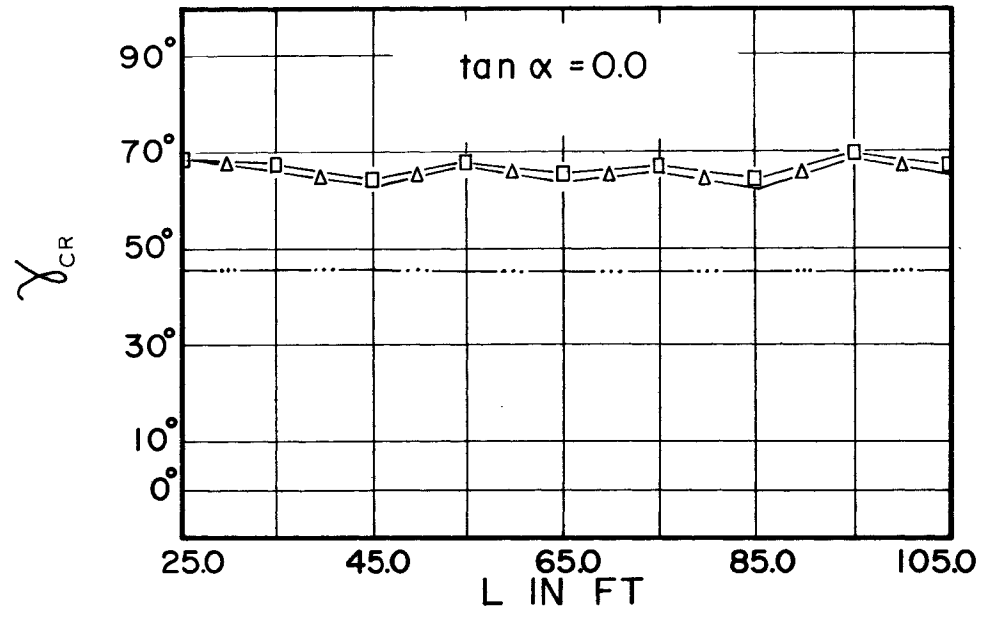
CASE II



## FIGURE 38

COMPARISON OF INCLINATIONS OF MAXIMUM PRINCIPAL TENSILE STRESSES WITH HORIZONTAL AXIS AT CRITICAL SECTIONS
BASED ON GENERAL COMPUTER SOLUTION PROGRAMME

CASE I
L = 80 FT
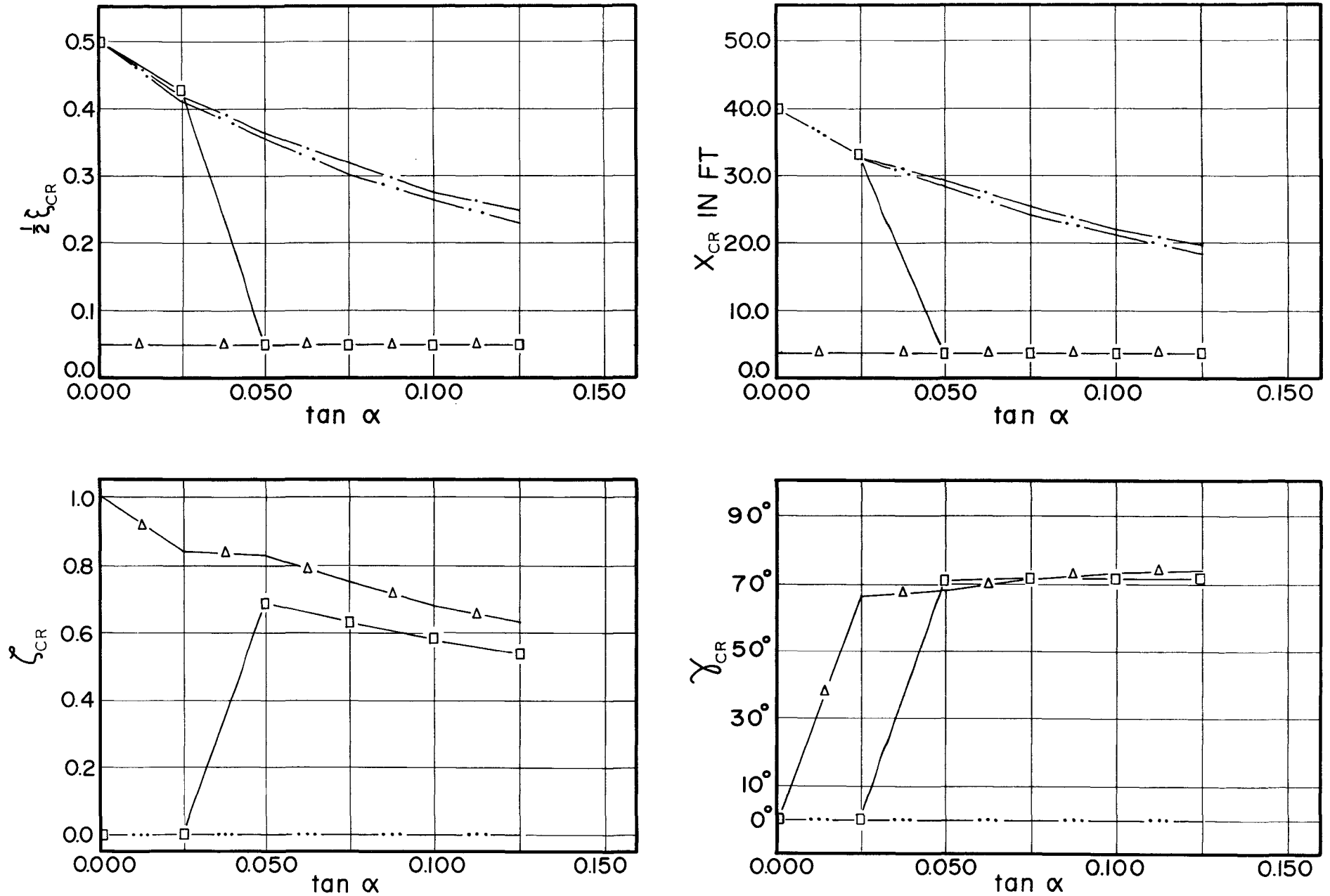
FIGURE 39

VARIATION OF CRITICAL SECTION LOCATIONS, POSITIONS RELATIVE TO SOFFIT OF GIRDER, AND INCLINATIONS
OF MAXIMUM PRINCIPAL TENSILE STRESSES WITH TAN α FOR 80 FT SPAN GIRDER
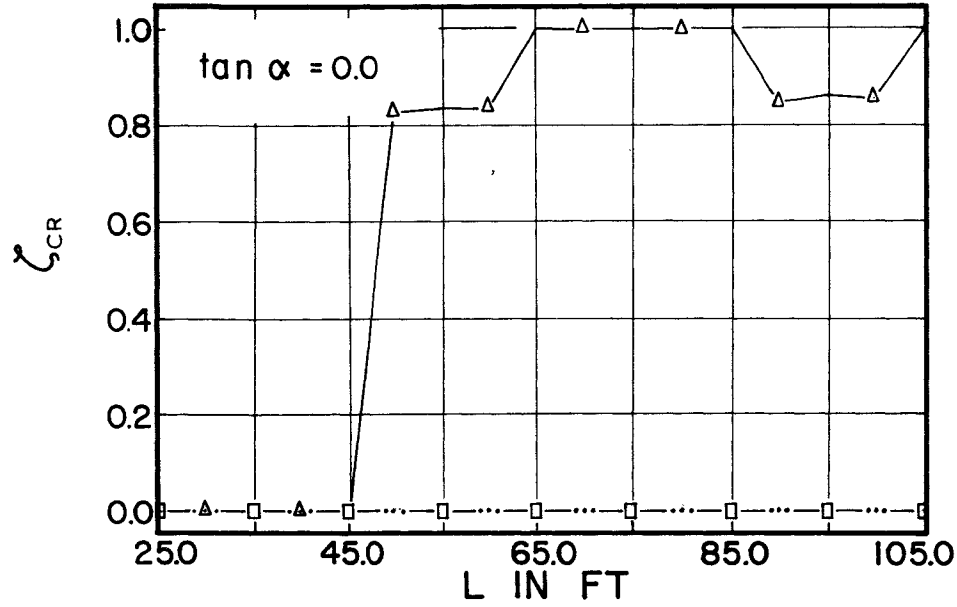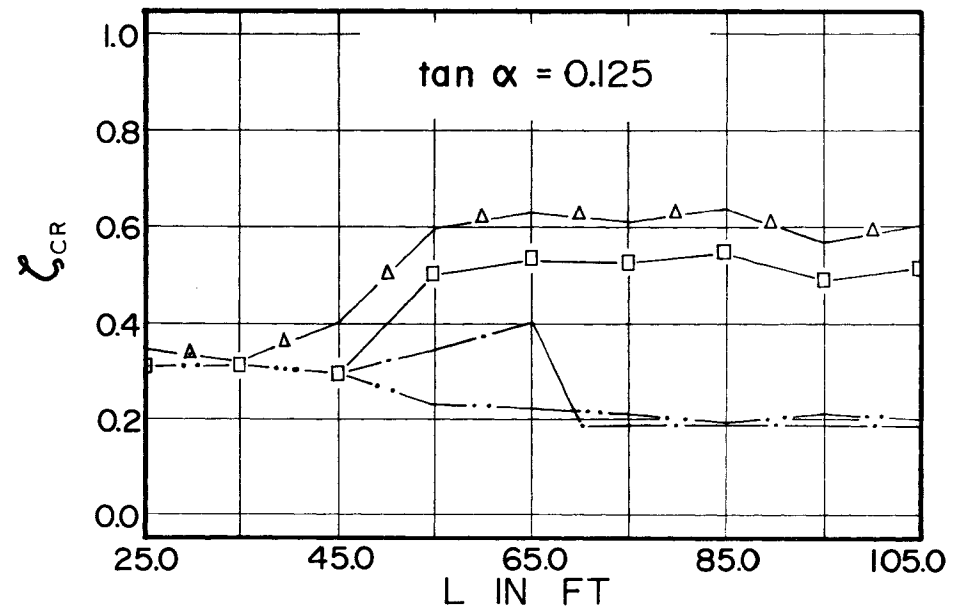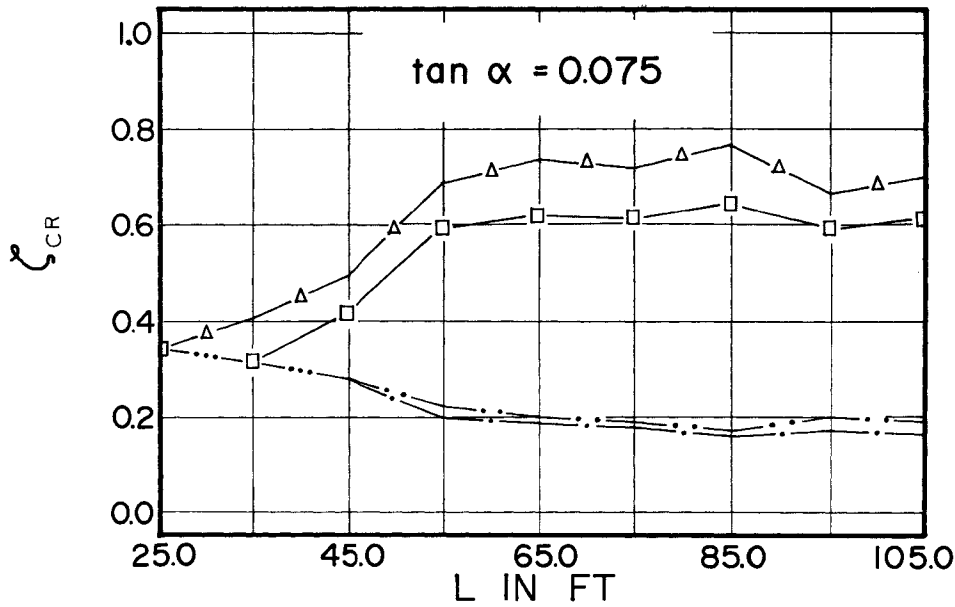BASED ON GENERAL COMPUTER SOLUTION PROGRAMME

CASE II
L = 80 FT
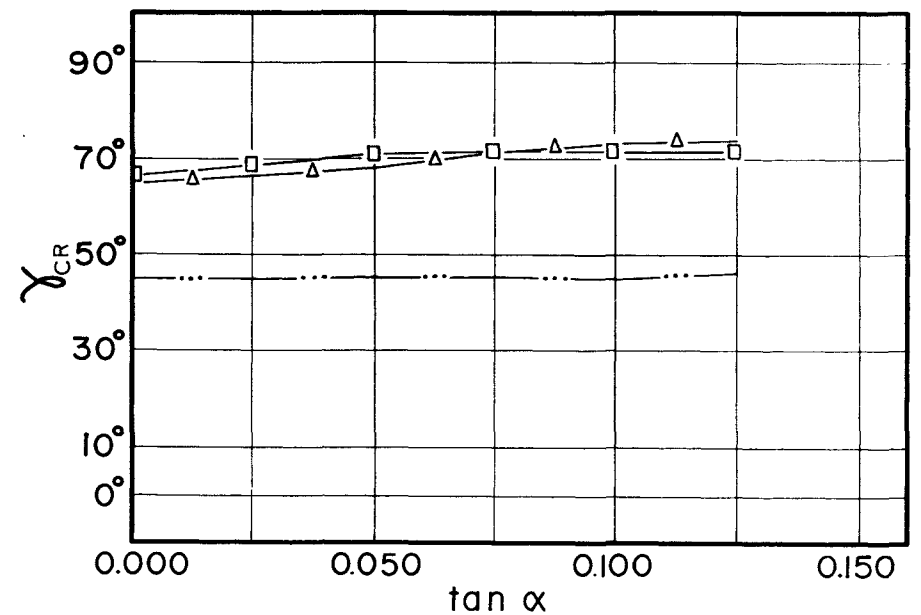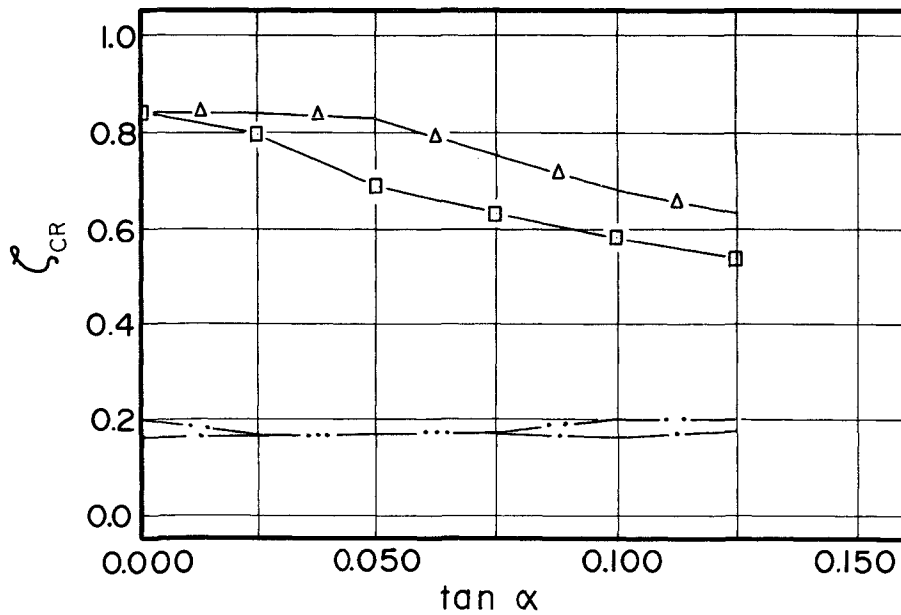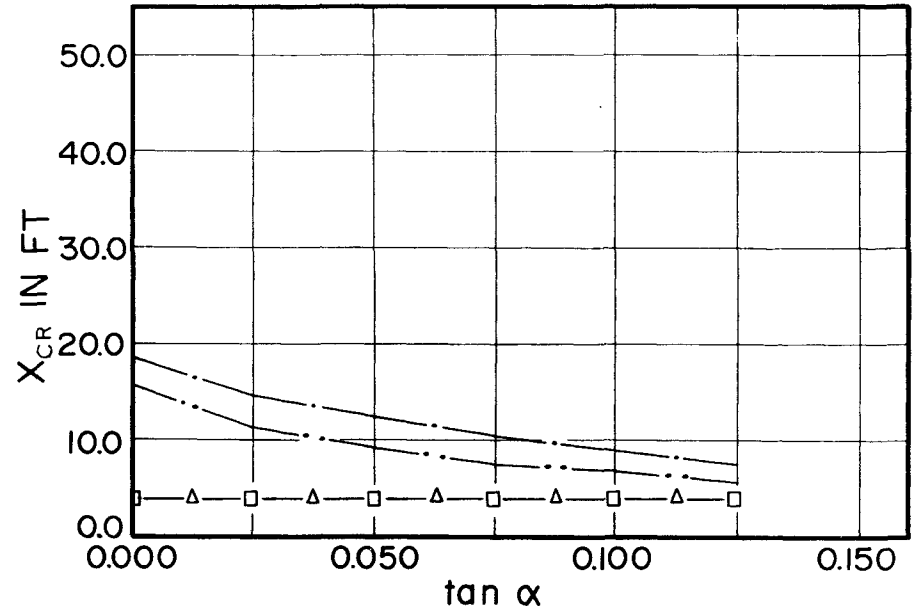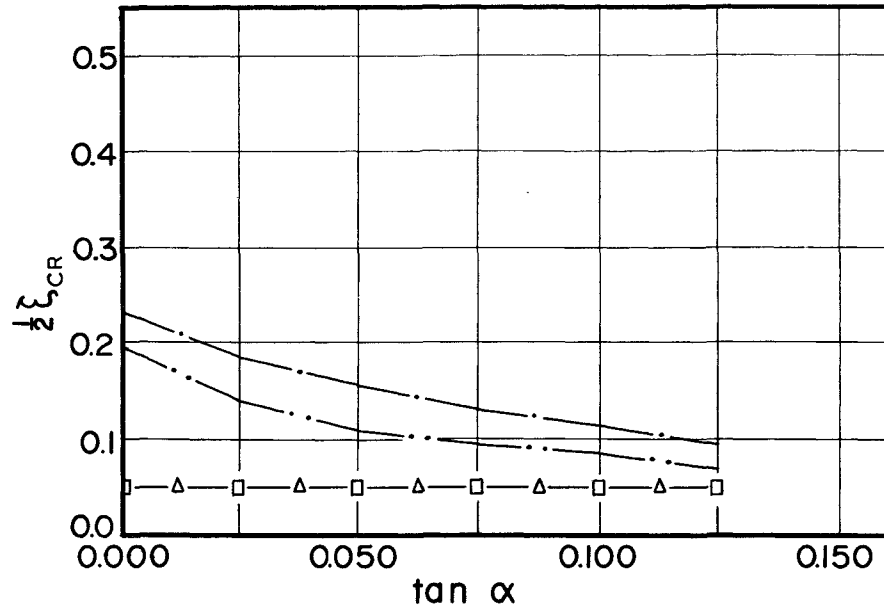
FIGURE 40

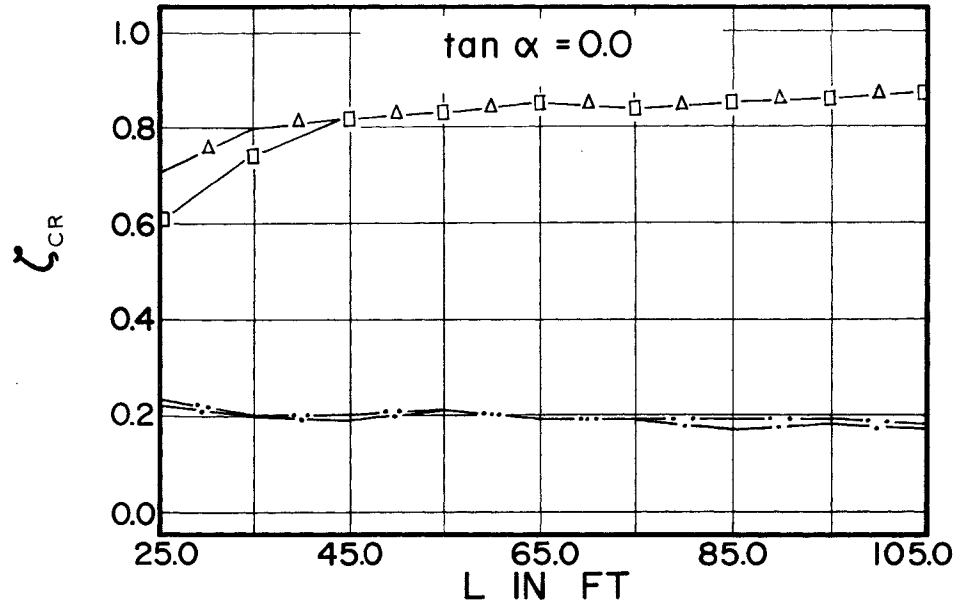VARIATION OF CRITICAL SECTION LOCATIONS, POSITIONS RELATIVE TO SOFFIT OF GIRDER, AND INCLINATIONS
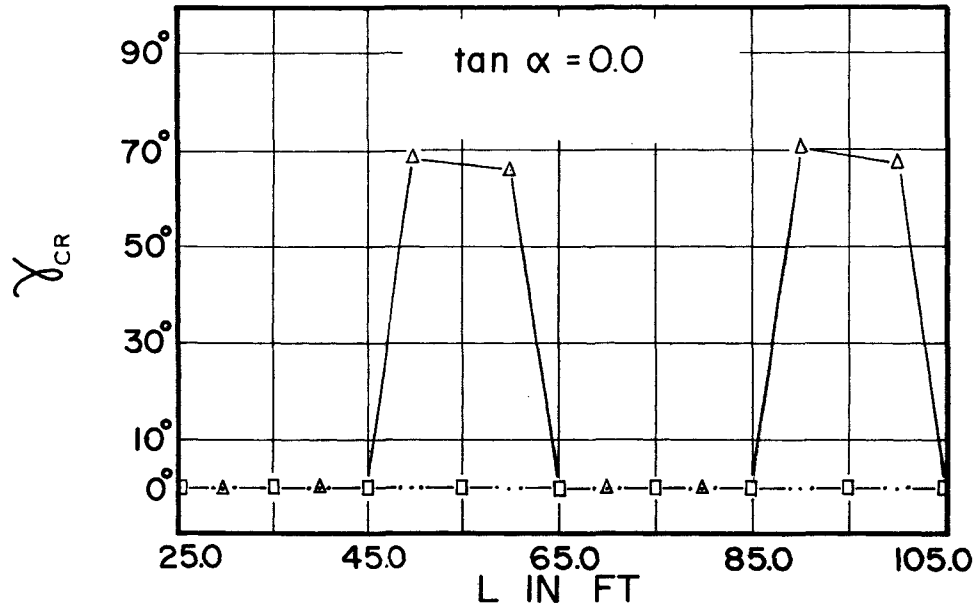OF MAXIMUM PRINCIPAL TENSILE STRESSES WITH TAN α FOR 80 FT SPAN GIRDER
BAS⎯ ⎯ ⎯ ⎯ ⎯ ⎯ :OGRAMME

# APPENDIX

## A.1 Shear Centre

The shear centre of a girder is a line made up of points through which the line of action of transverse loads must pass in order that the girder be subjected to bending alone, i.e., bending without torsion.

For I-section girder the shear centre lies on the axis of symmetry (vertical axis y - y) of the cross-section. In the case when the girder is subjected to transverse loads perpendicular to the axis of symmetry, torsional stresses are introduced unless such loads are applied through the shear centre. Considering the distribution of shear stresses perpendicular to the y - y axis, the distribution along y - y axis is not uniform, with small stresses in the web and the flanges taking practically all the shear. From the foregoing discussions, the two flanges may be considered as two seperate beams having moments of inertia $I_{yft}$ and $I_{yfb}$ about the y - y axis; the deflections of these flanges are equal, provided the proportion of the load taken by each flange is proportional to $I_{yft}$ and $I_{yfb}$; also, the shearing force carried by each flange will be in the same proportion. Refering to Fig. 8, this condition is satisfied when:

$$I_{yft}/I_{yfb} = h_{fb}/h_{ft} \qquad (53a)$$

where

$h_{ft}$ = the distance of the shear centre, s.c., to the centroid of the top flange

$h_{fb}$ = the distance of the shear centre, s.c., to the centroid of the bottom flange

Thus, the position of the shear centre, s.c., relative to the centroid of the section, c.g., could be determined.

## A.2 Torsional Resistance Constant J

St. Venant has established that for rectangular sections of thickness $t$ and length $h$ , ($t$ is always taken as the smaller side of the rectangle), the torsional resistance constant:

$$J = \frac{h\ t^3}{3} - 2\eta t^4 \tag{54a}$$

$$= (\ \frac{1}{3} - 2\eta \frac{t}{h}\ )\ h\ t^3 \tag{54b}$$

$$= k\ h\ t^3 \tag{54c}$$

where, $\eta$ and $k$ are coefficients depending upon the ratio $\frac{h}{t}$

For $\frac{h}{t} \leqslant 2$ , the values of $k$ are given in the following table:

| $\frac{h}{t}$ | 1.00 | 1.25 | 1.50 | 1.75 | 2.00 |
|---|---|---|---|---|---|
| $k$ | 0.141 | 0.171 | 0.196 | 0.214 | 0.229 |

For $\frac{h}{t} > 2$ , $\eta$ is practically constant and is equal to 0.105 , thus:

$$J \approx (\ \frac{1}{3} - 0.21\ \frac{t}{h}\ )\ h\ t^3 \tag{54d}$$

Eq. (54a) may be best visualized by the use of membrane analogy. For a very thin rectangular section ( $\frac{h}{t} \to \infty$ , $k \to \frac{1}{3}$ ), the deflected shape of the membrane is parabolic across the thickness $t$ and straight across the length $h$ . However, for ratios of $\frac{h}{t}$ other than infinity, the deflected

membrane shape deviates from the shape described above, especially at the ends. Coefficient $\eta$ accounts for such deviations.

In general

$$M_t = J \, G \, \theta \qquad (55a)$$

where

$M_t$ = the internal resisting torsional moment of the section, i.e., the internal resisting torque

$G$ = the shearing modulus of elasticity

$\theta$ = the unit angle of twist in radian per unit length

$J$ = the torsional resistance constant, depending upon the shape of the cross-section

By definition, the torsional regidity of a section, $JG$ , is given as:

$$JG = \text{torque per unit rotation} = M_t \qquad (56a)$$

Since for any material, $G$ , is constant, then:

$$J \propto M_t \qquad (56b)$$

And it can also be shown from the membrane analogy that the torsional resistance moment, $M_t$ , of a section is equal to twice the volume, $V$ , under the deflected membrane, thus:

$$J \propto V \qquad (56c)$$

The torsional resistance constant, $J$ , of an I-section can be

-144-

evaluated approximately by considering the section to be made up of several rectangles[11]. Thus:

$$J = \sum ( \frac{h\,t^3}{3} - 2\,\eta\,t^4 )$$  (57a)

$$= J_1 + J_2 + J_3 + \dots$$  (57b)

$$= k_1 h_1 t_1^3 + k_2 h_2 t_2^3 + k_3 h_3 t_3^3 + \dots$$  (57c)

In evaluating the rorsional resistance constant, $J$ , by this method, the following points should be observed:

1- Division of the section into rectangles is carried out in accordance to the priority of the rectangle with the largest possible thickness, i.e., the first rectangle with the largest possible thickness and the second rectangle with the next largest possible thickness and so on.

2- The deflected membrane is not immediately attached to the surface of the section along the inner lines resulting from the division of the section into rectangles. To allow for this effect, the $k$ values of the discontinued rectangles ( the overhanging rectangles), should be taken as $\frac{1}{3}$ for a long discontinued rectangle and for a short discontinued rectangle $k$ should be determined by assuming an equivalent length, $h_e$ , equal to

twice the length resulting from the subdivision. This modification would compensate for any underestimation of the volume under deflected membrane which would otherwise occur.

3- In I, T, and channel sections warping plays a very important role in inducing normal stresses which in turn reduces the shear stresses. The maximum shear stress occurs along the length of the rectangle with the largest thickness, $t_{max}$ , provided the reentrant corners (inner corners) are rounded, tapered or filleted.

-146-

### A.3 Concrete Stresses in Pretensioned Girders under Sustaining Loads with Effects of Creep and Shrinkage

Owing to the shrinkage and creep phenomena in the concrete, the concrete stresses in pretensioned members, or any uncracked composite members under sustaining load do not remain constant. This is due to the fact that concrete shrinks and creeps under sustained loads with time, while the steel reinforcements in the section do not[*].

In order to explain such behaviour of the concrete, let us consider the subject in the following order.

#### Creep and Shrinkage Deformations in Uncracked Plain Concrete

Subjecting a concrete cylinder of unit length (the shortening and the resulting strain are numerically equal) to a uniform compressive stress $f_c$ , an immediate shortening of such cylinder will occur and such shortening is termed as elastic shortening

$$\mathcal{E}_{cel} = \frac{f_c}{E_{co}} \tag{58a}$$

However, upon leaving the cylinder under the same compressive stress for longer times, further plastic shortening will occur,

---

[*]   The creep in the steel is small and takes place very rapidly, almost 75% of the creep takes place during the tensioning process, thus, the creep in the steel is usually ignored except for some kinds of cold drawn steels.

-147-

which is relatively rapid at the beginning and it slows down afterwards. Such plastic shortening, after a few years, reaches a limit which is almost constant . Such deformation is defined as creep deformation of the concrete.

It has been shown experimentally that concrete behaves in the same manner when subjected to tensile stresses as long as the concrete remains uncracked. It has been also confirmed by experiments that for the same period of time, the amount of such plastic deformation is proportional to the applied stress, $f_c$ , as long as this stress remains below 0.4 $f_c'$ , which is well within the working loads.

The foregoing mentioned fact signifies that for all practical purposes it can be assumed that the deformation follows Hooke's law.

Defining the ratio of the plastic deformation at any arbitrary given time t to the elastic deformation as creep factor, $\phi_t$ , one can write:

$$\phi_t = \frac{\text{plastic deformation in concrete}}{\text{elastic deformation in concrete}} \tag{59a}$$

$$= \frac{\varepsilon_{cpl}}{\varepsilon_{cel}} \tag{59b}$$

or.

$$\varepsilon_{cpl} = \varepsilon_{cel}\,\phi_t = \frac{f_c}{E_{co}}\,\phi_t \tag{59c}$$

-148-

Thus, the total deformation of the concrete under the sustained stress at any given time, t , is:

$$\Sigma_{ct} = \Sigma_{cel} + \Sigma_{cpl} = \frac{f_c}{E_{co}} + \frac{f_c}{E_{co}} \phi_t \qquad (60a)$$

$$= \frac{f_c}{E_{co}} (1 + \phi_t) \qquad (60b)$$

Furthermore, shortening, $\Sigma_{s,t}$ , of the unloaded cylinder, attributed to shrinkage of concrete, takes place in a similar manner to that due to creep. The shrinkage of the concrete is very rapid at the beginning and it decreases slowly to where after a few years it reaches almost a constant value. Experiments show that both shrinkage and creep have the same affine (resemblance curves) as regards to the time under the same ambient conditions, i.e.

$$\Sigma_{s,t} = \Sigma_{s\infty}(1 - \bar{e}^{\lambda t}) \qquad (61a)$$

$$\phi_t = \phi_\infty(1 - \bar{e}^{\lambda t}) \qquad (61b)$$

where

$\Sigma_{s\infty}$ = the final shrinkage strain, shrinkage strain at
    time $t = \infty$

$\phi_\infty$ = the final creep factor, the creep factor at time $t = \infty$

$\lambda$ = a constant depending on the concrete and the ambient
    conditions

-149-

In practice, the shrinkage strains and creep factors are considered to attain their final values after 5 years.

It follows from the foregoing 2 equations, that:

$$\mathcal{E}_{s,t} = \frac{\mathcal{E}_{s\infty}}{\phi_{\infty}} \phi_t \qquad\qquad (61c)$$

In general when there is composite action between steel and concrete deformations can be shown to be:

$$\frac{d\mathcal{E}_{ct}}{dt} = \frac{1}{E_{co}} \frac{df_c}{dt} + \frac{f_c}{E_{co}} \frac{d\phi_t}{dt} + \frac{\mathcal{E}_{s\infty}}{\phi_{\infty}} \frac{d\phi_t}{dt} \qquad\qquad (62a)$$

In reality, outdoor concrete structures are exposed to temperature changes and other climatic conditions, and shrinkage and creep do not follow a regular pattern, e.g. they slow down in the winter months. However, as Dischinger[8] has proven, these irregularities do not affect the internal forces in the section induced by shrinkage and creep of the concrete as such internal forces depend only on the final shrinkage strain and final creep factor.

## Effects of Creep and Shrinkage Deformations on Concrete Stresses in a Bonded Composite Section

For generality of the subject let us consider concrete creep and shrinkage deformations in a composite section comprised of a profile steel section encased in concrete, and investigate the effects of such time dependent deformations on the concrete stresses.

-150-

## 1- Compatibility Conditions

The strain and rate of the strain at any steel fibre is given as:

$$\dot{\varepsilon}_{st} = \frac{f_s}{E_s} \quad , \tag{63a}$$

$$d\varepsilon_{st} = \frac{1}{E_s} \, df_s \quad , \quad \text{and} \tag{63b}$$

$$\frac{d\varepsilon_{st}}{dt} = \frac{1}{E_s} \frac{df_s}{dt} \tag{63c}$$

assuming that the modulus of elasticity of steel, $E_s$ , is independent of time  $t$ .

From the compatibility conditions, the strains in both neighbouring concrete and steel fibres must be equal.  Thus:

$$d\varepsilon_{ct} = d\varepsilon_{st} \tag{64a}$$

Thus, the differential equation of the strains in the concrete will be reduced to:

$$\frac{df_c}{E_{co}} + \frac{f_c}{E_{co}} \, d\phi_t + \frac{\varepsilon_{s\infty}}{\phi_\infty} \, d\phi_t = \frac{df_s}{E_s} \tag{64b}$$

Furthermore, by considering the equilibrium conditions, the stress in steel  $f_s$  could be expressed in terms of the stress in concrete  $f_c$ .

-151-

## 2- Equilibrium Conditions

In considering the equilibrium conditions, let us imagine first that the bond between the concrete and the steel in the composite girder is no longer operative, and each of the concrete and the steel parts act independently with the exception that when they are subjected to a bending moment, both parts should have the same curvature.

To show the effect of the inter-play between the concrete and steel parts as hypothesized, let the concrete part be subjected to a moment $M_{co}$ applied about its own centroidal axis. From flexural consideration, it can be readily shown that the moment carried by the concrete alone, is:

$$M_c = \frac{E_{co} I_c}{E_{co} I_c + E_s I_s} M_{co} \tag{65a}$$

Thus, the strain due to $M_c$ at a distance $e_c$ from the centroidal axis of the concrete part is:

$$\overline{\Sigma}_{com} = \frac{M_c}{E_{co} I_c} e_c \tag{65b}$$

$$= \frac{M_{co}}{E_{co} I_c + E_s I_s} e_c \tag{65c}$$

or

$$\overline{\Sigma}_{com} = \frac{M_{co}}{E_{co}( I_c + \frac{E_s}{E_{co}} I_s)} e_c \qquad (65d)$$

The strain due to a moment applied to the steel part of the unbonded composite section could be found in the same way. Thus, for this special condition, we are introducing the so called 'construction moment of inertia' which is the sum of both of the individual moments of inertia, thus:

relative to the concrete part:

$$I_{const,c} = I_c + \frac{E_s'}{E_{co}} I_s \qquad (66a)$$

and relative to the steel part:

$$I_{const,s} = I_s + \frac{E_{co}}{E_s} I_c \qquad (66b)$$

Let two unit loads of opposite directions be applied at any arbitrary common level, one on the concrete part the other on the steel part at a distance $e_c$ from the centroid of the concrete part, and at a distance $e_s$ from the centroid of the steel profile as shown in Fig. 9. The concrete and steel strains at this common level are:

$$\overline{\Sigma}_{co} = \frac{1}{A_c E_{co}} + \frac{(1.e_c)e_c}{E_{co}( I_c + \frac{E_s}{E_{co}} I_s)} \qquad (67a)$$

-153-

$$\bar{\varepsilon}_{sto} = \frac{1}{A_s E_s} + \frac{(1.e_s)e_s}{E_s \left( I_s + \frac{E_{co}}{E_s} I_c \right)} \qquad (67b)$$

The resulting stresses in each of neighbouring concrete and steel fibres are:

$$\bar{f}_c = \bar{\varepsilon}_{co} E_{co} \qquad (68a)$$

$$\bar{f}_s = -\bar{\varepsilon}_{sto} E_s \qquad (68b)$$

Now, in a 'bonded composite section' at a location $e_c$ away from the centroid of the concrete section, or $e_s$ away from the centroid of the steel section, time dependent changes in the stresses, $f_c$ and $f_s$, due to the creep and shrinkage in the concrete, will take place. On the grounds of the equilibrium, the ratio of $df_s$ and $df_c$ should be equal to the ratio of $\bar{f}_s$ and $\bar{f}_c$, thus:

$$\frac{df_s}{df_c} = \frac{\bar{f}_s}{\bar{f}_c} \qquad (69a)$$

$$= - \frac{\bar{\varepsilon}_{sto}}{\bar{\varepsilon}_{co}} \frac{E_s}{E_{co}} \qquad (69b)$$

Hence, $f_s$, could be expressed in terms of $f_c$, then:

-154-

$$\frac{df_s}{E_s} = - \frac{\bar{\bar{\varepsilon}}_{sto}}{\bar{\varepsilon}_{co}} \frac{1}{E_{co}} \cdot df_c \qquad (69c)$$

Substituting the above equation into Eq. (64b) and rearranging:

$$\frac{df_c}{d\phi_t} + \frac{\bar{\varepsilon}_{co}}{\bar{\varepsilon}_{co} + \bar{\varepsilon}_{sto}} f_c + \frac{\bar{\varepsilon}_{co}}{\bar{\varepsilon}_{co} + \bar{\varepsilon}_{sto}} \frac{E_{co} \varepsilon_{s\infty}}{\phi_\infty} = 0 \qquad (70a)$$

### 3- Solution of the Differential Equation

Defining:

$$\alpha_o = \frac{\bar{\varepsilon}_{co}}{\bar{\varepsilon}_{co} + \bar{\varepsilon}_{sto}} \qquad (71a)$$

then Eq. (70a) reduces to:

$$\frac{df_c}{d\phi_t} + \alpha_o f_c + \alpha_o \frac{\varepsilon_{s\infty}}{\phi_\infty} E_{co} = 0 \qquad (71b)$$

The solution of the above differential equation is:

$$f_c = f_{co} - (1 - e^{-\alpha_o \phi_t})\left(f_{co} + \frac{\varepsilon_{s\infty}}{\phi_\infty} E_{co}\right) \qquad (71c)$$

where

$f_{co}$ = the initial concrete stress at the time $t = 0$, i.e., the stress in concrete before any deformation due to creep and shrinkage of concrete takes place.

-155-

## 4- Stiffness Coefficient

Substituting Eqs. (67a) and (67b) into Eq. (71a) one finds:

$$\alpha_o = \frac{\dfrac{1}{E_{co}A_c} + \dfrac{e_c^2}{E_{co}\left(I_c + \dfrac{E_s}{E_{co}}I_s\right)}}{\dfrac{1}{E_{co}A_c} + \dfrac{e_c^2}{E_{co}\left(I_c + \dfrac{E_s}{E_{co}}I_s\right)} + \dfrac{1}{E_sA_s} + \dfrac{e_s^2}{E_s\left(I_s + \dfrac{E_{co}}{E_s}I_c\right)}} \qquad (72a)$$

where $\alpha_o$ is defined as the stiffness coefficient for
the composite structure comprising of two parts (the
concrete and the steel parts). This coefficient signifies
the contribution of the steel section in supporting the
loads carried by the composite structure. It is func-
tion of the area and shape of the steel profile as well
as the position of the stress in the fibre considered.
In prestressed concrete, however, the cross-sectional
areas of the steel tendons are considered to be
concentrated at their centroid (c.g.s.) as a single
steel fibre, thus, the moment of inertia of the steel
tendons about their centroid is ignored, hence:

$$e_s = 0$$

$$I_s = 0$$

Now, by letting $e_c = y_s$ and $n = E_s/E_{co}$ , the stiffness

-156-

coefficient $\alpha_o$ in a prestressed concrete girder

reduces to:

$$\alpha_o = \frac{I_c + A_c \, y_s^2}{\dfrac{I_c A_c}{n \, A_s} + I_c + A_c \, y_s^2} \qquad\qquad (72b)$$

It can also be shown that $\alpha_o$ , in a prestressed

concrete girder, could be expressed as follows:

$$\alpha_o = \frac{n \, A_s}{A_e} \left( 1 + \frac{A_e}{I_e} \, y_e^2 \right) \qquad\qquad (72c)$$

where

$A_e$ = the effective area of the girder, i.e.,

$\quad A_e = A_c + A_s \, n$

$y_e$ = the distance of the prestressing steel to the

effective centroid of the section (c.g.e.)

$I_e$ = the effective moment of inertia about the

effective centroid of the section

## 5- Special Cases

### a) Permanent Loading with Effects of Creep

Neglecting the shrinkage deformation of the concrete,

Eq. (71c) for sustaining loads reduces to:

$$f_c = f_{co} \, e^{-\alpha_o \phi_t} \qquad\qquad (73a)$$

The stress losses in the concrete are then:

$$\Delta f_{co} = f_{co} - f_c \tag{73b}$$

$$= f_{co} ( 1 - \bar{e}^{\alpha_o \phi_t} ) \tag{73c}$$

b) <u>Concrete Shrinkage with Effects of Creep</u>

For composite structures with no initial stresses in the concrete ($f_{co} = 0$ at $t = 0$), Eq. (71c) reduces to:

$$f_c = - ( 1 - \bar{e}^{\alpha_o \phi_t} ) \frac{\mathcal{E}_{s\infty}}{\phi_\infty} E_{co} \tag{74a}$$

c) <u>Concrete Shrinkage without Effects of Creep</u>

By expanding $\bar{e}^{\alpha_o \phi_t}$ and letting $\phi_\infty$ and $\phi_t$ both $\longrightarrow 0$ in Eq. (74a), the stress in the concrete without effects of creep is:

$$f_c = - \mathcal{E}_{s\infty} E_{co} \alpha_o \tag{74b}$$

It is worthwhile to note that the creep in the concrete induces stress relaxation in the concrete which in turn leads to stress concentration in the neighbouring steel fibre. However, the shrinkage of concrete in general induces tensile stresses in the concrete and compressive stresses in the steel.

-158-

# VITA AUCTORIS

1931    Mohammed Amin Saeed born September 25, Koisanjak,
        Iraq.

1944    Graduated from Koisanjak Primary School, Koisanjak,
        Iraq.

1949    Graduated from Arbil Secondary School, Arbil, Iraq.

1950    Granted a Scholarship in Civil Engineering, College
        of Engineering, Baghdad, Iraq.

1951    On completion of first year Engineering with distinc-
        tion, was granted a scholarship to study Civil
        Engineering in the United Kingdom.

1955    Granted Bachelor of Science Degree, with honours, in
        Civil Engineering, University of Wales, Cardiff, U.K.

1955    September, entered employment in the Design Office,
        Bridge and Road Section, Ministry of Development,
        Baghdad, Iraq.

1956    November, entered employment as part time Engineer
        in the Rhein-Rohr Consulting Engineers, Baghdad, Iraq.

1958    Entered employment in the Design Office, Public Works
        Department, Ministry of Housing, Baghdad, Iraq.
        Entered also (as part time Engineer) in the Design
        Office of Abdul-Kader Hishmat, Baghdad.

1960    Entered employment in the Construction Company of
        Rashid Aref and Partner, Baghdad.

1962    Entered imployment with Betonwerk Hemmerlein, Neunkirchen
        am Brand, W. Germany.